Identification and analysis of the molecular components involved in the oil palm (Elaeis guineensis) fruit abscission processhuile (Elaeis guineensis)

Kim Fooyontphanich

Collège Doctoral du Languedoc-Roussillon

THÈSE

Pour obtenir le grade de

Docteur

Délivré par **Université de Montpellier**

Préparée au sein de l'école doctorale **SIBAGHE**

Et de l'unité de recherche **DIADE**

Spécialité : **Biologie Intégrative des Plantes**

Présentée par **Kim FOOYONTPHANICH**

Identification and analysis of the molecular components involved in the oil palm (*Elaeis guineensis*) fruit abscission process

Soutenue le 16 Décembre 2015 devant le jury composé de

Dr. Francisco R. Tadeo, IVIA, Espagne	Rapporteur
Professor Jens Wünsche, University of Hohenheim, Allemagne	Rapporteur
Professor Jeremy Roberts, University of Nottingham, UK	Examinateur
Dr. Evelyne Costes, INRA, France	Examinateur
Dr. Jean-Luc Verdeil, CIRAD, France	Examinateur
Dr. Timothy J. Tranbarger, IRD, France	Directeur de Thèse
Dr. Fabienne Morcillo, CIRAD, France	Invitée
Dr. Chatchawan Jantasuriyarat, Kasetsart University, Thaïlande	Invité

UNIVERSITÉ DE MONTPELLIER

Acknowledgements

I would like to acknowledge the French Embassy in Thailand (Franco-Thai scholarship) and Palmelit SAS for graduate scholarship support during my stays in France. I also thank Palmelit for financial support for the field trip to the plantations in Ecuador. In addition, I would also like to acknowledge IRD (Allocations de recherche pour une thèse au Sud, ARTS scholarship) and the Thailand Graduate Institute of Science and Technology (TGIST) (codes TG-22-11-56-005) for the co-financial support during my thesis project.

First of all, I would like to thank my thesis director Dr. Timothy Tranbarger for his brilliant guidance along the way of my thesis project and all types of support had given to me while I was working at IRD and during my stay in France. I also would like to thank Dr. Jean-Luc Verdeil for all of the suggestion during my thesis and accessibility to the confocal microscope.

I appreciate Dr. Fabienne Morcillo, Dr. Stephane Dussert, Dr. James W. Tregear and the members of oil palm group for their very kind of support on the technical and theory on the related topic in my thesis. I thank Myriam Collin, Julien Serret and Maxime Pizot for their help during my experiment in the laboratory and give me a lot of suggestion during my research experiments.

I would like to thank Dr. Chatchawan Jantasuriyarat whose first suggested me to Dr. Timothy for the collaboration that brought me to France and also give me a suggestion for supports while I performed research in Thailand. We especially thank Anek Limsrivilai and the staff at GoldenTenera Oil Palm Plantation in Thailand, Roberto Poveda and staffs at the PDA/Murrin Companies (DANEC group) and Claude Louise of PalmElit in Quinindé, Ecuador for the excellent plant material and logistical support for the study.

I would like to thank Dr. Atikorn Panya and Dr. Peeraya Ekchariyawat for their suggestion and give me a consult and suggestion on everything along my study in France and in Thailand. And also Dr. Uthaiwan Kanto for the ideas had given on the result figure design.

I also want to say thank you to all of the “doctorants” in IRD which I have known during my stay in France, Chloé for her support and the suggestion given on almost everything in every day life, Karina for her help in the Bioinformatics stuffs, Lucie, Céline, Mathilde, Sineewanlaya and Julien for sharing the good moment together during the weekend in France.

Last but not the least, I would like to thank my family: my parents, my brother, my uncle and aunt for supporting me spiritually throughout writing this thesis and my life in general.

Kim FOOYONTPHANICH

November 2015

Abstract

Plant organ abscission is a complex developmental process that involves cell separation regulated by the environment, stress, pathogens and the physiological status of the plant. In particular, seed and fruit abscission play a central role in seed dispersion and plant reproductive success, and are common domestication traits with important agronomic consequences for many crop species. Oil palm (*Elaeis guineensis*) is cultivated throughout the tropical regions as one of the most economically important oil crop species in the world. The unsynchronized ripening of the oil palm fruit bunch leads to the abscission of the ripest fruit and consequently high labor cost for harvest and loss of yield. In this context, the control of oil palm ripe fruit abscission is an important agricultural concern for the cultivation of oil palm in a sustainable and cost effective way. In the present study, a protocol to phenotype the oil palm fruit abscission process was developed and used to identify a tree in the field that does not undergo ripe fruit abscission. In parallel, transcriptome and proteome analyses of the oil palm ripe fruit abscission zone (AZ) during abscission induced experimentally by ethylene compared to the AZ undergoing natural abscission in the field was performed. A total of 1,957 candidate genes were identified statistically as differentially expressed in the ripe fruit AZ during ethylene-induced abscission. Furthermore, a total of 64 of these differentially abundant candidates were statistically specific or enriched at least during one time point of the ethylene induced abscission, compared to their profiles in the AZ of immature fruit and the pedicel of ripe fruit, where cell separation is not observed. The profiles of these gene candidates were examined in the ripe fruit AZ undergoing natural abscission in the field to validate their potential role during abscission. Finally, the profiles of selected candidate genes were then examined in the AZ of the tree observed not to undergo fruit abscission in the field. The combined approaches provide evidence of wide scale conservation of the molecular components involved in organ abscission of this monocot compared with the model dicot plants tomato and Arabidopsis. For example, the identification of polygalacturonases very similar to those that function during Arabidopsis floral organ abscission suggests a conservation of the components for pectin disassembly despite the phylogenetic distance between these species. In addition, the data from the global analysis and complementary molecular, cellular and biochemical approaches suggest novel components and provide a robust list of genes and processes important for AZ function during ripe fruit abscission of this important monocot crop species.

Key words: abscission, abscission zone, 454-seqencing, transcriptome, Illumina sequencing, proteome, histology, ethylene, oil palm, *Elaeis guineensis.*

Résumé

L'abscission des organes chez les végétaux est hautement régulée au cours du développement. Ce processus physiologique qui consiste à diminuer l'adhésion entre deux cellules adjacentes dépend de l'environnement, du stress, de l'attaque de pathogènes ou encore de l'état physiologique de la plante. L'abscission du fruit et de la graine jouent un rôle déterminant dans le cycle de vie de la plante et en particulier, un rôle central dans la dispersion des graines. C'est également un caractère commun de domestication avec des conséquences économiques pour la plus part des espèces cultivées. Le palmier à huile (*Elaeis guineensis*) est largement cultivé dans toutes les zones tropicales et l'huile de palme représente aujourd'hui plus d'un tiers des huiles végétales produites dans le monde. La maturation des fruits au sein des régimes est asynchrone. Ainsi, les fruits les plus murs tombent avant le murissement complet du régime, entrainant une baisse du rendement d'une part et rendant leur collecte manuelle fastidieuse et couteuse d'autre part. Dans ce context, le contrôle ou la réduction de la chute des fruits permettrait une meilleure gestion de la récolte à des couts réduits. Dans le cadre de cette étude, un protocole de phénotypage du processus d'abscission du fruit du palmier à huile a été développé et utilisé pour identifier des génotypes à faible ou retard d'abscision des fruits arrivés à maturité. En parallèle, des analyses comparatives de transcriptomes et de protéomes issus de la zone d'abscission (ZA) du fruit ont été conduites tout au long du processus de séparation cellulaire, déclenché au laboratoire par un traitement à l'éthylène ou bien de manière naturelle au champ. Au total 1957 gènes présentent une expression différentielle significative dans la ZA du fruit au cours du processus d'abscission induit par l'éthylène. Parmi ces gènes, 64 sont spécifiquement (ou majoritairement) exprimés dans la ZA des fruits arrivés à maturité par comparaison avec les tissus où le processus de séparation cellulaire n'est pas observé (pédicelle et mésocarpe des fruits murs ; ZA non fonctionnelle des fruits immatures). Le profil d'expression de ces 64 gènes candidats a été également analysé dans la ZA des fruits mûrs prélevés au champ, afin de conforter leur rôle potentiel au cours de l'abscission déclenchée naturellement. Ainsi, en utilisant les nouvelles technologies de séquençage du transcriptome et du protéome, couplées à une analyse biochimique et cellulaire des modifications de la paroi dans la ZA, ce travail a permis de mettre en évidence la conservation de certains processus moléculaires associés à l'abscission des organes chez les monocotylédones par comparaison avec les espèces modèles dicotylédones, telles que la tomate et Arabidopsis. Par exemple, l'identification de gènes codant des polygalacturonases très proches de celles qui sont impliquées dans l'abscission de la fleur chez Arabidopsis suggère la conservation de leur fonction dans l'hydrolyse de la pectine des cellules des ZA, malgré la divergence phylogénétique entre les espèces. Enfin, ce travail a permis également d'identifier de nouveaux

régulateurs associés au processus de séparation cellulaire et fournir une liste de gènes associés à des processus biologiques étroitement liés à la fonction de la ZA chez le fruit du palmier à huile.

Mots clés: abscission des fruits, ethylene, transcriptome, palmier à huile, séparation des cellules, zone d'abscission

Table of Contents

Chapter 1.
Introduction

Background and Context

The shedding of plant organs is a highly coordinated, developmentally regulated event that can occur in different contexts throughout the plant life cycle (Addicott, 1982; Sexton and Roberts, 1982; Roberts et al., 2002; Leslie et al., 2007; Roberts and Gonzalez-Carranza, 2007; Estornell et al., 2013). Organ shedding is important for both plant vegetative and reproductive development, including abscission of leaves, bunches, whole flowers, floral parts, seeds and immaturely aborted or ripe fruit. In particular, cell separation that occurs during fleshy fruit abscission and dry fruit dehiscence facilitates seed dispersal, the final stage of reproductive development, and therefore governs important characters in many crop species. For fruit to be shed, cell separation must occur in a precise location timed to optimize dispersal under the most favorable conditions. For crop species, if fruit are shed too early or late, economic consequences can be significant. Whereas our understanding of the evolutionary context for the organ abscission phenomenon is mainly limited to model systems such as tomato and Arabidopsis, less is known about the mechanisms underlying fruit abscission in non-model crop species in general and, monocot species in particular.

Oil palm is a tropical perennial monocotyledonous species in the family Arecaceae with an extraordinarily oil rich fleshy mesocarp, which is the number one source of edible vegetable oil worldwide. In addition, potential use of palm oil as a biofuel is predicted to cause constraints on the worldwide supply of edible palm oil and increase the pressure for higher yields and an expansion of cultivatable areas. While conventional breeding schemes have allowed increases in yield of palm oil up to 1% per year, non-synchronized ripening and subsequent shedding of the ripest fruit before harvest limit yield gains (Osborne et al., 1992; Rival, 2007). In addition, the difficulty to schedule regular harvests due to non-synchronized fruit shedding results in a labor-intensive logistics that increases overall production costs. Furthermore, several original characters of oil palm fruit shedding warrant further detailed investigations. In particular, the two-stage process involving primary and adjacent abscission zones (AZs), plus the extraordinary low amount of methylated pectin and high levels of polygalacturonase (PG) activity, collectively suggest that divergent mechanisms may underlie the cell separation process that leads to fruit shedding in this monocotyledonous species (Henderson and Osborne, 1990; Henderson and Osborne, 1994; Henderson et al., 2001).

In the context of a previous thesis project carried out by Peerapat Roongsattham at IRD in the Palm Development Group (PDG), UMR DIADE during 2008-2011, knowledge about original molecular and cellular characters of oil palm fruit abscission was extended. During the previous thesis project, a field experimental system was setup and used to define the precise timing of cell separation, and to examine and compare the response of the oil palm AZ, pedicle and mesocarp fruit

tissues to ethylene at different stages of development (Roongsattham et al., 2012). The results indicated that AZ is highly sensitive to the ethylene treatment, and that the response to ethylene is developmentally regulated, with separation that occurs most rapidly in the ripe fruit AZ within 9 h of ethylene treatment. Molecular approaches identified 14 polygalacturonase (PG) genes expressed in the fruit base containing the AZ and in particular, one PG transcript (*EgPG4*) increases dramatically 700-5000 fold during the ethylene treatment time course and preferential increased in the AZ cell layers in the base of the fruit, at least 6 hours prior to cell separation (Roongsattham et al., 2012). While expression of *EgPG4* is always associated with the cell separation and is an excellent marker of abscission, there is very little known about the other transcriptional changes that occur during oil palm fruit abscission, and how they compare to data acquired from model and other crop species.

Cell separation

Cell separation in plants is a process that takes place throughout the life cycle of a plant (Addicott, 1982; Sexton and Roberts, 1982; Roberts et al., 2002; Leslie et al., 2007; Roberts and Gonzalez-Carranza, 2007; Estornell et al., 2013) and plays roles in protecting and providing for plant growth development. This process is important during both vegetative and reproductive development, and can happen in almost all parts of plants (Figure 1) such as; radicles to appear from germinating seeds, primary roots grow through the soil and laterals root to emerge, cotyledons and leaves to expand and gaseous exchange to happen, formation of aerenchyma, formation of stomata, pollen development and to be released from anthers, microspore separation, fruit to soften, pods to dehisce in dry fruit or various organs to be shed (Roberts et al., 2002). Cell wall breakdown, in particular in the middle lamella, that result in cell separation is related to many biochemical activities while the precise mechanisms are not well understood, in addition to the molecular control of the complexity in the cell walls are still under investigation.

The organization of components within cell walls is not random and the plant cell wall plays important roles in defining the shape of plant cells as well as the ways the cells grow. Cell walls are primarily composed of rigid cellulose micro-fibrils embedded within a gel-like matrix of polysaccharides and glycoproteins, which vary among plant species, while pectin polysaccharides and xyloglucan are also abundant in the cell walls of most land plants (Cosgrove, 1997; Popper et al., 2011; Fangel et al., 2012). The primary cell wall of plant cells is composed of approximately 10% proteins and 90% polysaccharides and also contain structural proteins and many different enzymes. Those polysaccharides are composed of approximately 30% cellulose, 30% hemicellulose and 35% pectin. In addition, the middle lamella is a pectin-rich tissue and important for adhesion between adjacent cells. This combination of different cell wall components provides a plant with a strong

structure but also allows flexibility and adaptation to take place. A complete understanding of the biosynthesis of cell wall polysaccharides is still to be elucidated. It is known that cellulose is made at the plasma membrane and placed directly into the wall while most other matrix components, such as pectins, are made in the Golgi and transported to the wall in secretory vesicles (Carpita, 2000). Because wall components are synthesized in different locations, they must be assembled into a functional wall following their biosynthesis, and the molecular and biochemical differences between parts of the plant where separation takes place compared to areas where separation does not take place is not understood. Indeed, cell separation that leads to fruit and seed abscission must happen in precise locations and timed to optimize dispersal under the most favorable conditions. For example, for crop species, if fruit are separated from the plant at unsuitable times, economic consequences can be significant. Cell separation is very important for plants, without which, it would not have been possible for giant sequoia or red wood (*Sequoia giganteum*) to grow to a height of 115.2 meters or the root of wild fig tree that can grow through the soil for 120 meters.

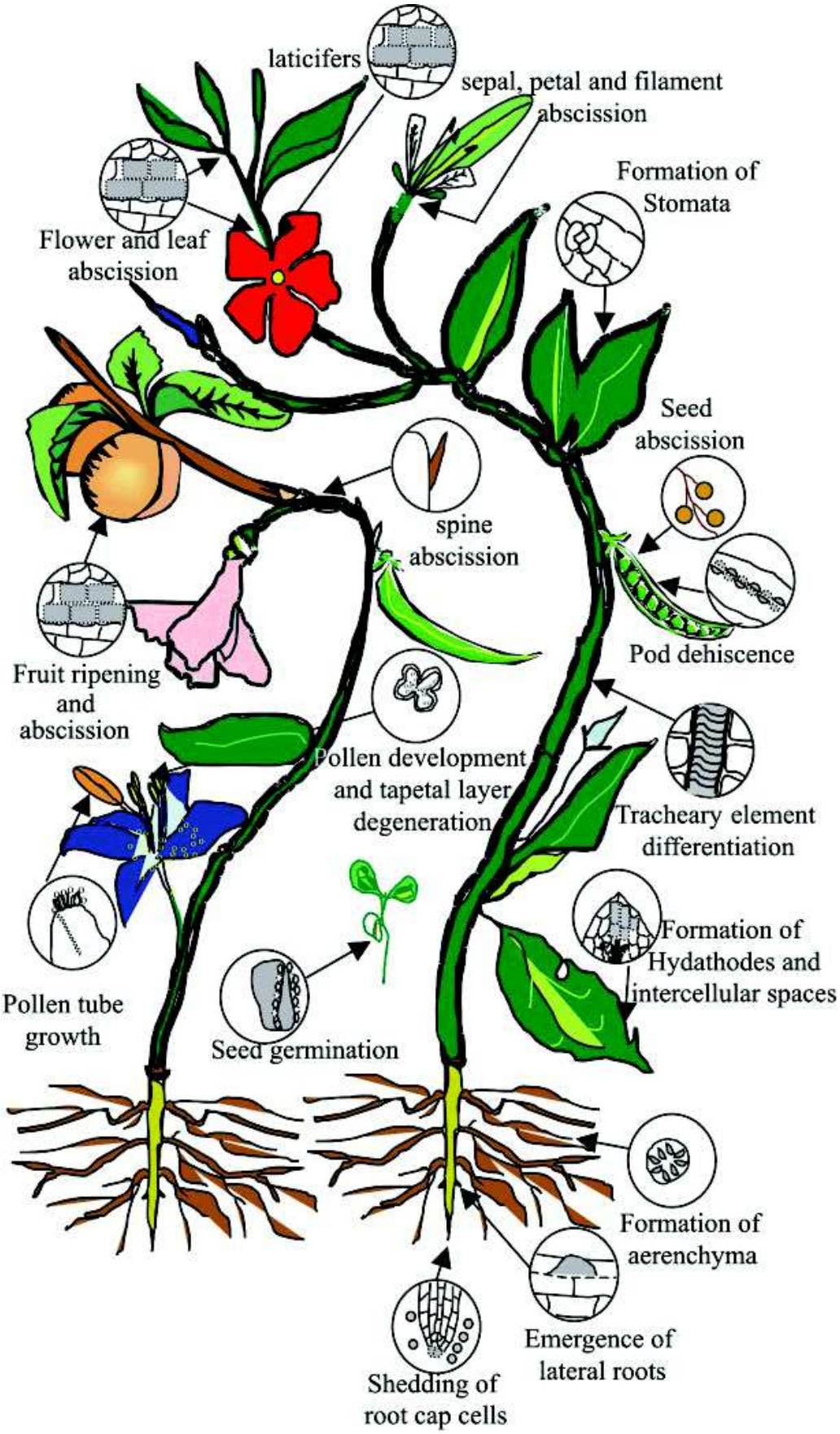

Figure 1. Locations of cell separation sites possible during the plant life cycle (adapted from (Roberts and Gonzalez-Carranza, 2007).

Organ Abscission

Organ shedding is the result of a sequence of cell separation events that occurs during abscission. The cell separation mechanisms that allow plant organs to be shed are determined by molecular and biochemical processes that must be strictly regulated. Organ shedding in plants happens at the base of the organ to be shed, in specialized cells referred to as the abscission zone (AZ), and facilitates several key processes in plants that can be divided into main topics (Leslie et al., 2007) as follows:

1) Reproduction: Cell separation events in plants are arranged to drop ripened fruit, disperse pollen after anther dehiscence, and seeds directly or after pod dehiscence.

2) Recycling: Many organs of plants are shed after they have served their biological function, senescent leaves fall from deciduous trees and fallen floral organs are released after fertilization.

3) Remodeling: Whole branches are often shed to allow for directed growth of plants that affects plant architecture.

4) Defense: Organ shedding can also produce protective scars or spines that prevent pathogen attack and shed affected organs or even eliminate infected organs when attacked by any pathogen to save the non infected area.

5) Competition: Normally plants will generate too many floral buds to be fertilized. After fertilization has occurred, the unfertilized and a portion of the remaining buds or the developing fruit will be dropped to ensure optimized growth of remaining fruit.

For shedding in a plant to occur at the correct time, cell wall modifying enzymes must be secreted from cells within AZs at the base of each organ to be shed (Roberts et al., 2002). If these enzymes are released too soon or in the wrong localization, premature organ loss could have an irreversible effect on reproduction (such as shedding of stamens before pollination, seeds before seed maturation, organs before senescence). Abscission is a process that can alter plant morphogenesis, is essential in the life cycle of plant, and is a physiological and cellular process frequently related to stress and senescence. The abscission process involves the breakdown of the cell-to-cell adhesion in the AZ (Patterson, 2001) located at the base of the organ to be shed. As the AZ develops, it must become competent for cell separation events required for organ abscission. Indeed, once the AZ develops, it responds differently from adjacent tissues to the signals that induce cell separation (Taylor and Whitelaw, 2001). After the AZ becomes competent for separation to be induced, cellular activity, in particular the expansion of the golgi vesicles and activation of the endomembrane system with the release of hydrolytic enzymes to the apoplast leads to the degradation of the middle lamella

and cell separation (Liljegren et al., 2009; Burr et al., 2011). Anatomical studies of the AZ have shown that before cell separation, the site where cell wall breakdown is destined to occur can frequently be morphologically identified as including a layer (or layers) of isodiametric cells containing dense cytoplasm and are joined by plasmodesmata, and are preprogrammed to respond to developmental or environmental cues (Sexton and Roberts, 1982; Roberts et al., 2002). The size of the AZs varies from as few as 1-2 rows of cells in the model plant *Arabidopsis thaliana* to multiple rows as in *Sambucus nigra* (Taylor et al., 1994; Bleecker and Patterson, 1997).

Abscission can be induced by various factors such as temperature, hormones, light, nutrient availability, water, photoperiod, wounding, pathogen and ozone (Addicott, 1982; Taylor and Whitelaw, 2001; Roberts et al., 2002). This suggests that AZ cells have the capacity to integrate many environmental inputs to correctly adapt the plant response. Plant organs are shed in response to stress and senescence mediated by the same hormones that are also involved in the regulation of AZ cell function. The timing of organ abscission is influenced through the plant hormone signaling pathways, including ethylene and auxin (Ellis et al., 2005; Patterson et al., 2007) and by transcriptional regulation and chromatin remodeling, which may globally affect both senescence and abscission (Fernandez et al., 2000; Kandasamy et al., 2005; Kandasamy et al., 2005). The two hormones that have the greatest effect on abscission are ethylene and auxin (Addicott, 1982; Henderson and Osborne, 1990; Taylor and Whitelaw, 2001; Roberts et al., 2002). Ethylene is a small, gaseous readily diffusible phytohormone that affects several developmental processes and is an abscission stimulator with an important role in integrating developmental signals and responses to biotic and abiotic external stimuli. Ethylene treatment enhances abscission of leaves, flowers and fruits whereas treatments with inhibitors of ethylene biosynthesis delay abscission. With Arabidopsis, plants were found to be sensitive to external ethylene at concentrations as low as 0.01 $\mu L.L^{-1}$ (Binder et al., 2004). AZ cells are sensitive to ethylene and respond by changes in gene expression, including those encoding hydrolytic enzymes that are required to remodel or degrade the cell wall (Brown, 1997). Differential gene expression has been studied in many ethylene response systems (Deikman, 1997). In contrast, auxin (indoleacetic acid, IAA**)** acts as abscission inhibitor, and active crosstalk with ethylene (Torrigiani et al., 2012). Auxin can delay abscission by decreasing the sensitivity of the AZ cell to ethylene, and also changing in gene expression necessary for abscission to occur (Roberts et al., 2002). In 2007 (Trainotti et al., 2007), have reported the existence of a cross-talk between auxin and ethylene during peach fruit ripening with auxin biosynthetic and signaling genes regulated by ethylene and ethylene-related genes regulated by auxin. Auxin affects abscission not only by regulating sensitivity to ethylene but also affected the intracellular transport of the hydrolytic enzyme PG associated with cell wall degradation (Meir et al., 2006, 2006). Abscisic acid

(ABA) has also been shown to modulate abscission (Sexton and Roberts, 1982; Suttle and Hultstrand, 1993) and the role during fruit ripening appears to be critical and participates in the regulation of ripening of both climacteric and non-climacteric fruit. Both IAA and ABA also plays important regulatory roles in many plant developmental processes. During abscising events, complex synthesis and activities of cell wall hydrolases has been detected which could be responsible for the degradation of middle lamella and the loosening of primary cell wall of separation layers (Taylor et al., 1993; Taylor et al., 1994). ABA can either antagonize or reinforce ethylene action in different experimental systems and fruit species (Soto et al., 2013). While ABA was discovered and named as a factor involved in cotton fruit abscission, its role is not universal and/or is not well understood at the molecular level. On the recent study of Sawicki et al. (2015) conclude the model showing major events that leading to the abscission process. The complete abscission required three phases; signaling phase, regulatory phase and execution phase (Figure 2).

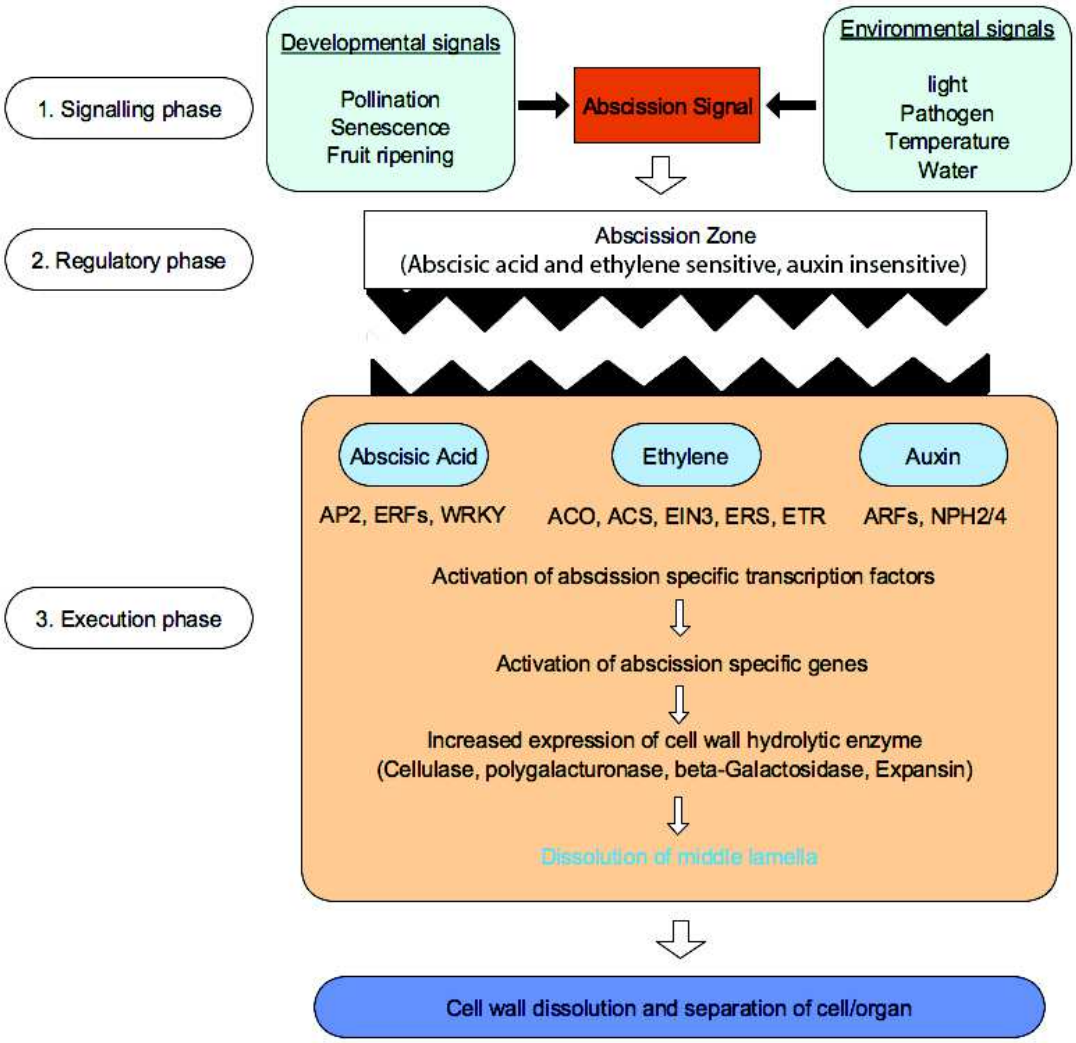

Figure 2. Model showing major events leading up to abscission. Describe steps common to organ abscission process of plants. (Adapted from Sawicki et al., 2015).

Genes that encode proteins related to cell wall softening during fruit ripening, for hydrolytic enzymes that dissolve the cell wall during abscission (organ shedding) and for proteinases during leaf senescence all contain promoter elements that are subject to regulation by ethylene (Bleecker and Patterson, 1997; Deikman, 1997). The abscission process has been broadly studied and many of the analyses have been performed using excised segments of tissue (or explants) exposed to non physiological concentrations of plant regulators such as ethylene or auxin for sustained periods of time (a various durations from a few hours to several days) (Osborne, 1958; Lamotte et al., 1969; Sexton and Roberts, 1982; Coupe et al., 1995; Gonzalez-Carranza et al., 2002; Whitelaw et al., 2002; Belfield et al., 2005; Tucker et al., 2007; Roongsattham et al., 2012).

There have been many studies done on morphological, cytological and biochemical events that occur upon activation of the AZ, but still little is known about the processes involved in AZ development. Controlling of abscission in fruit and grain crops is a key concerning for agricultural.

For examples during cereal crop domestication, mutants that reduce seed shattering have been preferentially selected for because shattering is a major limiting factor for yield (Li et al., 2006). In Arabidopsis and tomato (*Solanum lycopersicum*), which are model plants, many studies focus on what happens or the changes during abscission, such as the study that try to measure the petal abscission by use the special tools (Lease et al., 2001) to follow that what happen during abscission. Although the Arabidopsis silique and the tomato berry are regarded as models for dry and fleshy fruits, respectively, peach is now emerging as a model species for the drupe type of fruit too (Torrigiani et al., 2012). While most of the current molecular knowledge on the abscission process has been obtained from these model plant systems, it is largely unknown whether this knowledge is applicable to all species, in particular for monocot fruit species.

A large number of studies have focused on the factors expressed specifically in the AZ that lead to cell wall disassembly. For example, expression of the β-1,4-glucanase increased during ethylene promoted abscission was suppressed by the application of IAA and was restricted to the abscission zone tissue (Roberts et al., 2000). An increase in expression of β-1,4-glucanase has subsequently been reported during abscission of tomato flower (Lashbrook et al., 1994; Lashbrook et al., 1994) which are involved in cell wall loosening. Another family of genes related to abscission are the polygalacturonases (PGs). An increase in expression of PGs has been well studied during fruit ripening and abscission of tomato and other species (Berger and Reid, 1979; Bonghi et al., 1992; Taylor et al., 1993; Kalaitzis et al., 1997; Asif and Nath, 2005). From a previous study by Taylor (Taylor et al., 1991), it was found that transformed tomatoes with a construct that down regulated a fruit PG exhibited reduced pectin depolymerization in the fruit, but underwent leaf and flower abscission at the same time as controls, suggesting a specificity for abscission PGs. Furthermore, the antisense material did not exhibit a reduced activity of PG within the leaf abscission zone and the antibody raised against the fruit PG was not able to co-precipitate the abscission enzyme. Indeed, the abscission related PGs (TAPG1, TAPG2, TAPG4 and TAPG5) have been isolated from tomato and although they have close homology to each other (80-90% at the nucleotide level) they exhibit less than 50% identity with the fruit PG (Kalaitzis et al., 1997, 1997). In addition they encode a much smaller transcript (1.5 kB) than the fruit enzyme (1.9 kB). The expression pattern of these PGs varies with *TAPG4* being expressed in the flower abscission zone within 6 hours of exposure to ethylene while *TAPG1* mRNA does not accumulate until 6 hours later and predominantly detected at the proximal side of the separation layer, whereas the expression of other genes encoding a plant cell death (PCD) associated nuclease (TBN1), cellulase (Cel1) and ACC synthase (ACS) are predominantly detected at the distal side of the separation layer (Bar-Dror et al., 2011). These observations suggest an importance of tissue specific expression for processes

important for abscission. A small family of PG genes may also be responsible for abscission of *S. nigra* leaflets as two PG mRNAs have been shown to accumulate within 36 hours of ethylene treatment specifically in the zone tissue (Roberts, 2000). As we know that cell separation occurs at many sites during the life cycle of a plant, the coincident expression of PG during abscission strongly implicates PG enzymes in the events that lead to wall dissolution. An examination of the Arabidopsis EST Sequencing database revealed that a family of putative PGs could be identified on the basis of amino acid homology (Roberts et al., 2000). From other studies (Hadfield and Bennett, 1998) PGs are classified in three different clades based on full-length cDNAs that encode PGs (clade A, B and C). Members of clade A relate to fruit and/or AZ, of which clade B relate to fruit or dehiscence zone while clade C are involved in pollen and anther development. Finally, three PGs (ADPG1, ADPG2, and QRT2) from Arabidopsis have overlapping functions (Ogawa et al., 2009). ADPG1 and ADPG2 are essential for silique dehiscence, while ADPG2 and QRT2 contribute to floral organ abscission, and all three genes contribute to anther dehiscence (Ogawa et al., 2009). These observations point out a certain amount of functional redundancy function and combinations of gene functions may be important for abscission to take place.

Expansins are related with cell wall loosening during expansion growth and ripening. In Arabidopsis, *AtEXP10* is expressed in the petiole and midrib in leaves and also in the vestigial pedicel AZ (Cho and Cosgrove, 2000). Expansins alone can induce cell walls to extend, but in living cells they probably act together with a variety of enzymes that cut and restructure the wall (Cosgrove, 1998). In plants that overexpressing *AtEXP10*, the breakage of pedicel was easily broken than in control plants (Estornell et al., 2013). However, expression of *AtEXP10* at the base of floral organs has not been described. Other cell wall modifying enzymes like pectin methylesterases, pectate lyases and xyloglucan endotransglucosylases have also been proposed to be involved in leaf and floral organ abscission, but how these different cell wall targeted activities function together to promote abscission is unclear.

Ethylene activates expression of genes encoding cell wall remodeling enzymes and their secretion to cell walls (Estornell et al., 2013; Estornell et al., 2013). The *ETR1* gene was the first member of the ethylene receptor family of genes cloned from Arabidopsis (Chang et al., 1993). Studies with the *etr1-1* showed it is an ethylene insensitive mutant (Bleecker and Patterson, 1997), and that there are both ethylene dependent and independent pathways for the abscission process. Examination of Arabidopsis mutants lacking ethylene perception (*etr1-1*) and signaling (*ein2*) have suggested that ethylene may only play a secondary role in determining the timing of the onset of floral organ abscission in Arabidopsis, while it may not be essential for its activation. *ETR1*-like genes have also been reported from other plant species, the best characterized being from the tomato

family and the first of these tomato homologs to be discovered was the *never-ripe* (*NR*) gene, named as such because fruits of the *Nr* mutants do not ripen. The *Nr* mutants also show other indication of ethylene insensitivity (Wilkinson et al., 1995). Another group of genes related to abscission process are *MADS-box* genes known to be important for the development of flowers and fruit. The *MADS-BOX* genes *SHATTERPROOF1* and *2* (*SHP1* and *SHP2*) play key roles in regulating the formation of the dehiscence zone in Arabidopsis siliques (Liljegren et al., 2000). Another approach that proved effective to discover the molecular events that regulate abscission includes the isolation and characterization of mutants that exhibit impaired organ shedding. This approach revealed that the Arabidopsis *BLADE ON PETIOLE 1* (*BOP1*) and *BOP2* (*BOP1/BOP2*) genes are important for AZ differentiation. *BOP1/BOP2* encode proteins that belong to a family containing *BTB/POZ* domains and ankyrin repeats. *BOP1* and *BOP2* promote formation of the specialized AZ anatomy necessary for floral organ abscission; the bop1/bop2 double mutants retain all floral organs indefinitely and do not form a cytologically distinct and active floral AZ. *BOP1/BOP2* may have a wider role in differentiation necessary for AZ development, as they regulate leaf and flower development by controlling the activity of homeotic genes in leaves and inflorescences (Hepworth et al., 2005; Norberg et al., 2005; McKim et al., 2008). One function of BOP1/BOP2 is the activation of other transcription factors involved in differentiation that may also play direct or indirect roles in Arabidopsis AZ differentiation (Khan et al., 2014). Other genes found in Arabidopsis such as *NEVERSHED* (*NEV*) play key roles in regulating wall dissolution and remodeling including the membrane trafficking regulator and also influence plant development including fruit growth (Liljegren et al., 2009; Liljegren et al., 2009). From Figure 3 we can see that *NEV* acts at the same stage of abscission as *INFLORESCENCE DEFICIENT IN ABSCISSION* (*IDA*) and *HAESA* (*HAE*) and *HAESA-LIKE2* (*HSL2*). The peptide ligand *IDA* (Butenko et al., 2003), and the leucine-rich repeat receptor like kinases (*LRR-RLK*), *HAE*) and *HSL2* which are probably activated by the *IDA* and *IDA-LIKE* secreted peptides, act together to switch on a conserved mitogen-activated protein kinase signal transduction pathway essential for activating the separation process (Jinn et al., 2000; Jinn et al., 2000; Cho et al., 2008; Cho et al., 2008; Stenvik et al., 2008; Stenvik et al., 2008). *HAE* is expressed in the floral organ AZs and has been implicated in regulating floral abscission (Jinn et al., 2000). There are two *HSL* genes in the *LRR-RLK XI* subfamily that are closely related to *HAE* and share similar extracellular *LRR* and cytoplasmic Ser/Thr protein kinase domains (Shiu and Bleecker, 2001). Another family of genes involved in the abscission process is *ETHYLENE RECEPTOR* (*EIN)* involve of the ethylene-signaling pathway (Bleecker and Patterson, 1997; Tieman et al., 2001; Patterson and Bleecker, 2004). In a recent study of Arabidopsis, Liljegren (2012) proposed the process of organ abscission in flower that can be considered as a series of stages and associated gene

activity that lead to cell separation (Figure 3). Starting from organ boundaries, defects in the redundant organ boundary genes *BOP1* and *BOP2* appear to eliminate AZ formation (McKim et al., 2008), and F-box protein encoded by *HAWIIAN SKIRT* (*HWS*) is involved in distinguishing adjacent sepal primordia (Gonzalez-Carranza et al., 2007). Another genetic interaction study showed that *IDA*, *HAE* and *HSL2* act in the same pathway regulating floral abscission, in that plants overexpressing *IDA* in *hae*, *hsl2* were also deficient in abscission (Cho et al., 2008; Stenvik et al., 2008). In other experiments that studied the *MITOGEN-ACTIVATED PROTEIN KINASE* (*MAPK*) pathway found that members of MAPK act downstream of *IDA* and *HAE/HSL2* signaling (Cho et al., 2008). After a study on receptor-like kinases, Liljegren (2012) found the interaction and modification in the activity of ligand-binding receptor like kinases, it is possible that *Somatic Embryogenesis Receptor Kinase* (*SERK1*), *EVERSHED* (*EVR*) and *CAST AWAY* (*CST*) modulate abscission by mediating the availability of *HAE/HSL2* at the cell surface before their interactions with *IDA*. Overexpression of *AtDOF4.7* which is member of the *DOF* (DNA binding with one finger) gene family found to delay organ shedding without affecting abscission zone formation (Wei et al., 2010). Finally, the *ZINC FINGER BINDING PROTEIN 2* (*ZFP2*), a partner of *AtDOF4.7*, was initially identified within a cluster of genes upregulated in stamen AZ cells before abscission. In transgenic plants overexpressing *ZFP2* delay abscission was observed suggesting it is involved in the negative regulation of stamen abscission (Cai and Lashbrook, 2008). In tomato, ZFP2 suppresses ABA biosynthesis during fruit development and delays fruit ripening (Weng et al., 2015).

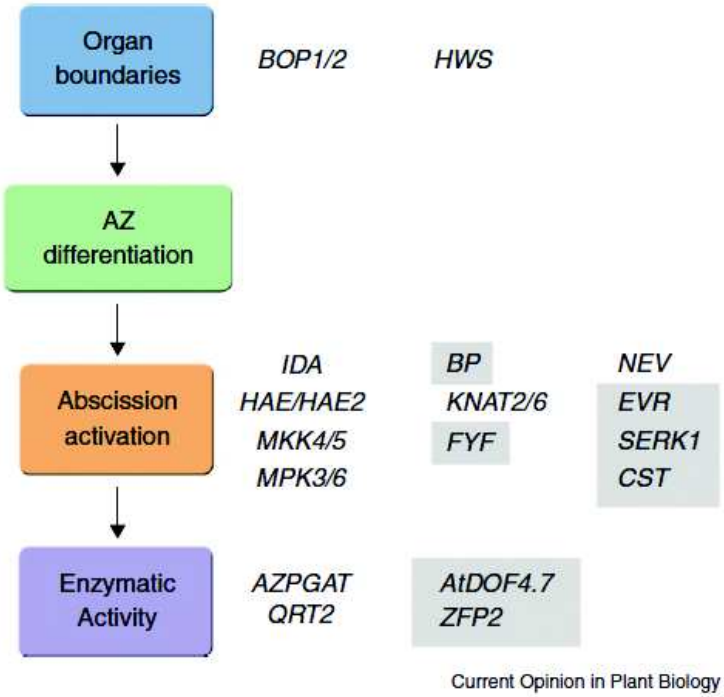

Figure 3 Process of the events and associated gene activities that lead to cell separation in Arabidopsis (Liljegren, 2012). Inhibitors of organ abscission appear within shaded boxes.

In the tomato pedicel, the expression of *JOINTLESS*, a MADS-box encoding gene (Mao et al., 2000) and *LATERAL SUPPRESSOR*, a VHIID transcriptional regulator gene encode a member of different groups of putative transcriptional activators that play a role AZ differentiation (Schumacher et al., 1999). In the *jointless* mutant, that is characterized by defective AZs in fruit pedicels, the nonabscission phenotype is an important trait for tomatoes that are processed into commercial tomato products. *Jointless-2* was discovered by Rick (1956) in a wild species of tomato (*Lycopersicon cheesmanii*) (LA166) found on the Galapagos Islands. *Jointless-2* was introduced into cultivated tomato and is still widely used in the processing tomato industry. This phenotype facilitates large scale harvesting of the tomatoes by saving time removing the calices, because when the *jointless* fruit is harvested, the calyx remains attached to the plant not to the fruit (Zahara and Scheuerman, 1988). The primary role of *JOINTLESS* is to suppress sympodial meristem identity in inflorescence meristems (Szymkowiak and Irish, 2006). Another tomato abscission phenotype is the *Never-ripe* (*Nr*) which results from the tomato mutation in the ethylene receptor similar to Arabidopsis *ETR1*, that results in ethylene insensitivity and a much slower rate of abscission (Lanahan et al., 1994; Wilkinson et al., 1995). From previous studies, (Bar-Dror et al., 2011) it was shown that genes associated to programmed cell death (PCD), cell wall remodeling and ethylene biosynthesis are expressed asymmetrically within the tomato pedicel AZ, but not in Arabidopsis. With relation to the cell wall there are at least seven cellulases have been cloned (*Cel1*-*Cel7*) from tomato. During pedicel abscission, *Cel1*, *Cel2* and *Cel5* increases in expression (delCampillo and Bennett, 1996). *Cel1* and *Cel2* share low nucleotide homology (55 %) and down regulation of these individual enzymes has been achieved using an antisense RNA strategy. Reduced expression of either of these genes (Lashbrook et al., 1998; Brummell et al., 1999) leads to an increase in the force required bringing about abscission, and these data indicate that the enzymes may have complementary roles during cell separation. Noticeably, both *Cel1* and *Cel2* accumulate during ripening but antisense fruit do not exhibit delayed or reduced softening (Brummell et al., 1999). From a recent study in tomato (Wang et al., 2013), it was found that the AZ was the most active site with the largest set of differentially expressed genes in comparison with basal and apical portions. Gene Ontology analyses also revealed enriched transcription regulation and hydrolase activities in the AZ. Furthermore they also found that the expression patterns of meristem activity genes support the clue that cells of the abscission zone confer meristem-like nature and overlap with the course of abscission and post-abscission cell differentiation. From all the information provided in both model plants, we can say that these mechanisms are well established in model species but it is still not known whether they are applicable for other species, in particular monocots, so it may be possible to benefit from studies with model plants and adapt to less studied species such oil palm.

The Oil Palm

Oil palm is a tropical perennial species in the family Arecaceae (formerly known as the Palmae). The Arecaceae are placed in the order Arecales and have always formed a distinct group of plants among the monocotyledons. Oil palm is grouped with the coconut and other genera in the tribe cocoseae. The oil palm normally is monoecious with male or female but maybe mixed inflorescences developing in the axils of the leaves. It is considered "temporally dioecious" given that separate male and female inflorescences occur on the same palm in an alternating cycle that depends on genetic factors, age and environmental (Adam et al., 2005). Oil palm is one of the most important tropical crops because of the fleshy mesocarp which edible oils are derived and recently became the number one source of edible vegetable oil worldwide (Rival, 2007). Oil palm fruit is a drupe whose thick fleshy mesocarp is especially rich in oil (80% dry mass) (Figure 4), making this species the highest oil-yielding crop in the world (Murphy, 2009). Mesocarp of oil palm presents an original model to examine the regulatory networks in a monocot fruit tissue subject to climacteric ripening and in which high amounts of lipids accumulate (Tranbarger et al., 2011).

Oil palm is used in big volume in the food industry for which the lipids and fats of mesocarp and kernel are major components of soaps, emulsifiers and pharmaceuticals. The kernel residues after oil extractions are still available to use as animal feed (Hartley, 1967). In addition, potential use of palm oil as a biofuel has also been developed. One problem for the oil palm business and oil palm growers is the difficulty to plan regular harvests due to non-synchronized fruit shedding which results in a harvest and logistics that increases overall production costs because nowadays, the only way to know the best time for harvesting is waiting until fruits drop to the floor and the labor will start to harvest. Normally labor will harvest the fruit at the nearly mature around at 180DAP, at this stage the fruit is ripening and accumulate amount of oil (Figure 5). If we can understand the process of abscission process in oil palm by biochemical and molecular approaches, we will able to provide tools and information to address the problem of non-synchronized fruit shedding.

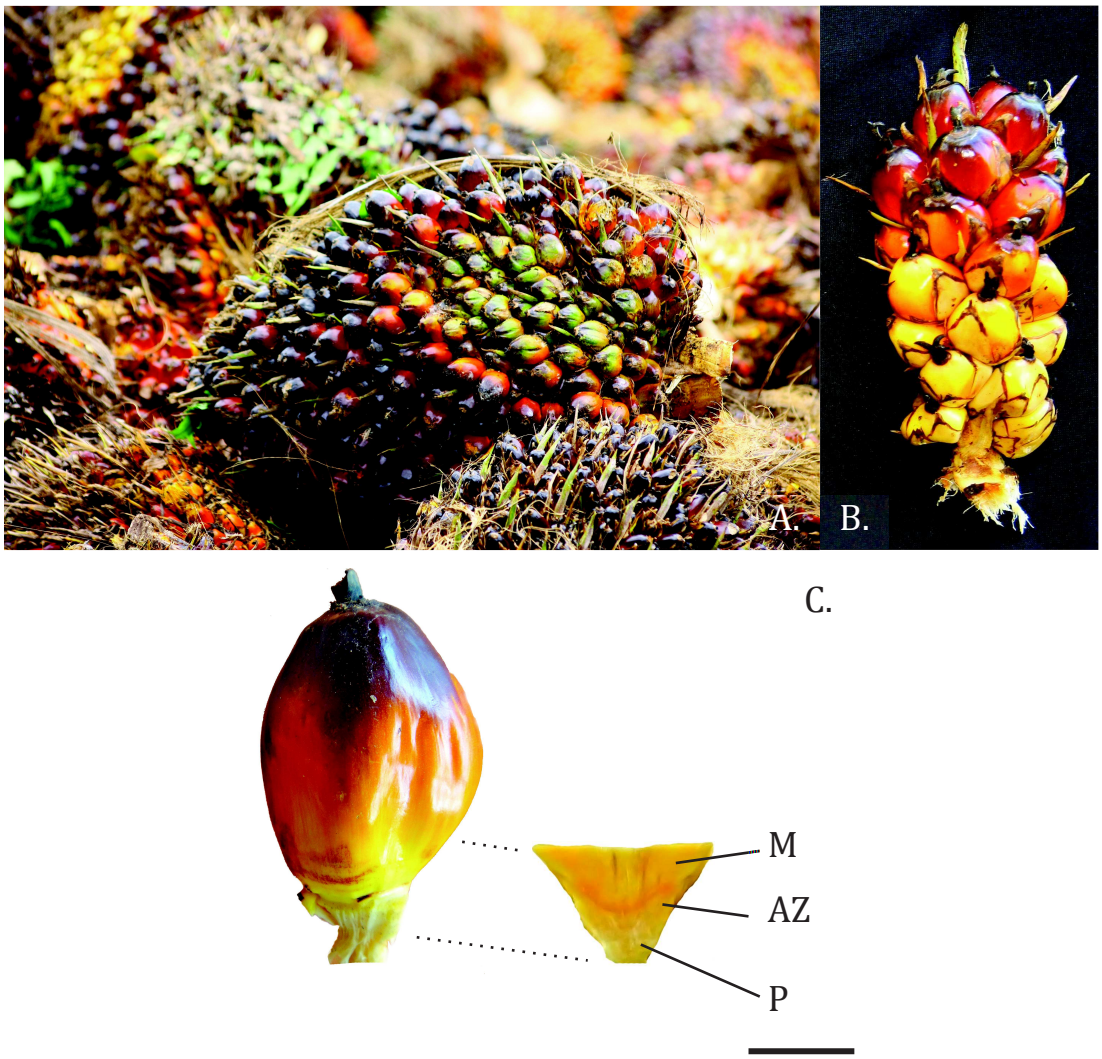

Figure 4 A. Oil palm (*E. guineensis*) fruit bunch.
B. Oil palm spikelet with fruits.
C. Oil palm fruit, base of mature oil palm (180 DAP) with primary AZ visible between pedicel (P) and mesocarp (M) tissues (bar, 1 cm.).

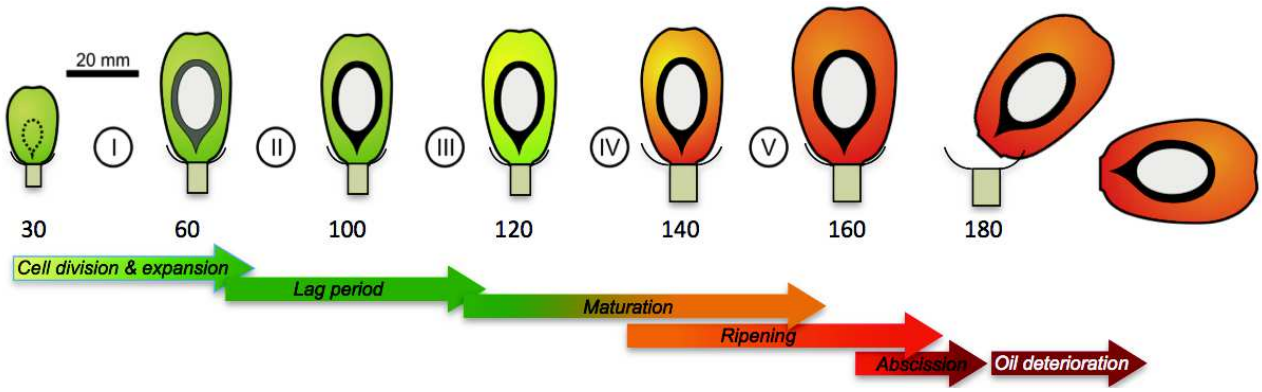

Figure 5 Development of the mature fruit in oil palm (*E. guineensis*) from immature fruit at 30DAP to mature fruit at 180DAP. Number on the bottom indicates the days after pollination (Tranbarger et al., 2011)

From previous studies (Henderson et al., 2001), the AZ and abscission process in oil palm was found to have a lot of interesting features. Firstly, shedding of the oil palm fruit takes place in two synchronized stages. The first, cell separation event is at a predefined AZ at the base of the fruit (primary AZ) and followed by further cell separation in peripheral tissues (adjacent AZs) at the junction with the rudimentary androecial ring and the tepals. The position of the second separation is determined by the age and ripeness of the fruit and the degree of pressure to which it is subjected; it is also dependent upon completion of the first stage (Henderson and Osborne, 1990). In the field, it is common that fruit shed at positions 1 and 2 (Figure 6) and is the reason most of the fruit are shed completely without the rudimentary androecium (Henderson and Osborne, 1990). Evidence also showed that the abscission cells separate at the middle lamellae while the primary walls remain intact with regions of plasmodesmatal connection being last to separate. In addition, while the vascular strands between the fruit base and the pedicel are continuous across the whole abscission region, they are much less lignified. In addition, AZ cells have specific characteristics including high levels of unmethylated pectin in the wall and a high level of inducible PG enzyme expression. Indeed, polygalacturonae activity in extracts of freshly abscinded abscission zone of ripe fruit show increase of at least 35 folds compared with the value for intact abscission zone or for the mesocarp and pedicel tissues above or below the shedding position (Henderson et al., 2001). Recent studies found that one PG transcript (*EgPG4*) in oil palm increases 700-5000 fold during the ethylene treatment time course with the confirmation by *in situ* hybridization indicating a preferential increase in the AZ cell layers in the base of the fruit in response to ethylene prior to cell separation (Roongsattham et al., 2012). Compared to the adjacent mesocarp and pedicel tissues, the *EgPG4* transcript undergoes a dramatic increase in abundance preferentially in the AZ that correlates with the onset of separation observed by 9 h of ethylene treatment. Ethylene or its precursor 1-aminocyclopropane-l-carboxylic acid (ACC) initiates while auxin inhibits cell separation in the primary AZ of the oil palm fruit, this suggests both of these hormones function to regulate abscission in oil palm as during the abscission processes with other species (Henderson and Osborne, 1994). Ethylene production is initiated at the ripe fruit stage and the progression of synthesis starts from the apex to base of the mesocarp in a positive correlation to the percentage of separation that occurs in the primary AZ. While the primary AZ, tepals and rudimentary androecium also increase in ethylene production during ripening, the amount is low which suggests the main source of ethylene production is in the mesocarp cells (Henderson and Osborne, 1994). From many previous studies, PGs not only play an important role in Arabidopsis and tomato, but also play an important role in oil palm too, and suggests some conservation of function between these distantly related species.

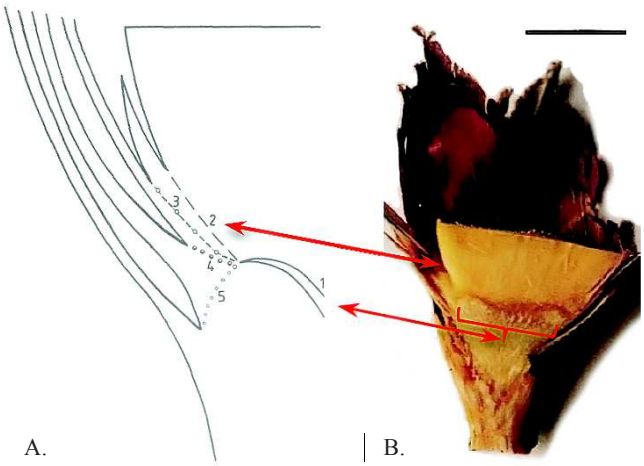

Figure 6 Positions where cell separation events can occur, especially in position 1 and 2 (arrow) in ripe fruit (adapted from Henderson and Osborne, 1990)

The anatomy of abscission of the oil palm differs from other commercial fruits. Instead of a synchronous series of cell separations across a plane of cells between the fruit and the stalk, resulting in immediate shedding of the fruit above, oil palm undergoes abscission in two distinct stages with a time lag of 1-2 days between the two (Osborne et al., 1992). From a recent study, it was found that pectin not only accumulates in the cell wall but also found high accumulation in the AZ cells during development, which is lost from the cells after separation, suggesting a possible relation to the capacity for AZ function (Roongsattham, 2011). Ultrastructural analysis also indicates a polarized vesicle accumulation at the tip of AZ cells occurs during development, and in immunohistological analysis indicated an increase in the JIM5 epitope in the AZ layers during ethylene treatments prior to separation is observed, followed by a polarized increase in both JIM5 and JIM7 on the separated cell surfaces. JIM5 and JIM7 are monoclonal antibodies, which detect epitopes of different degrees of pectin methyl-esterification. While it appears that oil palm fruit shedding has common and different process compared to model species, the process of oil palm fruit development and shedding in the AZ are not full understood and merit further examination.

Molecular approaches to identify genes involved in oil palm ripe fruit abscission

Transcriptome analysis has been a key tool of biological inquiry for decades. Transcriptome is a collection of all the transcripts present in a given cell. It can alter with external environmental conditions because it includes all mRNA transcripts in the cell. Things that we can determined from transcriptome have various benefits such as; the quantification of gene expression or expression profiling (Wang et al., 2010), and insights into the involvement of hormone and signal transduction pathways, enzymatic level changes in the plant cell and can determined when and where genes are

turned on or off in various types of cell and tissue. Gene expression is an important phenotype that informs about genetic and environmental effects on cellular status (Montgomery et al., 2010). For example, in a study of the maize leaf transcriptome, the aim was to understand the profiles of gene expression along the development gradient and define their relationship to differentiation of C4 photosynthesis (Emrich et al., 2007). Microarrays are an important tool to study variation for gene expression. However, microarray studies are limited by the number of genes included on the array to survey (Wang et al., 2010). A revolutionary way to study the transcriptome is based on Next Generation Sequencing (NGS), including 454 pyrosequencing (Roche) and Illumina, which are capable of generating hundreds of thousands or tens of millions of short DNA sequence reads at a relative low cost (Thudi et al., 2012). Pyrosequencing provides very deep coverage of the transcriptome data (Weber et al., 2007), and have been used to study the transcriptome of plants with no genome sequences including oil palm (Bourgis et al., 2011; Tranbarger et al., 2011). These techniques can serve as a very important resource for gene candidate studies to identify genes expressed specifically in plant tissues during physiological and developmental processes such as organ abscission.

The current project has the objective to determine the regulatory and molecular components underlying oil palm fruit shedding of the monocot species oil palm through transcriptome analysis. The strategy involves a detailed comparison with those of dicot model systems such as Arabidopsis and tomato, by using the advantage from next-generation sequencing 454 sequencing technology. Validation and expanded gene expression analysis of selected gene candidates will be done via qPCR in order to identify targets that could be used in molecular breeding strategies in oil palm improvement programs.

The integration of proteomics with other data, ranging from genomics to phenomics, will not only provide a comprehensive overview but also as a cross-validation of the results obtained; this being a necessary step not only to strengthen the interpretation of the data but also to increase the biological meaning of the proteomics-based studies (Jorrín‐Novo et al., 2015). A proteome analysis involves the measurement of changes in the proteome that occur during development and in response to changing physiological conditions. This can include analysis of the quantitative changes in protein expression in addition to changes in posttranslational modifications. From many experiments we know that proteins are the most complex and complicated biomolecules to work with due to their chemical complexity, variability, diversity and dynamic range. In the case of sequenced organisms proteomics allows us to identify gene products, but for non-sequenced organisms, this remains one of the challenges of the field (Champagne and Boutry, 2013). Ideally, proteome analysis is done with

species with sequenced genomes for annotation and gene discover, which is the case for oil palm (Singh et al., 2013). Overall, the application of both transcriptome and proteome approaches will provide a large-scale genome wide database that will be advantageous towards understanding the oil palm abscission process.

Objectives of Thesis

The present study has the objective of determining the regulatory components and molecular mechanisms underlying oil palm fruit shedding are as follows:

1. Transcriptome analysis complemented by proteome analysis to provide insight into the genes and process that underlies oil palm ripe fruit abscission.

2. Compare and contrast data obtained with that from model and other crop species to provide insight into the conservation or divergence of the molecular basis of organ abscission.

3. Examine the variability of the ripe fruit abscission process within the genetic diversity of oil palm available; search for non-shedding oil palm material.

4. Provide a robust list of gene candidates and processes involved in oil palm ripe fruit abscission.

REFERENCES

Adam H, Jouannic S, Escoute J, Duval Y, Verdeil JL, Tregear JW (2005) Reproductive developmental complexity in the African oil palm (Elaeis guineensis, Arecaceae). American Journal of Botany **92:** 1836-1852

Addicott FT (1982) Abscission. University of California Press, Berkeley and Los Angeles, California

Asif MH, Nath P (2005) Expression of multiple forms of polygalacturonase gene during ripening in banana fruit. Plant Physiology and Biochemistry **43:** 177-184

Bar-Dror T, Dermastia M, Kladnik A, Žnidarič MT, Novak MP, Meir S, Burd S, Philosoph-Hadas S, Ori N, Sonego L (2011) Programmed cell death occurs asymmetrically during abscission in tomato. The Plant Cell **23:** 4146-4163

Belfield EJ, Ruperti B, Roberts JA, McQueen-Mason S (2005) Changes in expansin activity and gene expression during ethylene-promoted leaflet abscission in Sambucus nigra. Journal of Experimental Botany **56:** 817-823

Berger RK, Reid PD (1979) Role of polygalacturonase in bean leaf abscission. Plant physiology **63:** 1133-1137

Binder BM, Mortimore LA, Stepanova AN, Ecker JR, Bleecker AB (2004) Short-term growth responses to ethylene in arabidopsis seedlings are EIN3/EIL1 independent. Plant Physiology **136:** 2921-2927

Bleecker AB, Patterson SE (1997) Last exit: senescence, abscission, and meristem arrest in Arabidopsis. The Plant cell **9:** 1169-1179

Bonghi C, Rascio N, Ramina A, Casadoro G (1992) Cellulase and Polygalacturonase Involvement in the Abscission of Leaf and Fruit Explants of Peach. Plant Molecular Biology **20:** 839-848

Bourgis F, Kilaru A, Cao X, Ngando-Ebongue GF, Drira N, Ohlrogge JB, Arondel V (2011) Comparative transcriptome and metabolite analysis of oil palm and date palm mesocarp that differ dramatically in carbon partitioning. Proceedings of the National Academy of Sciences of the United States of America **108:** 12527-12532

Brown KM (1997) Ethylene and abscission. Physiologia Plantarum **100:** 567-576

Brummell DA, Hall BD, Bennett AB (1999) Antisense suppression of tomato endo-1,4-beta-glucanase Cel2 mRNA accumulation increases the force required to break fruit abscission zones but does not affect fruit softening. Plant Molecular Biology **40:** 615-622

Burr CA, Leslie ME, Orlowski SK, Chen I, Wright CE, Daniels MJ, Liljegren SJ (2011) CAST AWAY, a membrane-associated receptor-like kinase, inhibits organ abscission in Arabidopsis. Plant Physiol **156:** 1837-1850

Butenko MA, Patterson SE, Grini PE, Stenvik GE, Amundsen SS, Mandal A, Aalen RB (2003) Inflorescence deficient in abscission controls floral organ abscission in Arabidopsis and identifies a novel family of putative ligands in plants. Plant Cell **15:** 2296-2307

Cai S, Lashbrook CC (2008) Stamen abscission zone transcriptome profiling reveals new candidates for abscission control: enhanced retention of floral organs in transgenic plants overexpressing Arabidopsis ZINC FINGER PROTEIN2. Plant Physiology **146:** 1305-1321

Carpita N (2000) The cell wall. Biochemistry and molecular biology of plants**:** 52-108

Champagne A, Boutry M (2013) Proteomics of nonmodel plant species. Proteomics **13:** 663-673

Chang C, Kwok SF, Bleecker AB, Meyerowitz EM (1993) Arabidopsis Ethylene-Response Gene Etr1 - Similarity of Product to 2-Component Regulators. Science **262:** 539-544

Cho H-T, Cosgrove DJ (2000) Altered expression of expansin modulates leaf growth and pedicel abscission in Arabidopsis thaliana. Proceedings of the National Academy of Sciences **97:** 9783-9788

Cho SK, Larue CT, Chevalier D, Wang H, Jinn T-L, Zhang S, Walker JC (2008) Regulation of floral organ abscission in Arabidopsis thaliana. Proceedings of the National Academy of Sciences **105:** 15629-15634

Cho SK, Larue CT, Chevalier D, Wang HC, Jinn TL, Zhang SQ, Walker JC (2008) Regulation of floral organ abscission in Arabidopsis thaliana. Proceedings of the National Academy of Sciences of the United States of America **105:** 15629-15634

Cosgrove DJ (1997) Assembly and enlargement of the primary cell wall in plants. Annual review of cell and developmental biology **13:** 171-201

Cosgrove DJ (1998) Cell wall loosening by expansins. Plant Physiology **118:** 333-339

Coupe SA, Taylor JE, Roberts JA (1995) Characterisation of an mRNA encoding a metallothionein-like protein that accumulates during ethylene-promoted abscission of Sambucus nigra L. leaflets. Planta **197:** 442-447

Deikman J (1997) Molecular mechanisms of ethylene regulation of gene transcription. Physiologia Plantarum **100:** 561-566

delCampillo E, Bennett AB (1996) Pedicel breakstrength and cellulase gene expression during tomato flower abscission. Plant Physiology **111:** 813-820

Ellis CM, Nagpal P, Young JC, Hagen G, Guilfoyle TJ, Reed JW (2005) AUXIN RESPONSE FACTOR1 and AUXIN RESPONSE FACTOR2 regulate senescence and floral organ abscission in Arabidopsis thaliana. Development **132:** 4563-4574

Emrich SJ, Barbazuk WB, Li L, Schnable PS (2007) Gene discovery and annotation using LCM-454 transcriptome sequencing. Genome Res **17:** 69-73

Estornell LH, Agusti J, Merelo P, Talon M, Tadeo FR (2013) Elucidating mechanisms underlying organ abscission. Plant Sci **199-200:** 48-60

Estornell LH, Agustí J, Merelo P, Talón M, Tadeo FR (2013) Elucidating mechanisms underlying organ abscission. Plant Science **199-200:** 48-60

Fangel JU, Ulvskov P, Knox JP, Mikkelsen MD, Harholt J, Popper ZA, Willats WGT (2012) Cell wall evolution and diversity. Frontiers in plant science **3:** 152

Fernandez DE, Heck GR, Perry SE, Patterson SE, Bleecker AB, Fang SC (2000) The embryo MADS domain factor AGL15 acts postembryonically: Inhibition of perianth senescence and abscission via constitutive expression. Plant Cell **12:** 183-197

Gonzalez-Carranza ZH, Rompa U, Peters JL, Bhatt AM, Wagstaff C, Stead AD, Roberts JA (2007) HAWAIIAN SKIRT: An F-box Gene that Regulates Organ Fusion and Growth in Arabidopsis. Plant Physiol

Gonzalez-Carranza ZH, Whitelaw CA, Swarup R, Roberts JA (2002) Temporal and spatial expression of a polygalacturonase during leaf and flower abscission in oilseed rape and Arabidopsis. Plant Physiology **128:** 534-543

Hadfield KA, Bennett AB (1998) Polygalacturonases: Many genes in search of a function. Plant Physiology **117:** 337-343

Hartley CWS (1967) The oil palm. The oil palm.

Henderson J, Davies HA, Heyes SJ, Osborne DJ (2001) The study of a monocotyledon abscission zone using microscopic, chemical, enzymatic and solid state C-13 CP/MAS NMR analyses. Phytochemistry **56:** 131-139

Henderson J, Lyne L, Osborne DJ (2001) Failed expression of an endo-beta-1,4-glucanhydrolase (cellulase) in a non-abscinding mutant of Lupinus angustifolius cv Danja. Phytochemistry **58:** 1025-1034

Henderson J, Osborne DJ (1990) Cell Separation and Anatomy of Abscission in the Oil Palm, Elaeis guineensis Jacq. Journal of Experimental Botany **41:** 203-210

Henderson J, Osborne DJ (1994) Intertissue Signaling during the 2-Phase Abscission in Oil Palm Fruit. Journal of Experimental Botany **45:** 943-951

Hepworth SR, Zhang YL, McKim S, Li X, Haughn G (2005) BLADE-ON-PETIOLE-dependent signaling controls leaf and floral patterning in Arabidopsis. Plant Cell **17:** 1434-1448

Jinn T-L, Stone JM, Walker JC (2000) HAESA, an Arabidopsis leucine-rich repeat receptor kinase, controls floral organ abscission. Genes & Development **14:** 108-117

Jinn TL, Stone JM, Walker JC (2000) HAESA, an Arabidopsis leucine-rich repeat receptor kinase, controls floral organ abscission. Genes & Development **14:** 108-117

Jorrín‐Novo JV, Pascual J, Sánchez‐Lucas R, Romero‐Rodríguez MC, Rodríguez‐Ortega MJ, Lenz C, Valledor L (2015) Fourteen years of plant proteomics reflected in Proteomics: Moving from model species and 2DE‐based approaches to orphan species and gel‐free platforms. Proteomics **15:** 1089-1112

Kalaitzis P, Solomos T, Tucker ML (1997) Three different polygalacturonases are expressed in tomato leaf and flower abscission, each with a different temporal expression pattern. Plant Physiology **113:** 1303-1308

Kalaitzis P, Solomos T, Tucker ML (1997) Three different polygalacturonases are expressed in tomato leaf and flower abscission, each with a different temporal expression pattern. Plant Physiology **114:** 1314-1314

Kandasamy MK, Deal RB, McKinney EC, Meagher RB (2005) Silencing the nuclear actin‐related protein AtARP4 in Arabidopsis has multiple effects on plant development, including early flowering and delayed floral senescence. The Plant Journal **41:** 845-858

Kandasamy MK, McKinney EC, Deal RB, Meagher RB (2005) Arabidopsis ARP7 is an essential actin-related protein required for normal embryogenesis, plant architecture, and floral organ abscission. Plant physiology **138:** 2019-2032

Khan M, Xu H, Hepworth SR (2014) BLADE-ON-PETIOLE genes: setting boundaries in development and defense. Plant Sci **215-216:** 157-171

Lamotte CE, Gochnauer C, Lamotte LR, Mathur JR, Davies LL (1969) Pectin esterase in relation to leaf abscission in Coleus and Phaseolus. Plant physiology **44:** 21-26

Lanahan MB, Yen HC, Giovannoni JJ, Klee HJ (1994) The Never Ripe Mutation Blocks Ethylene Perception in Tomato. Plant Cell **6:** 521-530

Lashbrook CC, Giovannoni JJ, Hall BD, Fischer RL, Bennett AB (1998) Transgenic analysis of tomato endo-beta-1,4-glucanase gene function. Role of cel1 in floral abscission. Plant Journal **13:** 303-310

Lashbrook CC, Gonzalez-Bosch C, Bennett AB (1994) Two divergent endo-beta-1,4-glucanase genes exhibit overlapping expression in ripening fruit and abscising flowers. The Plant cell **6:** 1485-1493

Lashbrook CC, Gonzalez-Bosch C, Bennett AB (1994) Two Divergent Endo-ß-1,4-glucanase Genes Exhibit Overlapping Expression in Ripening Fruit and Abscising Flowers. The Plant Cell **6:** 1485-1493

Lease KA, Wen JQ, Li J, Doke JT, Liscum E, Walker JC (2001) A mutant Arabidopsis heterotrimeric G-protein beta subunit affects leaf, flower, and fruit development. Plant Cell **13:** 2631-2641

Leslie ME, Lewis MW, Liljegren SJ (2007) Organ Abscission. *In* JA Roberts, Z Gonzalez-Carranza, eds, Plant Cell Separation and Adhesion. Blackwell Publishing, Oxford, UK

Li DP, Xu YF, Sun LP, Liu LX, Hu XL, Li DQ, Shu HR (2006) Salicylic acid, ethephon, and methyl jasmonate enhance ester regeneration in 1-MCP-treated apple fruit after long-term cold storage. J Agric Food Chem **54:** 3887-3895

Liljegren SJ (2012) Organ abscission: exit strategies require signals and moving traffic. Curr Opin Plant Biol **15:** 670-676

Liljegren SJ, Ditta GS, Eshed Y, Savidge B, Bowman JL, Yanofsky MF (2000) SHATTERPROOF MADS-box genes control seed dispersal in Arabidopsis. Nature **404:** 766-770

Liljegren SJ, Leslie ME, Darnielle L, Lewis MW, Taylor SM, Luo R, Geldner N, Chory J, Randazzo PA, Yanofsky MF, Ecker JR (2009) Regulation of membrane trafficking and organ separation by the NEVERSHED ARF-GAP protein. Development **136:** 1909-1918

Liljegren SJ, Leslie ME, Darnielle L, Lewis MW, Taylor SM, Luo RB, Geldner N, Chory J, Randazzo PA, Yanofsky MF, Ecker JR (2009) Regulation of membrane trafficking and organ separation by the NEVERSHED ARF-GAP protein. Development **136:** 1909-1918

Mao L, Begum D, Chuang HW, Budiman MA, Szymkowiak EJ, Irish EE, Wing RA (2000) JOINTLESS is a MADS-box gene controlling tomato flower abscission zone development. Nature **406:** 910-913

McKim SM, Stenvik GE, Butenko MA, Kristiansen W, Cho SK, Hepworth SR, Aalen RB, Haughn GW (2008) The BLADE-ON-PETIOLE genes are essential for abscission zone formation in Arabidopsis. Development **135:** 1537-1546

Meir S, Hunter DA, Chen JC, Halaly V, Reid MS (2006) Molecular changes occurring during acquisition of abscission competence following auxin depletion in Mirabilis jalapa. Plant Physiology **141:** 1604-1616

Meir S, Hunter DA, Chen JC, Halaly V, Reid MS (2006) Molecular changes occurring during acquisition of abscission competence following auxin depletion in Mirabilis jalapa. Plant Physiol **141:** 1604-1616

Montgomery SB, Sammeth M, Gutierrez-Arcelus M, Lach RP, Ingle C, Nisbett J, Guigo R, Dermitzakis ET (2010) Transcriptome genetics using second generation sequencing in a Caucasian population. Nature **464:** 773-777

Murphy DJ (2009) Oil palm: future prospects for yield and quality improvements. Lipid Technology **21:** 257-260

Norberg M, Holmlund M, Nilsson O (2005) The BLADE ON PETIOLE genes act redundantly to control the growth and development of lateral organs. Development **132:** 2203-2213

Ogawa M, Kay P, Wilson S, Swain SM (2009) ARABIDOPSIS DEHISCENCE ZONE POLYGALACTURONASE1 (ADPG1), ADPG2, and QUARTET2 are Polygalacturonases required for cell separation during reproductive development in Arabidopsis. Plant Cell **21:** 216-233

Osborne DJ (1958) Growth of Etiolated Sections of Pea Internode Following Exposures to Indole-3-Acetic Acid, 2,4-Dichlorophenoxyacetic Acid and 2,5-Dichlorobenzoic Acid. Plant Physiol **33:** 46-57

Osborne DJ, Henderson J, Corley RHV (1992) Controlling Fruit Shedding in the Oil Palm. Endeavour **16:** 173-177

Patterson S, Butenko M, Kim J (2007) Ethylene responses in abscission and other processes of cell separation in Arabidopsis. *In* Advances in Plant Ethylene Research. Springer, pp 271-278

Patterson SE (2001) Cutting loose. Abscission and dehiscence in Arabidopsis. Plant Physiology **126:** 494-500

Patterson SE, Bleecker AB (2004) Ethylene-dependent and -independent processes associated with floral organ abscission in Arabidopsis. Plant Physiology **134:** 194-203

Popper ZA, Michel G, Hervé C, Domozych DS, Willats WG, Tuohy MG, Kloareg B, Stengel DB (2011) Evolution and diversity of plant cell walls: from algae to flowering plants. Annual review of plant biology **62:** 567-590

Rick CM (1956) Genetic and Systematic Studies on Accessions of Lycospersicon from the Galapagos Islands. American Journal of Botany **43:** 687-696

Rival A (2007) Oil Palm, Vol 61. Springer-Verlag, Berlin Heidelberg

Roberts JA (2000) Abscission and dehiscence. Symp Soc Exp Biol **52:** 203-211

Roberts JA, Elliott KA, Gonzalez-Carranza ZH (2002) Abscission,dehiscence, and other cell separation processes. Annual Review of Plant Biology **53:** 131-158

Roberts JA, Gonzalez-Carranza Z (2007) Cell Separation and Adhesion Processes in Plants *In* JA Roberts, Z Gonzalez-Carranza, eds, Plant Cell Separation and Adhesion, Annual Plant Reviews. Blackwell Publishing Ltd, pp 1-7

Roberts JA, Whitelaw CA, Gonzalez-Carranza ZH, McManus MT (2000) Cell separation processes in plants - Models, mechanisms and manipulation. Annals of Botany **86:** 223-235

Roongsattham P (2011) Cell separation processes that underlie fruit abscission and shedding in oil palm (Elaeis guineensis Jacq.). UNIVERSITÉ MONTPELLIER 2, Montpellier, France

Roongsattham P, Morcillo F, Jantasuriyarat C, Pizot M, Moussu S, Jayaweera D, Collin M, Gonzalez-Carranza Z, Amblard P, Tregear JW, Tragoonrung S, Verdeil JL, Tranbarger TJ (2012) Temporal and spatial expression of polygalacturonase gene family members reveals divergent regulation during fleshy fruit ripening and abscission in the monocot species oil palm. BMC Plant Biology **12:** 150

Sawicki M, Barka EA, Clément C, Vaillant-Gaveau N, Jacquard C (2015) Cross-talk between environmental stresses and plant metabolism during reproductive organ abscission. Journal of experimental botany **66:** 1707-1719

Schumacher K, Schmitt T, Rossberg M, Schmitz G, Theres K (1999) The Lateral suppressor (Ls) gene of tomato encodes a new member of the VHIID protein family. Proc Natl Acad Sci U S A **96:** 290-295

Sexton R, Roberts JA (1982) Cell Biology of Abscission. Annual Review of Plant Physiology **33:** 133-162

Shiu S-H, Bleecker AB (2001) Receptor-like kinases from Arabidopsis form a monophyletic gene family related to animal receptor kinases. Proceedings of the National Academy of Sciences **98:** 10763-10768

Singh R, Ong-Abdullah M, Low ETL, Manaf MAA, Rosli R, Nookiah R, Ooi LCL, Ooi SE, Chan KL, Halim MA, Azizi N, Nagappan J, Bacher B, Lakey N, Smith SW, He D, Hogan M, Budiman MA, Lee EK, DeSalle R, Kudrna D, Goicoechea JL, Wing RA, Wilson RK, Fulton RS, Ordway JM, Martienssen RA, Sambanthamurthi R (2013) Oil palm genome sequence reveals divergence of interfertile species in Old and New Worlds. Nature **500:** 335-339

Soto A, Ruiz KB, Ravaglia D, Costa G, Torrigiani P (2013) ABA may promote or delay peach fruit ripening through modulation of ripening-and hormone-related gene expression depending on the developmental stage. Plant Physiology and Biochemistry **64:** 11-24

Stenvik G-E, Tandstad NM, Guo Y, Shi C-L, Kristiansen W, Holmgren A, Clark SE, Aalen RB, Butenko MA (2008) The EPIP peptide of INFLORESCENCE DEFICIENT IN ABSCISSION is sufficient to induce abscission in Arabidopsis through the receptor-like kinases HAESA and HAESA-LIKE2. The Plant Cell **20:** 1805-1817

Stenvik GE, Tandstad NM, Guo Y, Shi CL, Kristiansen W, Holmgren A, Clark SE, Aalen RB, Butenko MA (2008) The EPIP peptide of INFLORESCENCE DEFICIENT IN ABSCISSION is sufficient to induce abscission in Arabidopsis through the receptor-like kinases HAESA and HAESA-LIKE2. Plant Cell **20:** 1805-1817

Suttle JC, Hultstrand JF (1993) Involvement of abscisic acid in ethylene-induced cotyledon abscission in cotton seedlings. Plant physiology **101:** 641-646

Szymkowiak EJ, Irish EE (2006) JOINTLESS suppresses sympodial identity in inflorescence meristems of tomato. Planta **223:** 646-658

Taylor JE, Coupe SA, Picton S, Roberts JA (1994) Characterization and Accumulation Pattern of an Messenger-Rna Encoding an Abscission-Related Beta-1,4-Glucanase from Leaflets of Sambucus-Nigra. Plant Molecular Biology **24:** 961-964

Taylor JE, Tucker GA, Lasslett Y, Smith CJS, Arnold CM, Watson CF, Schuch W, Grierson D, Roberts JA (1991) Polygalacturonase Expression during Leaf Abscission of Normal and Transgenic Tomato Plants. Planta **183:** 133-138

Taylor JE, Webb STJ, Coupe SA, Tucker GA, Roberts JA (1993) Changes in Polygalacturonase Activity and Solubility of Poluronides during Ethylene-Stimulated Leaf Abscission in Sambucus-Nigra. Journal of Experimental Botany **44:** 93-98

Taylor JE, Whitelaw CA (2001) Signals in abscission. New Phytologist **151:** 323-340

Thudi M, Li YP, Jackson SA, May GD, Varshney RK (2012) Current state-of-art of sequencing technologies for plant genomics research. Briefings in Functional Genomics **11:** 3-11

Tieman DM, Ciardi JA, Taylor MG, Klee HJ (2001) Members of the tomato LeEIL (EIN3-like) gene family are functionally redundant and regulate ethylene responses throughout plant development. The Plant journal : for cell and molecular biology **26:** 47-58

Torrigiani P, Bressanin D, Beatriz Ruiz K, Tadiello A, Trainotti L, Bonghi C, Ziosi V, Costa G (2012) Spermidine application to young developing peach fruits leads to a slowing down of ripening by impairing ripening-related ethylene and auxin metabolism and signaling. Physiologia Plantarum **146:** 86-98

Torrigiani P, Bressanin D, Beatriz Ruiz K, Tadiello A, Trainotti L, Bonghi C, Ziosi V, Costa G (2012) Spermidine application to young developing peach fruits leads to a slowing down of ripening by impairing ripening‐related ethylene and auxin metabolism and signaling. Physiologia plantarum **146:** 86-98

Trainotti L, Tadiello A, Casadoro G (2007) The involvement of auxin in the ripening of climacteric fruits comes of age: the hormone plays a role of its own and has an intense interplay with ethylene in ripening peaches. Journal of Experimental Botany **58:** 3299-3308

Tranbarger TJ, Dussert S, Joet T, Argout X, Summo M, Champion A, Cros D, Omore A, Nouy B, Morcillo F (2011) Regulatory mechanisms underlying oil palm fruit mesocarp maturation, ripening, and functional specialization in lipid and carotenoid metabolism. Plant Physiol **156:** 564-584

Tucker ML, Burke A, Murphy CA, Thai VK, Ehrenfried ML (2007) Gene expression profiles for cell wall-modifying proteins associated with soybean cyst nematode infection, petiole abscission, root tips, flowers, apical buds, and leaves. J Exp Bot **58:** 3395-3406

Wang L, Li P, Brutnell TP (2010) Exploring plant transcriptomes using ultra high-throughput sequencing. Briefings in Functional Genomics **9:** 118-128

Wang X, Liu D, Li A, Sun X, Zhang R, Wu L, Liang Y, Mao L (2013) Transcriptome analysis of tomato flower pedicel tissues reveals abscission zone-specific modulation of key meristem activity genes. PLoS One **8:** e55238

Weber AP, Weber KL, Carr K, Wilkerson C, Ohlrogge JB (2007) Sampling the Arabidopsis transcriptome with massively parallel pyrosequencing. Plant physiology **144:** 32-42

Wei P-C, Tan F, Gao X-Q, Zhang X-Q, Wang G-Q, Xu H, Li L-J, Chen J, Wang X-C (2010) Overexpression of AtDOF4. 7, an Arabidopsis DOF family transcription factor, induces floral organ abscission deficiency in Arabidopsis. Plant physiology **153:** 1031-1045

Weng L, Zhao F, Li R, Xu C, Chen K, Xiao H (2015) The Zinc Finger Transcription Factor SlZFP2 Negatively Regulates Abscisic Acid Biosynthesis and Fruit Ripening in Tomato. Plant physiology **167:** 931-949

Whitelaw CA, Lyssenko NN, Chen LW, Zhou DB, Mattoo AK, Tucker ML (2002) Delayed abscission and shorter internodes correlate with a reduction in the ethylene receptor LeETR1 transcript in transgenic tomato. Plant Physiology **128:** 978-987

Wilkinson JQ, Lanahan MB, Yen HC, Giovannoni JJ, Klee HJ (1995) An ethylene-inducible component of signal transduction encoded by never-ripe. Science **270:** 1807-1809

Zahara MB, Scheuerman RW (1988) Hand-harvesting jointless vs. jointed-stem tomatoes. Calif Agric **42:** 14.

Chapter 2

A phenotypic test for delay of abscission and non-abscission oil palm fruit and validation by abscission marker gene expression analysis

This chapter was adapted from a manuscript accepted for publication in Acta Horticulturae, 2015

Authors: K. Fooyontphanich, M. Collin, F. Morcillo, P. Amblard, C. Jantasuriyarat and T.J. Tranbarger

Chapter 2

A phenotypic test for delay of abscission and non-abscission oil palm fruit and validation by abscission marker gene expression analysis

INTRODUCTION

There are two species in the genus *Elaeis*, including *E. guineensis* and *E. oleifera* which are interfetile. *E. guineensis* is known as the African oil palm. The world-wide cultivated crop is the African oil palm naturally abundant in all the African rain forests (Barcelos et al., 2015) (Barcelos et al., 2015). The description, biology and agronomic importance of the oil palm is well documented (Corley and Tinker, 2003). It is a large pinnate-leaved palm having a solitary columnar stem with short internodes. Development of the leaf is initially very slow and there are some 40–60 leaves within the apical bud. The number of leaves produced annually by a plantation palm increases to between 30 and 40 at 2–4 years of age. The fruit is a sessile drupe and grows in large bunches and matures in 5–6 months after pollination. Oil palm accessions show great variation in fruit shape and size from nearly spherical to ovoid or elongated and bulging on the top. Fruit color in the external appearance the normal fruit varies considerably, particularly when ripening. The most common type of fruit is deep violet to black at the apex and pale greenish yellow at the base before ripening (Figure 2A). The pericarp of the oil palm fruit is subdivided into the outer layer exocarp, fleshy mesocarp, and endocarp that in oil palm, is called the shell. The shell encases the seed or kernel, i.e., embryo and endosperm. The crude palm oil (80% of dry mass (DM)) and palm kernel oil (50% of DM) are extracted from mesocarp and kernel, respectively making this crop unique in that it produces two oils of major economic importance. Using the presence or absence of endocarp (shell) fruits are separated into three types, *dura*, *pisifera* and *tenera*. The *dura* type produces thick-shelled fruit with little pulp and is generally used as female parents for breeding. The *pisifera* type rarely bears fruits and does not generally contain kernels or only kernels without shells (Mezui et al., 2013). The *tenera* type, a hybrid of *dura* (female) and *pisifera* (male) produces fruits with thick pulp and thin shells. Thus, *tenera* type is widely grown in commercial plantations due to its high oil yield from the fruit mesocarp tissue (Muniran et al., 2008). Analysis of the species natural genetic diversity suggests that wild populations could be separated into three groups located at the extreme west of Africa, equatorial Africa and on Madagascar Island. The highest allelic diversity was found among Nigerian palm populations, indicating the possible center of origin (Bakoumé et al., 2015).

E. oleifera or the American oil palm occurs naturally in the tropical countries of South and Central America and has been described or collected from Brazil, Colombia, Venezuela, Panama,

Costa Rica, Nicaragua, Honduras, French Guiana and Surinam. Many of *E. oleifera* populations are found on Amazonian Dark Earths, Terra Preta de Índio in Portuguese. A feature of the palm that distinguishes it from *E. guineensis* is its much shorter growth, and often procumbent, trunk. The leaf of *E. oleifera* also readily distinguishes it from *E. guineensis*. All of the leaflets lie in one plane and have no basal swellings, the spines on the petiole are short and thick and leaflets are larger than those of *E. guineensis*. The male inflorescence differs little from that of *E. guineensis*. The spikelets are pressed together until they burst through the spathe just before anthesis. The male flower is somewhat smaller with shorter anthers. Fruit:bunch ratios are often low. There is some variation in fruit color. About 90% of palms have orange fruit at maturity, these having developed from immature fruit which were at first yellowish green, then ivory color at the base and orange above (Figure 2B). Like *E.* guineensis, *E. olifera* accumulates oil in the mesocarp but to a lesser extent (15-25% DM) (Montoya et al., 2013). Compared with *E. guineensis* the oil has a higher oleic acid content and iodine value and the carotene content is higher than that of the African palm (Barcelos et al., 2015). American oil palm is a source of many economically valuable traits, of which most important are slow height increment, which simplifies harvest (Corley and Tinker, 2003), higher proportion of desaturated FAs in palm oil (Montoya et al., 2014), lower lipase activity in mature fruit mesocarp, extending a period between harvest and fruit processing (Cadena et al., 2013), higher vitamins A and E contents, improving oil nutritional value (Rajanaidu et al., 2000) and finally the broader environmental adaptability (Barcelos, 1998).

For the interspecific hybrid *E. oleifera* × *E. guineensis*. This interspecific hybrid has emerged as a promising solution to diseases such as the bud rot of oil palm because of the apparent partial resistance of this genotype to the disease (Torres et al., 2010). The color of the fruit is yellow or very light green in the basal part, light green in the middle and dark green at the apex with soft endocarp, liquid endosperm. Between 101 to 105 days after anthesis the fruit color at the base is very light green-yellow, green-yellow in the center and light green at the apex. At the ripening stage the overall external color of the bunch is intense orange. Fruits are medium orange at the base, intense orange in the middle and dark orange at the apex. Fruits start shedding and presence of stretch marks arranged in a circular pattern around the apical part of the fruit.

The commercial plantations consist mostly of the African palm *E. guineensis*. However, producers in Latin America are increasingly planting hybrids (Hormaza et al., 2012).

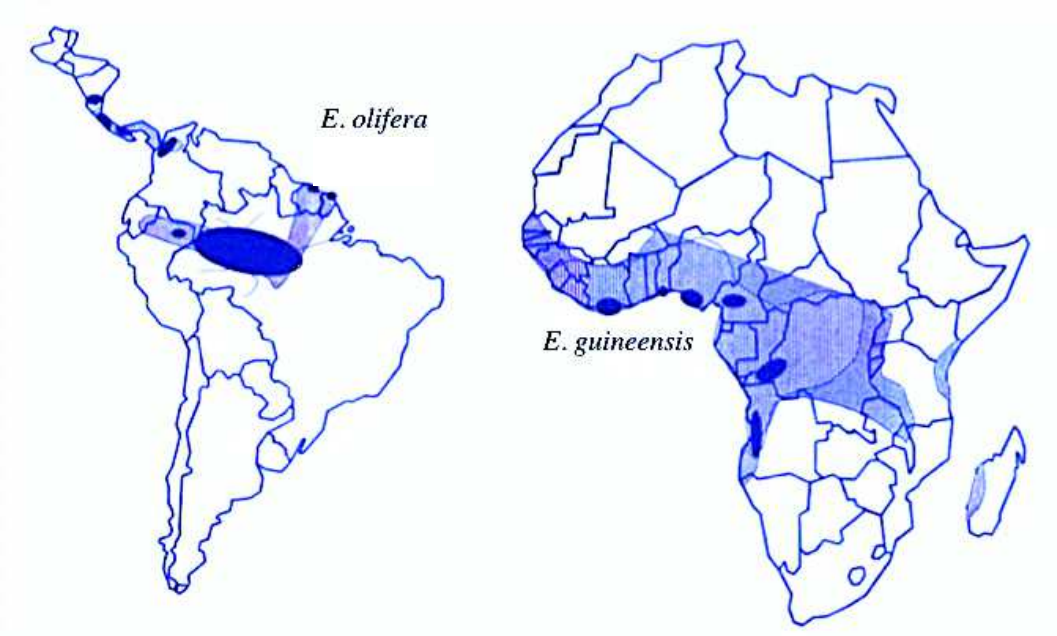

Figure 1. Origin (Blue oval) of the oil palm and the distribution (blue shade) of the species *E. guineensis and E. olifera* (from (Barcelos, 1998)).

Figure 2. Fruit bunch of A. *E. guineensis* from Thailand shows the mature fruit with the black color and the ripe fruit with red color. B. *E. oleifera* from Ecuador show the young fruit with green color and the ripe fruit in orange color.

Commercially, preharvest abscission and abscission of fruit during harvesting and transportation of fruit bunches are problems for the oil palm industry (Osborne et al., 1992). In addition, it is difficult for oil palm growers to schedule regular harvests due to non-synchronized fruit shedding, which results in higher production costs. If genetic material could be identified that does not undergo or is delayed in cell separation and abscission, this non-abscising fruit material

could be a valuable contribution to oil palm breeding programs. The African oil palm *E. guineensis* has a relatively large primary AZ and multiple adjacent AZs that have been previously defined (Henderson and Osborne, 1990; Osborne et al., 1992), while nothing is known about the AZ of the American oil palm species *E. oleifera*. In this study, we tested and compared the fruit abscission process in diverse genetic material from oil palm using a simple *in vitro* phenotypic screen that assesses cell separation that occurs in the AZ at the base of the oil palm fruit.

MATERIALS AND METHODS

Preparation of fruit bases containing the AZ and the *in vitro* abscission phenotypic test

The first analysis included the use of an *in vitro* phenotypic test developed to study the abscission process in both species of oil palm (*E. guineensis* and *E. oleifera)*. This method can be used in the field to quickly screen for plants with altered abscission phenotypes.

Spikelets of ripe fruit, indicated by Days After Pollination (DAP), were removed from the upper middle section of the fruit bunches from different genetic material including *E. guineensis* (African oil palm), *E. oleifera* (American oil palm), interspecific hybrids (*E. guineensis* x *E. oleifera*), and backcrosses (interspecific hybrid x *E. guineensis*). All of the plant materials were collected from Palmeras de los Andes (PDA) and Murrin private company plantations in Ecuador. Spikelets were rinsed in water and then individual fruit that included the base of the fruit (containing the AZ) and a portion of the spikelet stalk were removed. The fruit was then cut away from the base just above the AZ so as to include a small portion of the fruit mesocarp. Tepals were not removed for the phenotypic test analysis. A total of between 15-30 slices of fruit bases were collected from a bunch (from each individual tree) and placed in petri plates on dampened Whatman filter paper, and photographs of each petri plate were taken for a phenotypic record of the plant material examined (Figure 3A). The fruit base with the AZ were then incubated at room temperature for approximately 24 hours, and then pressure was applied with two forceps by twisting the slices to test for separation at both the primary and secondary AZs (Figure 3B). Photographs were again taken after the twist test (Figure 3C).

Sample preparation for histology and microscopy analysis

For histological analysis, the bases of fruit containing the AZ were collected from approximately 50 spikelets that were rinsed in water. The individual fruit containing the base of the fruit with the AZ were removed from spikelets and then the base of the fruit was cut off as described

above. Fruit bases were then cut in half longitudinally and immersed in fixation solution for classic histology (CH), i.e., 0.2 M phosphate buffer containing 2% [w/v] paraformaldehyde, 1% [w/v] caffeine, and 2% [v/v] glutaraldehyde (Buffardmorel et al., 1992). Samples for CH were vacuum infiltrated for 5 minutes/3 times, and then incubated overnight between 16 to 20h. After incubation, the AZ samples were rinsed twice for 15 minutes in 1X PBS + glycine 0.2 M and then rinsed twice again for 15 min in 1X PBS. After rinsing, the samples were dehydrated step-wise in ethanol (EtOH 30%, 50%, 70% for 1 hour) to a final concentration of 70% ethanol. The samples remained in 70% ethanol solution for transport back to France. In France, samples were then rinsed with 70% ethanol and serial dehydrated with ethanol from 70% to 100%, then 50% ethanol/ 50% butanol (v/v), and finally 100% butanol. Samples were then infiltrated with resin, and thin sections prepared with a microtome with the thicknesses of 5 µm for staining with Ruthenium Red and DAPI for comparison to previous samples collected from *E. guineensis*.

Figure 3. A. Slices of fruit bases; B. The pressure test of AZ separation; C. Slices of fruit bases after 24 hours incubation at room temperature when pressure test was performed.

Primer design and qPCR for expression analysis

In a previous study, *EgPG4* displayed an abscission associated gene expression profile that made it an ideal marker for the present study (Roongsattham et al., 2012). In addition, *ACO* expression was previously observed to be associated with ethylene evolution in the mesocarp during fruit ripening, and therefore also selected to examine ethylene production capacity in the collected plant materials (Tranbarger et al., 2011). Primer pairs were designed using Primer3 and Primer3plus and then tested with Amplify (http://engels.genetics.wisc.edu/amplify) for amplified sequence(s) to check primer pair specificity and primer dimer formation. Primers that were used for *EgPG4* amplification were as previously published (Roongsattham et al., 2012), and for *ACO* as follows:

EgACO1QS1: ATCCCAGGTTTGTGTTCGAG
EgACO1QAS1: TCCATCCTGTGATTTGACCA

The first step after primer design was to test for the efficiency of each primer pair to ensure that the Efficiency Values ranged between 1.95 and 2.0. The estimates were derived from a standard curve generated from a serial dilution of pooled cDNA (1, 10, 100, and 1000 fold dilutions). RNA was isolated as previously described (Morcillo et al., 2006). qPCR was conducted on a LightCycler 480 (Roche) in 96 well plates in a volume of 10 µl that included 2 µl of cDNA diluted 1/100, 1.5 µl of forward primer (2 µM), 1.5 µl of reverse primer (2 µM) and 5 µl SYBR® Green Mastermix (Roche). The qPCR process was initiated by denaturation at 95 °C for 10 min, followed by 45 cycles of 95 °C for 15 s, 60 °C for 15 s, and a final extension at 70 °C for 1 min. Expression was then normalized to that of *EgEf1α* (accession number: AY550990), with the primers:

EgEF1-Q-S4: TATCAAAGGATGGGCAGACC
EgEF1-Q-AS4: TCCAAGGCAAGGTATGATGA

For the relative transcript abundance was determined with the formula described previously (Pfaffl, 2001). *EgEf1α* transcript accumulation was relatively constant in all tissues examined. A control using RNA matrices was also conducted to validate the absence of DNA in each sample. Each time point was replicated three times and all amplified cDNA fragments were sequenced by Beckman-Cogenics to verify the amplification products. Each individual sample was comprised of 3-5 biological repetitions that were pooled and submitted to qPCR analysis with three technical

replicates. Gene expression was reported as the mean and standard error bars are calculated from the technical replicates.

RESULTS AND DISCUSSION

The *in vitro* phenotypic test allow the identification of delay and non-shedding material

The phenotypic test was performed with the fruit bases from at total of 47 different oil palm trees of different origins including *E. oleifera* (Taisha, Coari and Manicoré), hybrids (HTT) and backcrosses (MTC) and the results are presented in Figure 4. Firstly, the results provided evidence for the non-shedding or shedding resistant character of *E. oleifera* of Taisha origin (Figure 4, TA37, TA43 and TA60). Of the three individuals that did not undergo any detectable separation during the phenotypic test, two are Taisha (TA37 and TA43). In addition to Taisha, individuals from backcross origin also displayed a low separation in the phenotypic test; in particular, one clone (MTC180) displayed no cell separation. Two other MTC180 samples from the same individual also displayed 70% non-separation in the phenotypic test, which validates the abscission resistant phenotype of this individual. Other backcross clones with high percentage of non-separation (or delayed separation) in the phenotypic test included MTC159, MTC68, MTC153, MTC150, MTC159 and MTC151. Samples for selected clones were collected for histology and RNA analyses to compare the different materials and determine the basis of the non-separating character of the MTC180 material.

qPCR validation of marker genes during natural abscission and their decreased expression in non-shedding material MTC180

After the phenotypic test was performed on the samples, AZ containing samples were tested for expression of the marker genes *EgPG4* and *EgACO* during natural abscission in material including *E. guineensis*, hybrids and backcrosses, and in the non-shedding backcross material MTC180 (Figure 5). Material for RNA extraction from the Taisha material was not obtained and hence qPCR analysis was not done with this material. However, with the material tested, the results revealed that the expression of *EgPG4* is always associated with material undergoing abscission (S) and much lower in material not undergoing abscission (NS). Interestingly, the *EgPG4* transcript was consistently low in the AZ of the not-shedding (ns) MTC180 material (Figure 5). Surprisingly, while ACO expression was not significantly higher in the *E. guineensis* material undergoing abscission compared to NS material, expression was higher in hybrid and backcross material undergoing

abscission. Most importantly, ACO was greatly reduced in the ns MTC180 material suggesting the non-shedding character could be related to reduced ethylene production. Overall, results validate that expression of these two genes are associated with the abscission process and are highly reduced in the non-shedding MTC180 material.

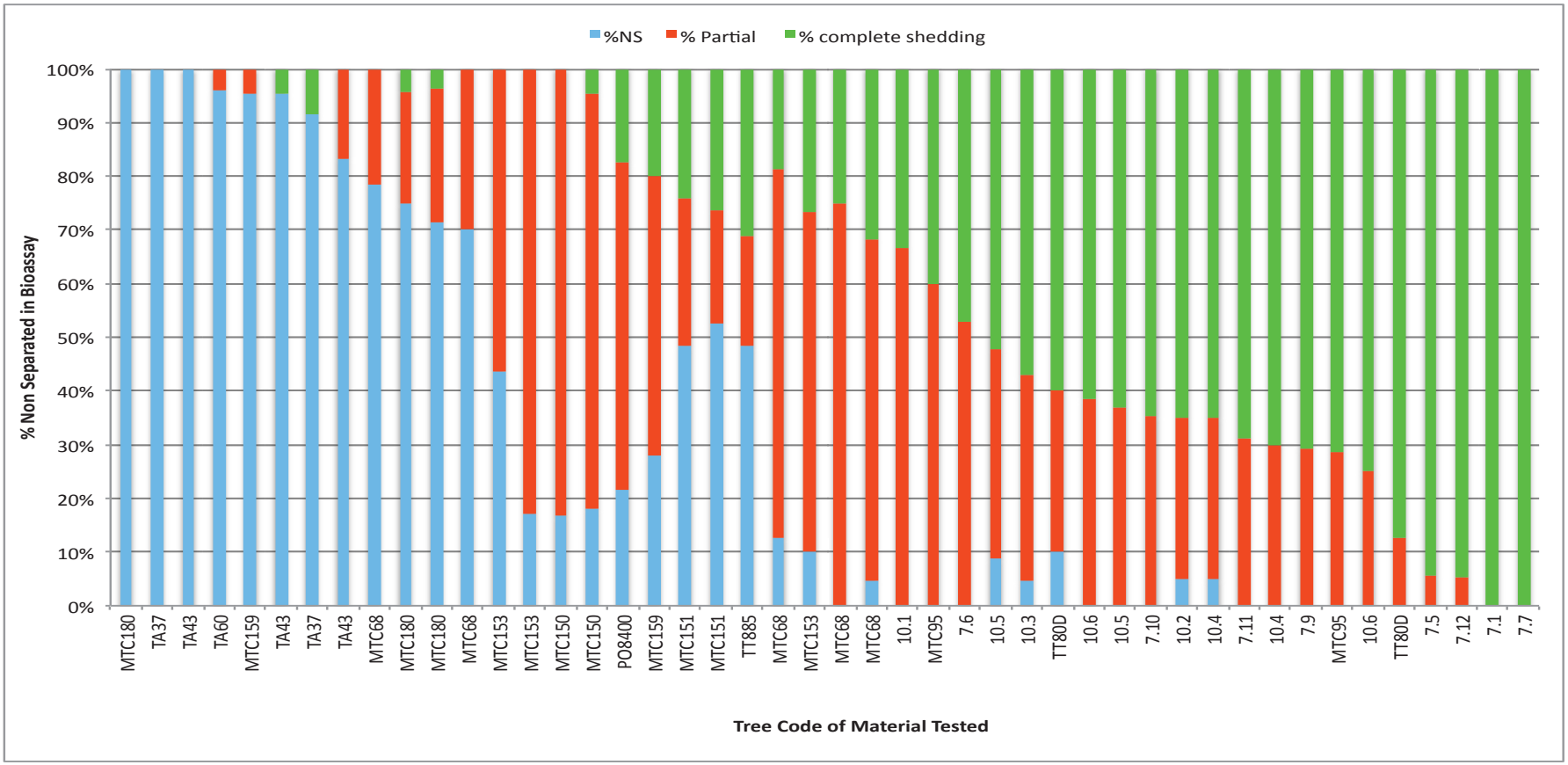

Figure 4. Graph of phenotypic test results. NS, no separation; Partial, separation only in primary AZ; complete shedding, separation in both 1 primary and adjacent AZs; MTC and number, code for backcross clones; TA and number, codes for Taisha (*E. oleifera*); TT and number codes for *E. oleifera* hybrid Coari x Taisha; PO plus number, code for *E. oleifera* hybrid Manicoré x Taisha; number codes from 7.1 to 10.6 are *E. oleifera* x E. guineensis hybrids as follows: 7.1, Mangenot x La Mé; 7.5, Manicoré x La Mé; 7.6, Manicoré (Bacabal) x La Mé; 7.7 Caracarai x La Mé; 7.11, Rio Negro (Caburis) x La Mé; 7.12, Rio Negro (Carvoeiro) x La Mé; 10.1 and 10.2, Coari x La Mé; 10.3, Coari x Yangambi; 10.4 and 10.5, Taisha x La Mé; 10.6, Taisha x Yangambi.

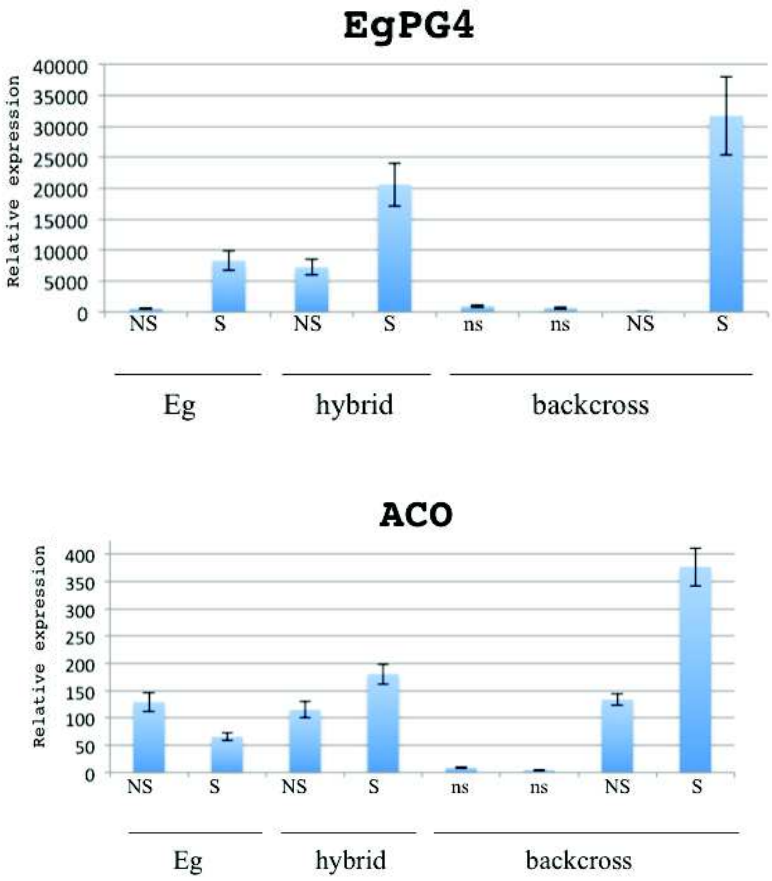

Figure 5. Relative expression profiles of *EgPG4* and *ACO* in the AZ of fruit not undergoing abscission where no fruit was shed (NS), in non-shedding material (ns) and in material undergoing abscission that results in fruit shedding (S). *E. guineensis*, Eg.

Histological analysis reveals differences between the AZ of *E. guineenesis* and *E. oleifera*

Longitudinal sections of the fruit bases of the plant material stained with Ruthenium Red allowed an overview of the structure of the AZ of the diverse oil palm material. The major difference between *E. guineensis* and *E. oleifera* AZs was the reduction in the number of layers that constitute the AZ in *E. oleifera* (Figures 6 and 7). While multiple layers were easily observed in the DAPI stained sections of *E. guineensis*, hybrid and backcross material, very few layers were observed in the *E. oleifera* (Figures 6 and 7). In addition, we also found lignified vascular strands, which pass through the AZ of *E. oleifera* in contrast to that of *E. guineensis* in which the vascular strands are less lignified within the AZ. It also appears that there are more phenolic containing cells in *E. oleifera* than *E. guineensis* (Figure 6). Finally, the transition from mesocarp to pedicel is much more abrupt and the pedicel appears more highly lignified in *E. oleifera* than *E. guineensis* (Figures 6 and 7) These features may be important for the non-shedding character of the *E. oleifera* of Taisha origin. The analysis of the AZ of the non-shedding BC MTC180 is not yet completed but the AZ appears to be normal (data not shown).

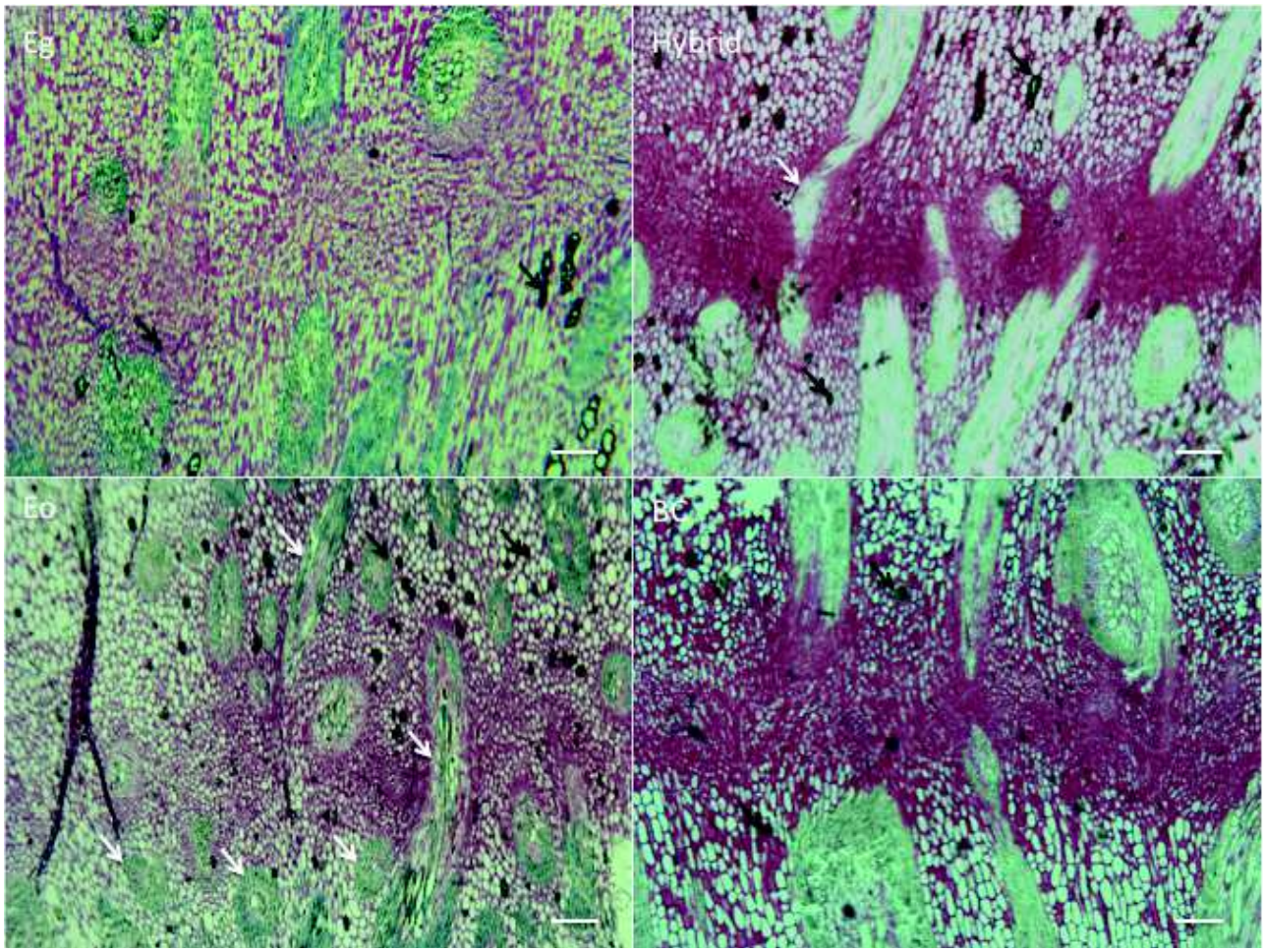

Figure 6. Ruthenium Red stained longitudinal sections of selected examples of oil palm fruit bases Eg (*E. guineensis*), Eo (*E. oleifera*), Hybrid and BC (Backcross). White arrows, lignified vascular strands; Black arrows, phenolic cells; Scale bar, 100 µm.

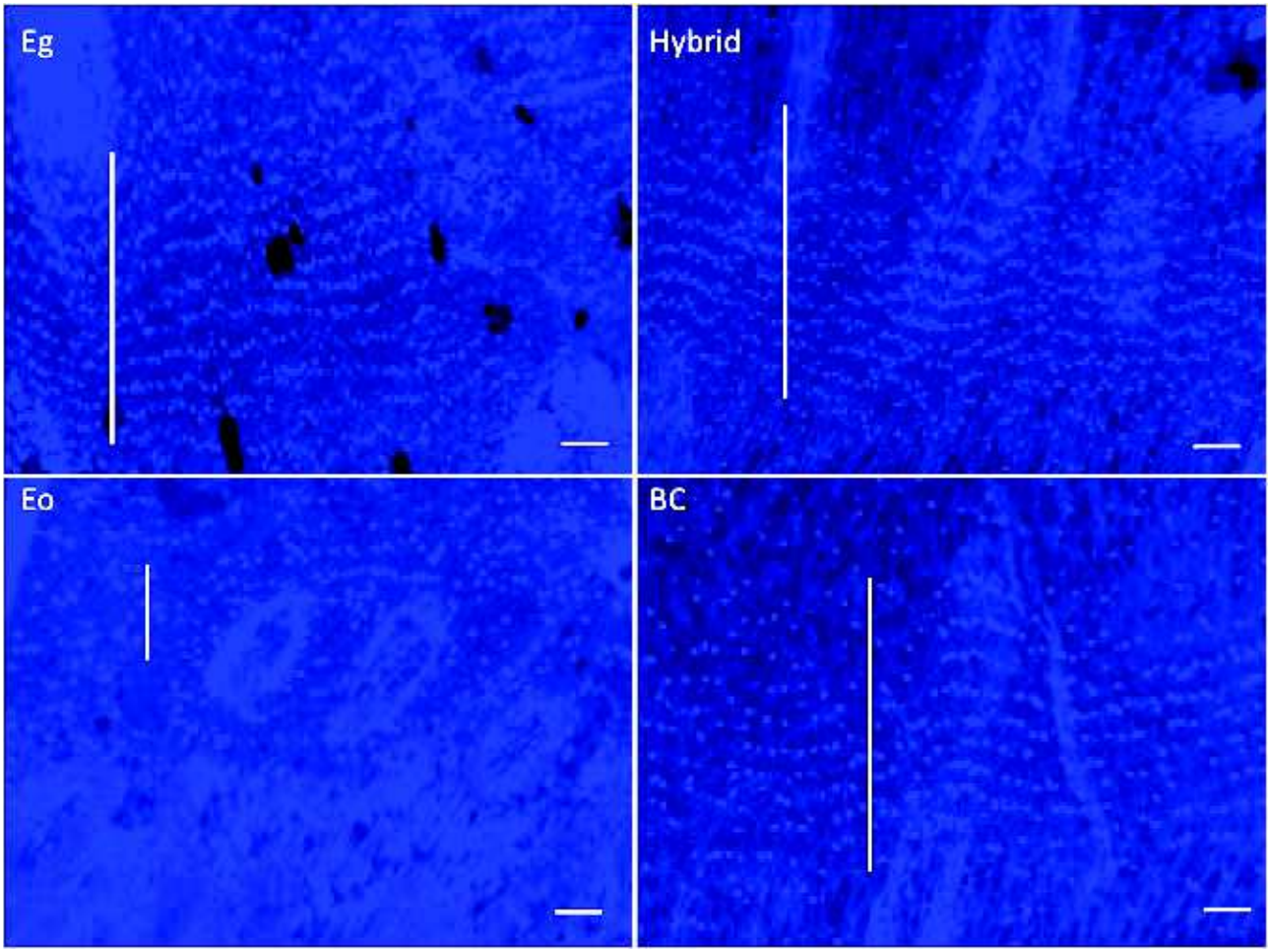

Figure 7. DAPI stained longitudinal sections of selected examples of oil palm fruit bases from Eg (*E. guineensis*), Eo (*E. oleifera*), Hybrid and BC (Backcross). Vertical white lines, AZ cell layers; horizontal scale bar, 100 µm.

CONCLUSIONS

The results provide evidence for the non-shedding character of the Taisha *E. oleifera* material, and of an individual (MTC180) in the BC population. The differences in the structure of the AZ observed between *E. guineensis* and *E. oleifera* may be associated with the non-shedding or abscission resistant nature of the *E. oleifera* Taisha material. The structure of the BC MTC180 AZ has been studied in some detail and it appears to differentiate normally in comparison to *E. guineensis* (Chapter 3). However, an expression marker for ethylene synthesis (ACO) was low and suggests the phenotype may be related to a lack of ethylene production. The combination of the phenotypic test and expression analysis of both *EgPG4* and *ACO* allowed a robust methodology to identify non-shedding material. Future work aims to determine the basis of the non-separating character of this material and the differences in the AZ observed between *E. guineensis* and *E. oleifera*.

ACKNOWLEDGEMENTS

This work was supported by Franco-Thai and Thailand Graduate Institute of Science and Technology (TGIST) scholarships to KF. Financial support for the project also came from PalmElit and IRD/CIRAD to KF, FM and TJT, and from the Kasetsart University Research and Development Institute (KURDI) to CJ.

We especially thank Anek Limsrivilai and the staff at GoldenTenera Oil Palm Plantation in Thailand, Roberto Poveda and staff at the PDA/Murrin Companies (DANEC group) and Claude Louise of PalmElit in Quinindé, Ecuador for the excellent plant material and logistical support for the study.

REFERENCES

Bakoumé C, Wickneswari R, Siju S, Rajanaidu N, Kushairi A, Billotte N (2015) Genetic diversity of the world's largest oil palm (Elaeis guineensis Jacq.) field genebank accessions using microsatellite markers. Genetic Resources and Crop Evolution **62:** 349-360

Barcelos E (1998) Etude de la diversité géaétique du genre Elaeis (E. oleifera (Kunth) Cortés et E. guineensis Jacq.) par marqueurs moléculaires (RFLP et AFLP). Université Montpellier

Barcelos E, de Almeida Rios S, Cunha RN, Lopes R, Motoike SY, Babiychuk E, Skirycz A, Kushnir S (2015) Oil palm natural diversity and the potential for yield improvement. Frontiers in plant science **6**

Buffardmorel J, Verdeil JL, Pannetier C (1992) Somatic Embryogenesis of Coconut-Palms (Cocos-Nucifera-L.) from Leaf Explants - Histology. Canadian Journal of Botany-Revue Canadienne De Botanique **70:** 735-741

Cadena T, Prada F, Perea A, Romero HM (2013) Lipase activity, mesocarp oil content, and iodine value in oil palm fruits of Elaeis guineensis, Elaeis oleifera, and the interspecific hybrid O x G (E. oleifera x E. guineensis). Journal of the Science of Food and Agriculture **93:** 674-680

Corley RHV, Tinker PB (2003) The Oil Palm, Ed Fourth. Blackwell Science, Oxford, UK

Henderson J, Osborne DJ (1990) Cell Separation and Anatomy of Abscission in the Oil Palm, Elaeis guineensis Jacq. Journal of Experimental Botany **41:** 203-210

Hormaza P, Fuquen EM, Romero HM (2012) Phenology of the oil palm interspecific hybrid Elaeis oleifera× Elaeis guineensis. Scientia Agricola **69:** 275-280

Mezui MA, Tchouamo I, Baudouin M (2013) Adoption of the tenera hybrid of oil palm (Elaeis guineensis Jacquin) among smallholder farmers in Cameroon. Tropicultura **31:** 103-109

Montoya C, Cochard B, Flori A, Cros D, Lopes R, Cuellar T, Espeout S, Syaputra I, Villeneuve P, Pina M (2014) Genetic architecture of palm oil fatty acid composition in cultivated oil palm (Elaeis guineensis Jacq.) Compared to its wild relative E. oleifera (HBK) Cortés.

Montoya C, Lopes R, Flori A, Cros D, Cuellar T, Summo M, Espeout S, Rivallan R, Risterucci A-M, Bittencourt D (2013) Quantitative trait loci (QTLs) analysis of palm oil fatty acid composition in an interspecific pseudo-backcross from Elaeis oleifera (HBK) Cortés and oil palm (Elaeis guineensis Jacq.). Tree genetics & genomes **9:** 1207-1225

Morcillo F, Gagneur C, Adam H, Richaud F, Singh R, Cheah SC, Rival A, Duval Y, Tregear JW (2006) Somaclonal variation in micropropagated oil palm. Characterization of two novel genes with enhanced expression in epigenetically abnormal cell lines and in response to auxin. Tree Physiology **26:** 585-594

Muniran F, Bhore SJ, Shah FH (2008) Micropropagation of Elaeis guineensis Jacq.'Dura': Comparison of three basal media for efficient regeneration. Indian journal of experimental biology **46:** 79

Osborne DJ, Henderson J, Corley RHV (1992) Controlling Fruit Shedding in the Oil Palm. Endeavour **16:** 173-177

Pfaffl MW (2001) A new mathematical model for relative quantification in real-time RT-PCR. Nucleic Acids Res **29:** e45

Rajanaidu N, Kushairi A, Rafii M, Din M, Maizura I, Jalani B (2000) Oil palm breeding and genetic resources. Advances in oil palm research, Vol. 1**:** 171-237

Roongsattham P, Morcillo F, Jantasuriyarat C, Pizot M, Moussu S, Jayaweera D, Collin M, Gonzalez-Carranza Z, Amblard P, Tregear JW, Tragoonrung S, Verdeil JL, Tranbarger TJ (2012) Temporal and spatial expression of polygalacturonase gene family members reveals divergent regulation during fleshy fruit ripening and abscission in the monocot species oil palm. BMC Plant Biology **12:** 150

Torres G, Sarria G, Varon F, Coffey M, Elliott M, Martinez G (2010) First report of bud rot caused by Phytophthora palmivora on African oil palm in Colombia. Plant Disease **94:** 1163-1163

Tranbarger TJ, Dussert S, Joet T, Argout X, Summo M, Champion A, Cros D, Omore A, Nouy B, Morcillo F (2011) Regulatory mechanisms underlying oil palm fruit mesocarp maturation, ripening, and functional specialization in lipid and carotenoid metabolism. Plant Physiol **156:** 564-584

Chapter3

Global analysis to identify key genes and processes underlying ripe fruit abscission of oil palm

This chapter is in preparation as a manuscript to be submitted 2016.

Authors: Authors: Fooyontphanich K, Morcillo F, Collin M, S. Tangphatsornruang, J. Serret, Dussert S, Jantasuriyarat C, Amblard P, Verdeil J and Tranbarger TJ.

INTRODUCTION

Organ shedding in plants occurs through the function of a specialized tissue referred to as the abscission zone (AZ) located at the base of the organ to be shed where breakdown of the cell-to-cell adhesion occurs (Patterson, 2001). There are two groups of AZ anatomy observed: 1) at the boundary region at the base of the organ to be shed and the neighboring tissue, for example between a floral organ and the pedicel as observed in Arabidopsis, and 2) within a tissue as observed in the pedicel of the tomato fruit or flower (Estornell et al., 2013). In either case, once differentiation of the AZ takes place at the base of the organ to be shed, it acquires competence to respond to signals required for cell separation and organ abscission (Taylor and Whitelaw, 2001). After the AZ becomes competent for separation to be induced, cellular activity, in particular the expansion of the golgi vesicles and activation of the endomembrane system with the release of hydrolytic enzymes to the apoplast leads to the degradation of the middle lamella and cell separation (Liljegren et al., 2009; Burr et al., 2011).

Organ detachment mechanisms have also been a target of domestication, and a well-known domestication example is the non-abscising *jointless* mutant, which has been used to develop non-shedding tomato fruit cultivars (Butler, 1936). Organ abscission is an important agronomic trait with widespread economic consequences. Crop species with overly abundant flowers or immature fruit need to be thinned to obtain the optimal size and highest quality final product, or crops with flowers or immature fruit that shed prematurely need to be inhibited to allow appropriate yields, or mature fruit that shed too soon need to be inhibited to facilitate harvest and avoid economic losses (Addicott, 1982). While some solutions to these problems can be resolved with chemical treatments that either inhibit or induce abscission, genetic solutions are desired to limit the environmental problems and the high cost associated with such treatments. Indeed, the modification of the abscission character is an important breeding target for many crop species. While research with dicot model plants, namely floral organ abscission in Arabidopsis and leaf, flower and fruit abscission of tomato has provided new insights into the molecular mechanisms underlying abscission, little is known about how these mechanisms have diversified during plant evolution and differ between species, plant families and in particular between dicots and monocots.

The monocot oil palm ripe fruit abscission process and AZ have commonalities and originalities to other organ abscission systems (Henderson and Osborne, 1990; Henderson and Osborne, 1994; Henderson et al., 2001). Common to organ abscission in many species, ethylene or its precursor 1-aminocyclopropane-l-carboxylic acid (ACC) promotes while auxin inhibits cell separation in the primary AZ of the oil palm fruit (Henderson and Osborne, 1994; Roongsattham et

al., 2012). Ethylene production is initiated in the ripe fruit apex in the mesocarp and progresses to the base of the mesocarp in a positive correlation to the percentage of separation that occurs in the primary AZ (Henderson and Osborne, 1994). An originality of oil palm fruit shedding is that it takes place in two synchronized stages. First, cell separation occurs in a very large multi-cell-layer primary AZ in the base of the fruit at the boundary between the mesocarp and pedicel tissues in the base of the fruit, followed by subsequent cell separation in peripheral tissues (adjacent AZs) at the junction with the rudimentary androecial ring and the tepals. The precise position of the second separation is determined by the age and ripeness of the fruit and depends upon completion of separation in the primary AZ (Henderson and Osborne, 1990). Evidence also showed that the abscission cells separate at the middle lamellae while the primary walls remain intact with regions of plasmodesmatal connection being last to separate (Roongsattham, 2011). In addition, while the vascular strands between the fruit base and the pedicel are continuous across the AZ, they are much less lignified and may facilitate organ removal (Chapter2).

The oil palm fruit primary AZ cells have high levels of unmethylated pectin in the cell wall, in addition to a high level of inducible polygalacturonase (PG) enzyme activity that is also observed during organ abscission of many species (Henderson et al., 2001). A recent study found an oil palm fruit PG transcript (*EgPG4*) is highly expressed in the AZ during the ethylene treatment time course and *in situ* hybridization showed a preferential increase in the AZ cell layers in response to ethylene prior to cell separation (Roongsattham et al., 2012). Interestingly, *EgPG4* is also expressed in the mesocarp during ripening and is not specific to the AZ, and may function in both cell wall dismantling processes. Surprisingly, the previous study did not identify homologs to the well-characterized Arabidopsis abscission and/or dehiscent PGs, including QRT2, PGAZAT and PGDAT (Ogawa et al., 2009).

In the present study, we report the first global molecular analysis of the oil palm ripe fruit AZ induced by ethylene with a combination of both transcriptomic and proteomic approaches, in addition to validation of selected candidates by qPCR with AZ samples undergoing natural abscission in the field. The combined approaches allow an integrated view into the originalities of the abscission process along with a robust list of genes involved in fruit abscission of this monocot compared with dicot models and other crop species.

RESULTS

Cell separation occurs in the ripe fruit AZ in response to ethylene while no separation occurs in the AZ at earlier stages of development or in adjacent pedicel tissues

Oil palm fruit abscission occurs first through the function of a very large multi-layer primary AZ at the interface of the mesocarp and pedicel tissues in the base of the oil palm fruit, then subsequently in less distinguishable AZs adjacent to the primary zone (Figure 1A) (Henderson and Osborne, 1990). While the primary AZ is fully distinguishable by 30 DAP, it is non-functional; cells do not undergo cell separation even when treated with ethylene (Figure 1B-E) (Roongsattham et al., 2012). We previously showed that ethylene induces fruit abscission and that the response is developmentally dependent; the most rapid response is with the ripest fruit which is also when abscission is observed naturally in the field (Figure 1F-K). Furthermore, ethylene induces cell separation in the primary AZ of ripe fruit, while no separation is visible in the adjacent pedicel cells (Figure 1L). To examine the transcriptional response that occurs in the functional ripe fruit AZ during ethylene induced abscission, we used these differences in ethylene response to compare the ripe fruit (150 DAP) functional AZ (AZ150) with that of the non-functional 30 DAP AZ (AZ30) and the pedicel cells of ripe fruit (P150) where no cell separation is observed in response to ethylene.

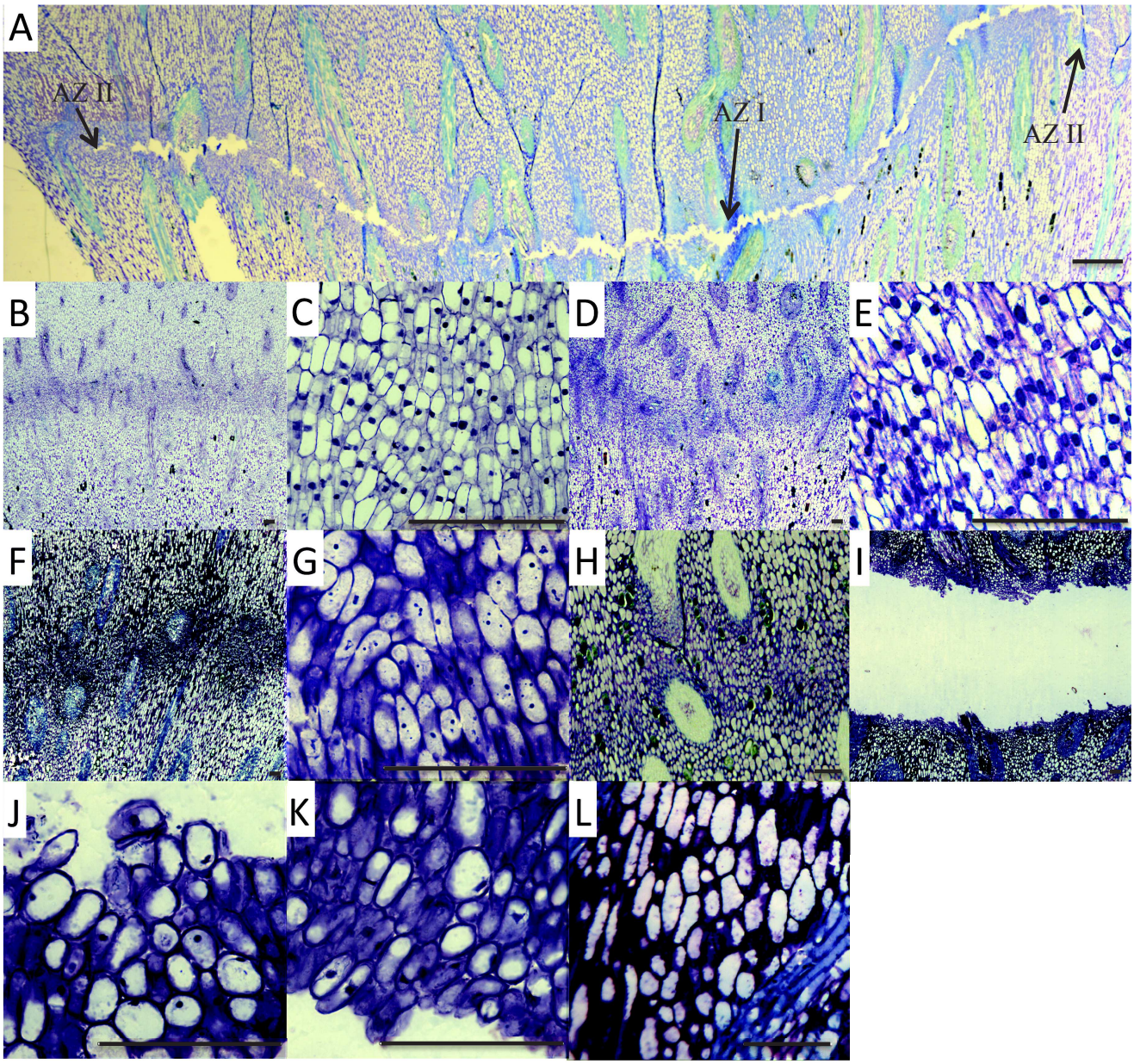

Figure 1. Cell separation occurs in the ripe fruit AZ and not in developing fruit AZ or adjacent pedicel tissue of ripe fruit. Comparison of different tissues of oil palm fruit in response to ethylene. **A**, cell separation has occurred in the primary AZ but not yet in adjacent AZs of ripe 180 DAP fruit. **B** and **C**, 30 DAP AZ before ethylene treatment. **D** and **E**, 30 DAP AZ after ethylene 9h of treatment. **F** and **G**, 120 DAP AZ from fruit not undergoing natural abscission in the field. **H** and **I** 160 DAP AZ not undergoing or undergoing natural abscission in the field respectively. **J**, 160 DAP AZ separated pedicel side 40x. **K**, 160 DAP NA AZ separated mesocarp side 40x. **L**, 160 DAP NA pedicel. Scale bar, 100 µm. Black arrow primary AZ (AZ I), adjacent AZ (AZ II).

454 Sequencing and *de novo* assembly of the ethylene induced abscission transcriptome

In this study, we obtained a total of 2,311,009 reads with the average length of 415 bp and a total of 971 Mbp of sequence data with subtotals of 326,484, 553,805 and 1,099,385 reads for the AZ30, AZ150 and P150 samples respectively (Table 1). The reads were processed and assembled using an automated pipeline as previously described (Argout et al., 2008; Tranbarger et al., 2011). After initial processing, we obtained a total of 1,563,975 reads (68% total reads) that were assembled into 51,804 contigs, in addition to 747,034 singleton reads (Table 1). A comparison of the assembled contigs revealed that the highest number of unique contigs was found in the P150 sample (6,930 contigs), followed by the AZ30 (4,669 contigs) and AZ150 (2,856 contigs), while there were 22,067 contigs common to all samples (Supplementary Figure S1).

Analysis of the abscission transcriptome suggests gene function conservation between dicots and monocot fruit abscission

To assess whether homologous genes from model species may function during oil palm monocot fruit abscission, a total of 67 genes involved in abscission, fruit ripening, seed shattering and ethylene response were selected from a review of the literature to provide an initial evaluation of the *de novo* 454 transcriptome (Figure 2) (Tranbarger et al., 2011) raw data see appendix Table S5. The objective was to determine the relative abundance of this group of genes, with predicted roles in abscission or ethylene related ripening in different species, in the tissue samples of the oil palm fruit. We first examined the abundance of the abscission and AZ expressed *EgPG4,* previously identified in a study of oil palm fruit abscission, and found it to be highly represented in the AZ150 as predicted (Roongsattham et al., 2012). Notably, a large number of putative homologues for ethylene biosynthesis (*ACO1* and *ACO2)*, ethylene signaling (*ERS1, EIL1, EIL2* and *ERF*), abscission signaling (*NEVERSHED* and *HSL2*), and pectin metabolism during abscission (*ADPG1* and *ADPG2*) were highly represented in our transcriptome data. Notably, transcripts for *ACO* (*AtACO1* and *2*), PG (*ADPG1* and *2*) and MADS-box proteins (MACROCALYX, SHATTERPROOF (SHP2) and AtAGL15) were preferentially abundant in the AZ150 sample suggesting conserved roles during ethylene induced oil palm fruit abscission. While several monocot genes involved in seed shattering from sorghum (*Sorghum bicolor*) and rice (*Oryza sativa*) were found in the P150 trancriptome they are represented by very few read numbers. Overall, these results provide evidence for some conservation of genes involved in abscission between dicots and monocots, in particular those related to ethylene or known to be induced by ethylene. In contrast, while genes involved in monocot

seed shattering are present, they are not amongst the most highly represented nor preferentially expressed in the ripe fruit AZ.

Statistical analysis of the AZ150 ethylene induced transcriptome identifies transcripts enriched or specifically expressed in the AZ during abscission

One objective of the current study is to identify genes differentially expressed in the ripe fruit AZ (AZ150) during the ethylene induction time course, and in particular, those with specific expression in the AZ150 where cell separation is induced. Read amounts from each of the AZ150 contigs (33,740 contigs) were analyzed using Audic-Claverie and false discovery rate (FDR) statistics (P = 0.05), to identify 1,957 differentially abundant contigs during at least one time point of the ethylene treatment in the AZ150 sample compared to untreated fruit (Figure 3A). Hierarchical clustering analysis (HCA) identified 4 clusters of contigs with similar read abundance profiles; A (9h), B (6h), C (3h) and D (0h) with different sub-clusters A1-A7, B1-B6, C1-C7, D1-D10 (Figure 3B). At 0h (Cluster D), the highest number (762 contigs) of differentially abundant contigs (38% of total) was found, while cluster B (6h) showed the lowest (309 contigs, 16% of total; Figure 3B). The cluster profiles and graphs obtained were based on the read averages (appendix Figure S1).

Samples	Number of reads	Avg. length (bp)	Total bp (Mbp)	Subtotals
AZ-0h-30DAP	46,048	413	19	
AZ-3h-30DAP	164,920	398.2	65	
AZ-6h-30DAP	120,367	422	50	
AZ-9h-30DAP	326,484	425	138.6	326,484
AZ-0h-150DAP	164,027	437	71.6	
AZ-3h-150DAP	86,217	371.7	32	
AZ-6h-150DAP	121,711	431.5	52	
AZ-9h-150DAP	181,850	399	72	553,805
P-0h-150DAP	339,657	427	145	
P-3h-150DAP	278,933	407.8	113	
P-6h-150DAP	416,935	450	187.8	
P-9h-150DAP	63,860	395	25	1,099,385
Totals/Averages	2,311,009	415	971	

454 Sequencing data	Numbers
Number of raw reads	2,311,009
Reads Assembled	1,563,975
Reads not assembled (singeltons)	747,034
Percentage singeltons	32%
Total contigs	51,804

Table 1 Summary of 454 sequencing

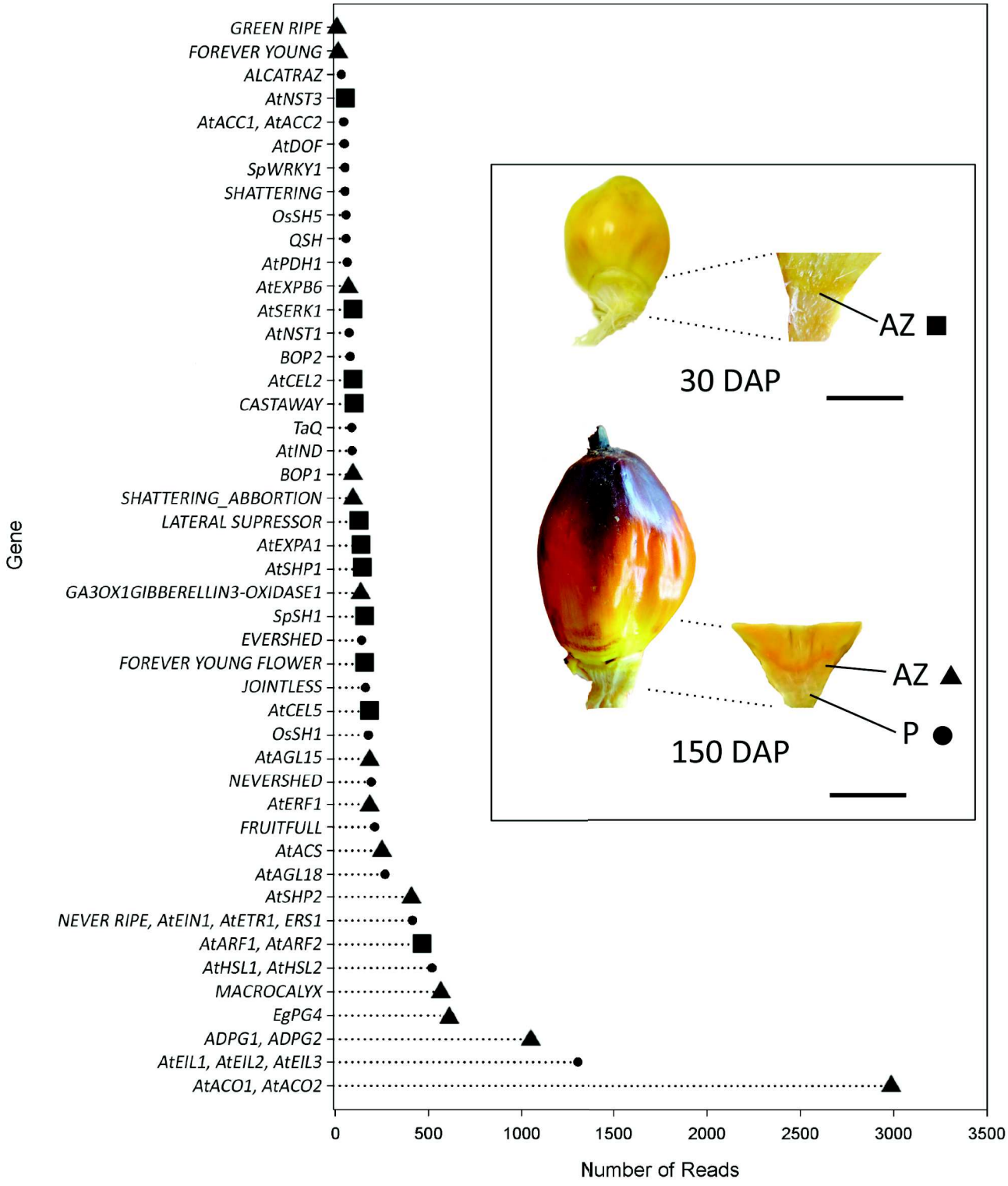

Figure 2. Homologues for many known abscission and ripening related genes are found in the abscission transcriptome. The Y axes is the name of the genes and the X axes is the number of reads and the summary of their relative abundance created by using the highest top 5 contigs then calculate for the total number of reads and represent of read in symbol. Preferentially abundant in AZ150, solid triangle (▲), AZ30, solid square (■), P150, solid circle (●) Scale bar, 1 cm. (*NAC Transcription Factor* (*AtNST3*), *Acetyl-CoA carboxylase* (*ACC1, 2*), *DNA-binding with one finger* (*AtDOF*), *Solanum pimpinellifolium WRKY* (*SpWRKY1*), *Seed Shattering* (*OsSH1*, *OsSH5*, *QSH,*

TaQ, AtSHP1, 2, SpSH1, OsSH1), Pyruvate dehydrogenase (*AtPDH1*), *Expansin B6* (*AtEXPB6*), *Somatic Embryogenesis Receptor Kinase* (*AtSERK1*), *NAC Secondary Wall Thickening Promoting Factor1* (*AtNST1*), *Blade On Petiole* (*BOP1, 2*), *Endoglucanase* (*AtCEL2, AtCEL5*), *Indehiscent* (*AtIND*), *Expansin* (*AtEXPA1*), AGAMOUS-Like15,18 (*AtAGL15, AtAGL18*), *Ethylene Responsive Factor* (*AtERF1*), 1-aminocyclopropane-1-carboxylate synthase (*AtACS*), *Ethylene Insensitive* (*AtEIN*), *Ethylene Insensitive-Like* (AtEIL1, AtEIL2, AtEIL3) *Ethylene Receptor* (*AtETR*), *Ethylene Responsive Element* (*AtERS1*), *HAESA-Like* (*AtHSL1*, *AtHSL2*), *Polygalacturonase* (*EgPG4*, *ADPG1*, *ADPG2*), *1-aminocyclopropane-1-carboxylate oxidase* (*AtACO1*, *AtACO2*))

A

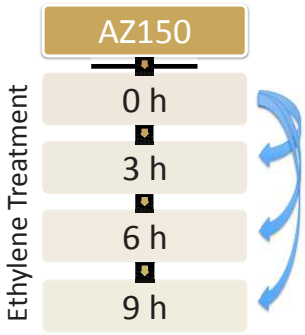

B

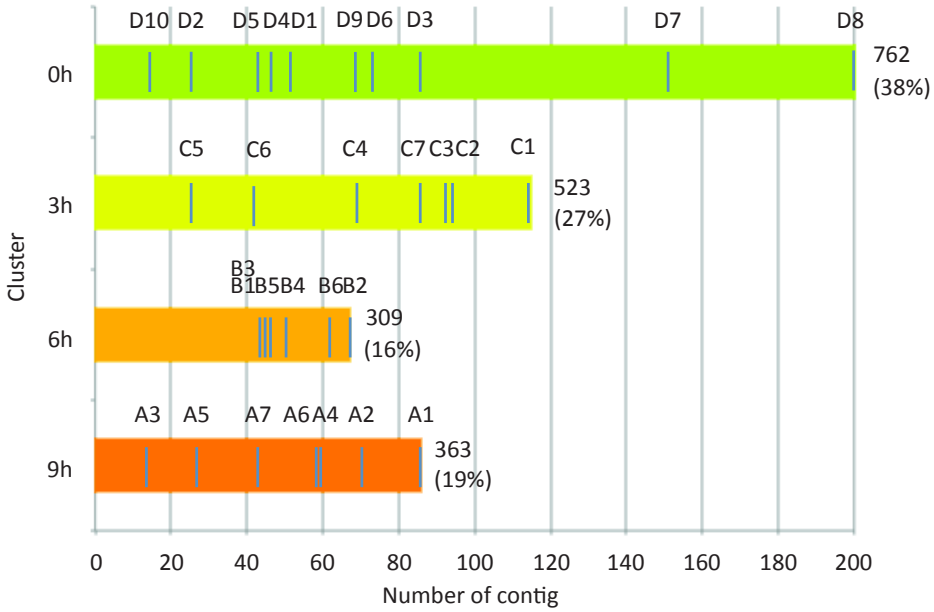

C

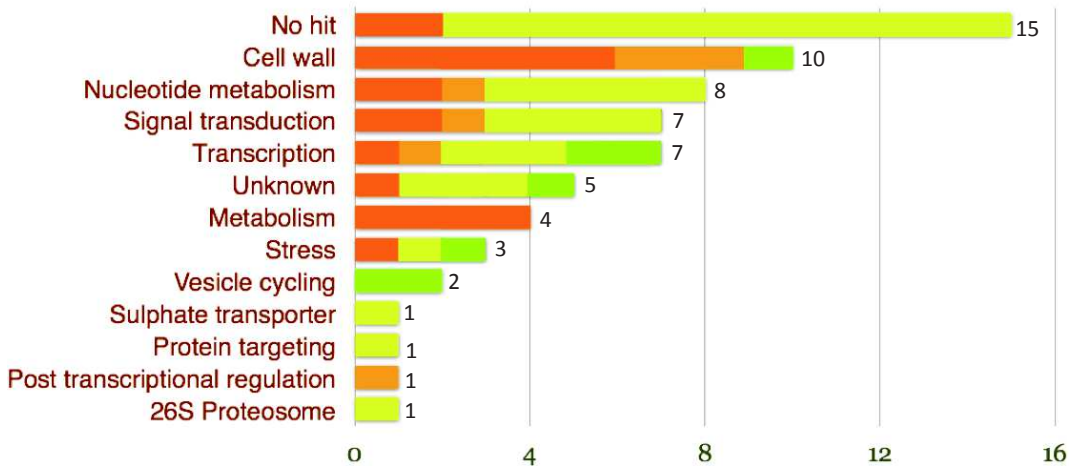

Figure 3. The identification of genes preferentially or specifically differentially expressed in the ripe fruit AZ. **A**, contigs with statistically significant (P = 0.05) in the AZ150 at the different ethylene time points when compared to the untreated field control. **B**, Overview of the four main clusters and multiple sub-clusters found by HCA analysis. Sub-clusters are labeled above the bars, while total number of contigs and percentage of each cluster are indicated at the left end of bars. **C**, The 13 functional categories of the 64 candidates identified by the combined statistical analysis (color of the bar related to the cluster on Figure **B**).

The 1,957 differentially abundant contigs identified were annotated with Gene Ontology (GO) tools to provide insight into the functions that occur in the AZ during ripe fruit abscission. Overall, GO annotations (level 2) of the 4 clusters were very similar (Figure S2). The 3 most prevalent GO annotations for the cellular component of the clusters were cell (28-33%), organelle (25-28%), and membrane (15-17%). The most abundant GO annotations for molecular function were binding (41-45%) and catalytic activity (34-42%), while the 4 highest GO biological process annotations were cellular process (13-14%), metabolic process (12-14%), signal-organism process (11%), and response to stimulus (10-11%) (Figure S2). To identify GO annotations enriched in each cluster, the FISHER's exact test (P value = 0.01) was performed on each cluster (test set) in comparison with the reference set of 1,957 differentially abundant contigs (Figure 4). Cluster D (0h) had the most enriched GO terms, followed by cluster A (9h) and Cluster C (3h). There were no enriched GO terms in Cluster B (6h). The 0h cluster D was especially enriched in GO terms for macromolecule annotations, and in particular, several annotations for gene expression and regulation. Notably annotations for auxin mediated signaling are also significantly enriched. Annotations for macromolecule metabolic processes remain enriched at 3h cluster C, in addition to annotations for secretion and endomembrane processes. Finally, at 9h cluster A the most enriched annotations included hydrolase activity, in particular, those targeting O-glycosyl bonds (Figure 4).

To identify AZ150 specific contigs, the next step was to compare the abundance of the differentially expressed AZ150 contigs statistically (P = 0.05) with the AZ30 and P150 samples at each ethylene treatment time point. The contigs identified were subjected to another screening step by examining their abundance in the mesocarp transcriptome database (Tranbarger et al., 2011), and only those with low or no expression in the mesocarp during ripening were kept for further analysis. From this analysis a total of 64 contigs were identified with AZ150 specific or enriched abundance at least during one time point of the ethylene treatment, compared to the AZ30 and P150 samples (Table S2). To validate these candidates, the sequences were aligned to the oil palm genome to determine their location and they were found throughout the genome on all 15 chromosomes except chromosome 13 (Supplementary Figure S3). The highest number of candidates was positioned on the "Unplaced Scaffold" (12%), Chromosome 2 (12%), Chromosome 1 (11%) and Chromosome 4 (11%). This step validated the assembly of our transcriptome by alignment of all 64 contig sequences to the oil palm genome.

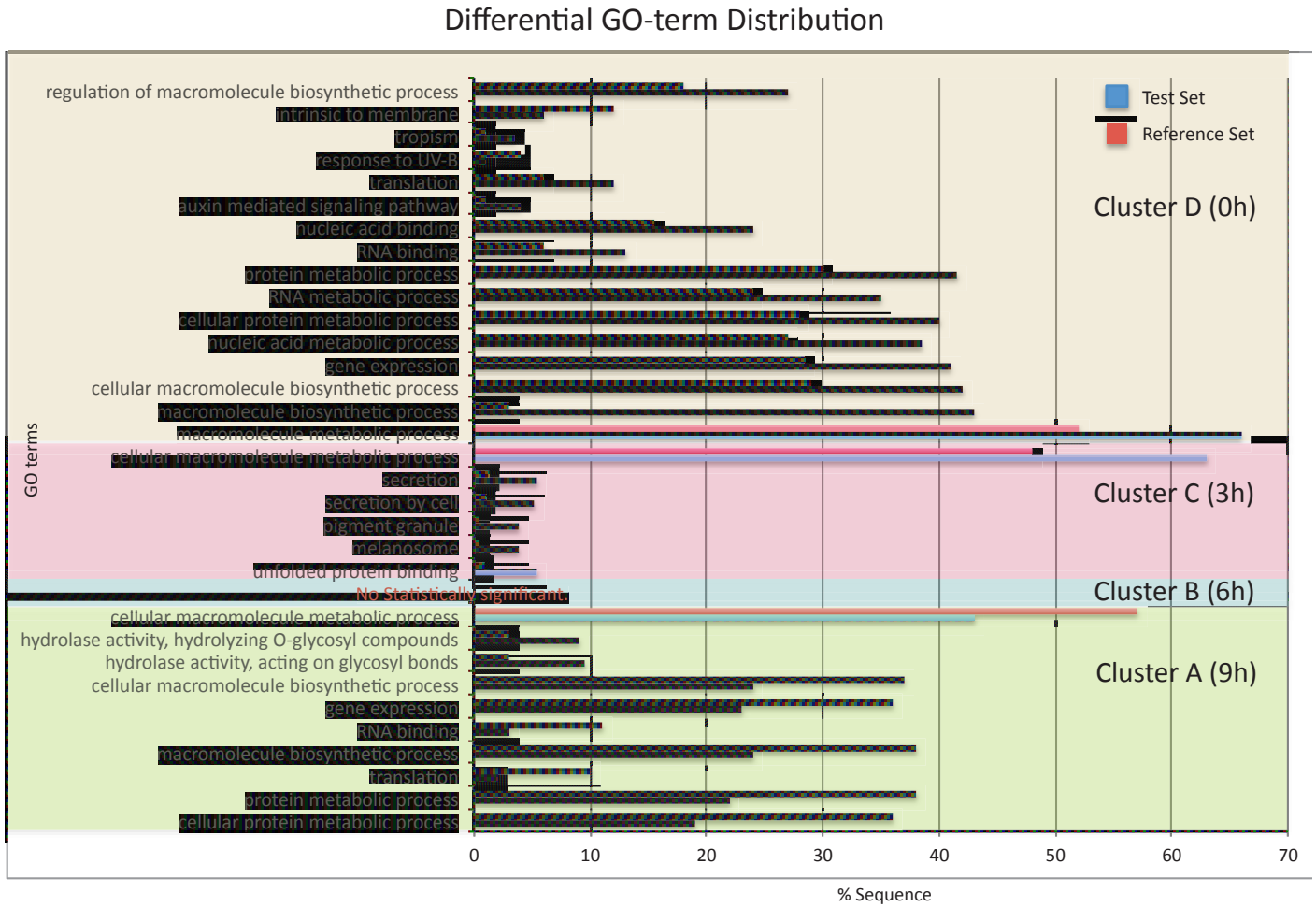

Figure 4. Differential GO-terms enriched in the clusters of A (9h), B (6h), C (3h) and D (0h) in comparison with the 1,957 differential contigs. The X axes as % of the sequences the Y axes as the GO terms.

From the 64 candidates, a total of 45 candidates could be assigned a functional annotation based on similarity to known sequences in the available databases. The highest number of contigs (15 contigs) did not have sequence similarity in the available databases (No hit), and were mostly found at 3h cluster C and a few at 9h Cluster A (Figure 3C). While these sequences and 4 other sequences similar to proteins of unknown function are found in the oil palm genome and are not an artifact of assembly, there is no annotation information to assess their potential functions, hence no further work was done (appendix Table S2). The 45 annotated contigs can be separated into 12 functional categories including cell wall, nucleotide metabolism, signal transduction, transcription, metabolism, stress, vesicle cycling, and others (Figure 3C and appendix Table S2). The first highest category is cell wall related genes (10 contigs) found mostly at 6h cluster B and 9h cluster A. In particular, several of the cell wall genes encode proteins related to pectin metabolism including pectinesterase (PME) and two PGs, in addition to those related to lignification (laccase) cell expansion (expansin) and other functions (leaf senescence protein-like and leucine-rich repeat extensin-like protein). The second highest number of contigs correspond to genes encoding proteins related to nucleotide metabolism, including adenine nucleotide translocator 1, survival protein Sur E-like phosphatase/nucleotidase, 2 cytidine deaminase, nitrilase/cyanide hydratases, universal stress protein/adenine nucleotide alpha hydrolases-like and 2 ATP-sulfurylases. Contigs with functions in transcription and signal transduction were also highly represented with 7 in each category (Figure 3C).

A comparison between ethylene induced and natural abscission that occurs in the field identifies key genes and processes

To validate gene candidates identified from the ethylene transcriptome analysis, Illumina sequencing was performed from AZ samples undergoing natural abscission in the field. The study was conducted with 3 different samples including the AZ from 30 DAP (AZ30DAP), 120 DAP (AZ120DAP) during which time no abscission was observed, and 160 DAP (AZ160DAP) collected from a fruit bunch where abscission was observed (Figure 1 F-I). The resulting sequences were mapped to the predicted coding sequences (CDS) derived from the oil palm genome (Singh et al., 2013). The ripe fruit undergoing abscission (AZ160DAP) were first identified by the presence of recently abscised fruit observed below a ripe fruit bunch, then further characterized by a simple pull test to determine whether abscission was underway. The result revealed that fruits from both the lower and upper parts of the 120 DAP spikelet could not be removed when pulled, while the fruit from the lower (65%) and upper portion (92%) of the spikelet were easily removed and the fruit

separated at least along the primary AZ (Figure S4). This test verified that abscission was underway or had already occurred in the ripe fruit spikelet and not in the spikelets of the less mature fruit bunch (120 DAP).

During oil palm fruit ripening, ethylene is produced in the mesocarp and is thought to be the main signal to induce abscission in the AZ (Henderson and Osborne, 1994; Tranbarger et al., 2011). Therefore, we predicted that the candidates that increased or decreased during at least one time point of the ethylene treatment should also increase or decrease in the AZ of ripe fruit undergoing abscission in the field. To test this hypothesis, we examined transcript profiles during natural abscission of 45 annotated statistically significant ethylene transcriptome candidates described above in addition to other selected candidates (34 contigs) that were highly differentially expressed in the ripe fruit AZ, but not statistically different to the comparison tissues (Figure 5 and Table S4. The predicted CDS was found for 79 contigs and they were used as reference to map Illumina sequences to obtain the corresponding expression profiles in AZ during ripe fruit abscission (Figure 5). Firstly, the contig corresponding to *EgPG4* was highly expressed in the AZ of ripe fruit undergoing natural abscission as predicted, which is further validation that the fruit sampled is undergoing abscission (Roongsattham et al. 2012). In addition to *EgPG4*, we found 26 other candidates also had expression during natural abscission as we predicted (peak or lowest expression in the ripe fruit AZ), 7 were close to the prediction (high or low expression in the ripe fruit AZ), while 9 did not conform to our predicted expression profile (Figure 5). From those that followed our prediction, 21 were validated to have high expression and 5 were validated to have low expression in the AZ during abscission. Interestingly, amongst the statistically significant candidates with high expression in the AZ during abscission, 5 (including *EgPG4*) have cell wall related functions, including 2 newly identified PGs, a pectinesterase and an expansin. From the other 33 candidates examined, 16 conformed, 11 were close, and 7 did not conform to our predictions. 10 were validated to have high expression while 5 were validated to have low expression in the AZ during abscission. Other transcripts highly expressed in the AZ during abscission encode products for nucleotide metabolism, signal transduction, sulfate transport and metabolism. Interestingly, two contigs that decrease in expression in the ripe fruit AZ are TFs, including an ERF. The other candidates with comparable profiles during ethylene induced and natural abscission, encoded products include cell wall, transcription, metabolism, membrane transport, hormone metabolism or response, endomembrane and cytoskeleton related functions. The results provide evidence that during natural abscission, ethylene induced transcription occurs in the AZ and coordinates the expression of key genes involved in oil palm fruit abscission.

Gene expression in the AZ of non-shedding oil palm tree is perturbed and corroborates key genes and processes

To provide further evidence for roles during the abscission process, we examined the expression profiles of 48 gene candidates in the fruit AZ from oil palm trees that do not shed their fruit (Fooyontphanich et al, 2015). Indeed, the AZ of the ripe fruit MTC180 are differentiated with similar cellular characteristics as observed with *E. guineensis*, but the fruit remain on the trees and no natural abscission in the field was observed (Figure 7). Our hypothesis was that the non-shedding character of these trees is due to perturbations in gene expression required for abscission to occur, so we could use this material to examine this hypothesis and to provide evidence for roles of selected candidates. We predicted that genes important for abscission would have the opposite expression profiles in the non-shedding (MTC180) fruit AZ than observed in the AZ during natural abscission and in response to ethylene induced abscission. A qPCR analysis of AZ samples revealed 33 genes (including *EgPG4*) with expression that corresponded to our prediction; expression profiles in the non-shedding fruit AZ were opposite to those observed in the AZ during natural and the ethylene induced abscission (Figure 5).

Does similar expression of candidates in adjacent mesocarp and pedicel tissues suggest possible signals and an importance for abscission in the AZ?

EgPG4 is not only expressed in the AZ in response to ethylene, but also in the mesocarp during ripening (Roongsattham et al., 2012). The observation suggests that ethylene produced in the mesocarp may be the signal to induce expression in the AZ, and that EgPG4 may also be involved in mesocarp ripening. While *EgPG4* expression is not specific to the AZ, a coordination of *EgPG4* expression between the AZ and mesocarp tissues may be important for the timing of cell separation in the AZ, and insure that only the ripest fruit abscise. In addition, in the current study, it was a surprise to find so few AZ specific or enriched transcripts (only 64 candidates) when compared to the control ripe pedicel and immature AZ at 30 DAP (Chapter 3). This raised the question whether expression coordinated between adjacent tissues may be important for the abscission process, in addition to AZ specific expression. To examine this in further detail, the expression of the most robust candidates (EgPG4, EgPGAZ1, EgPGAZ2, pectinesterase, hydroxy-methylglutaryl-coenzyme A reductase, inositol oxygenase, thioesterase superfamily, alpha/beta hydrolase, beta-galactosidase, serine/threonine protein kinase, helix-loop-helix and thaumatin-like) were examined in the mesocarp (M) pedicel (P), and AZ during the ethylene time course (0h, 3h, 6h and 9h; Figure 6). The results

can be separated into 3 groups; the first group with the expression in all 3 tissues (M, AZ and P) including transcripts for beta-galactosidase and serine/threonine protein kinase; the second group with expression in the M and AZ including those encoding EgPG4, pectinesterase, hydroxy-methylglutaryl-coenzyme A reductase, thioesterase superfamily, alpha/beta hydrolase, helix-loop-helix and thaumatin-like; and the last group with the expression only in the AZ including transcripts for EgPGAZ1, EgPGAZ2 and inositol oxygenase. The results suggest overlapping and coordinated expression exists between the AZ and adjacent tissue.

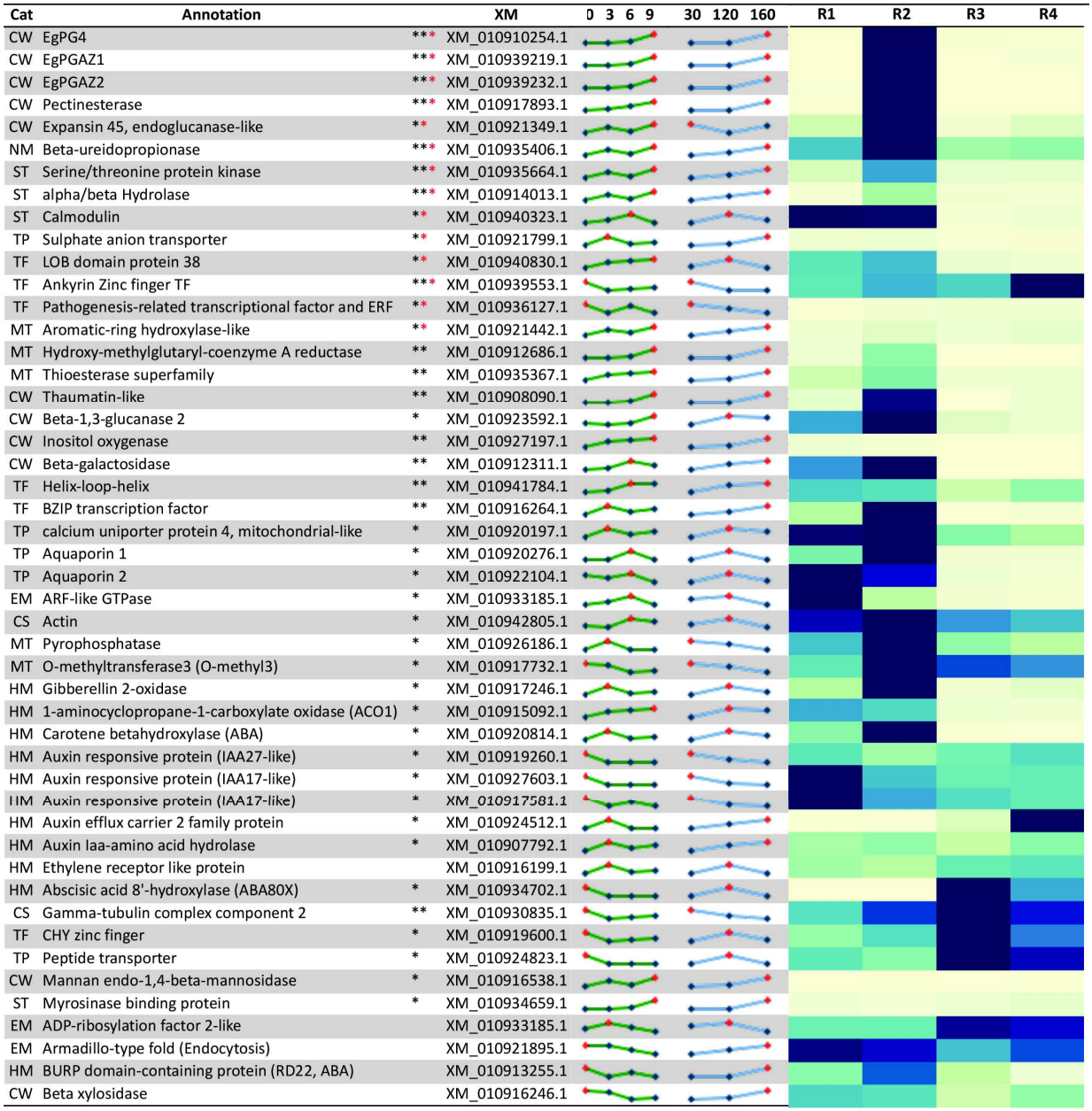

Figure 5. A comparison of expression profiles during ethylene induced abscission with natural abscission that occurs in the field and in the AZ during natural abscission are opposite to that found in the non-shedding fruit AZ. Normal backcross R1 (not undergoing abscission) and R2 (undergoing abscission) and non-shedding (no abscission observed) backcross R3 and R4 from the different DAP. The 0, 3, 6 and 9 h column are profiles during ethylene-induced abscission (calculated from read abundance as in Tranbarger et al., 2011). The 30, 120 and 160 DAP column are Illumina profiles during ripe fruit abscission that occurs naturally in the field (calculated as RPKM, see Methods and Materials). Overview of expression profiles from qPCR analysis is shown by the heat map (highest relative expression was calculated as 1 for each candidate). Cat, Annotation Category; CDS came from blast against the NCBI website). The symbol in front of the Contig indicates the following: *** Statistically validated candidate and validated during both natural abscission and in the non-shedding backcross R3 and R4; ** Statistically validated candidate by one of the approaches (either natural abscission or in the non-shedding backcross R3 and R4); ** Validated candidate by both approaches (validated during both natural abscission and in the non-shedding backcross R3 and R4); * Validated candidate by one of the two approaches; No * no validation

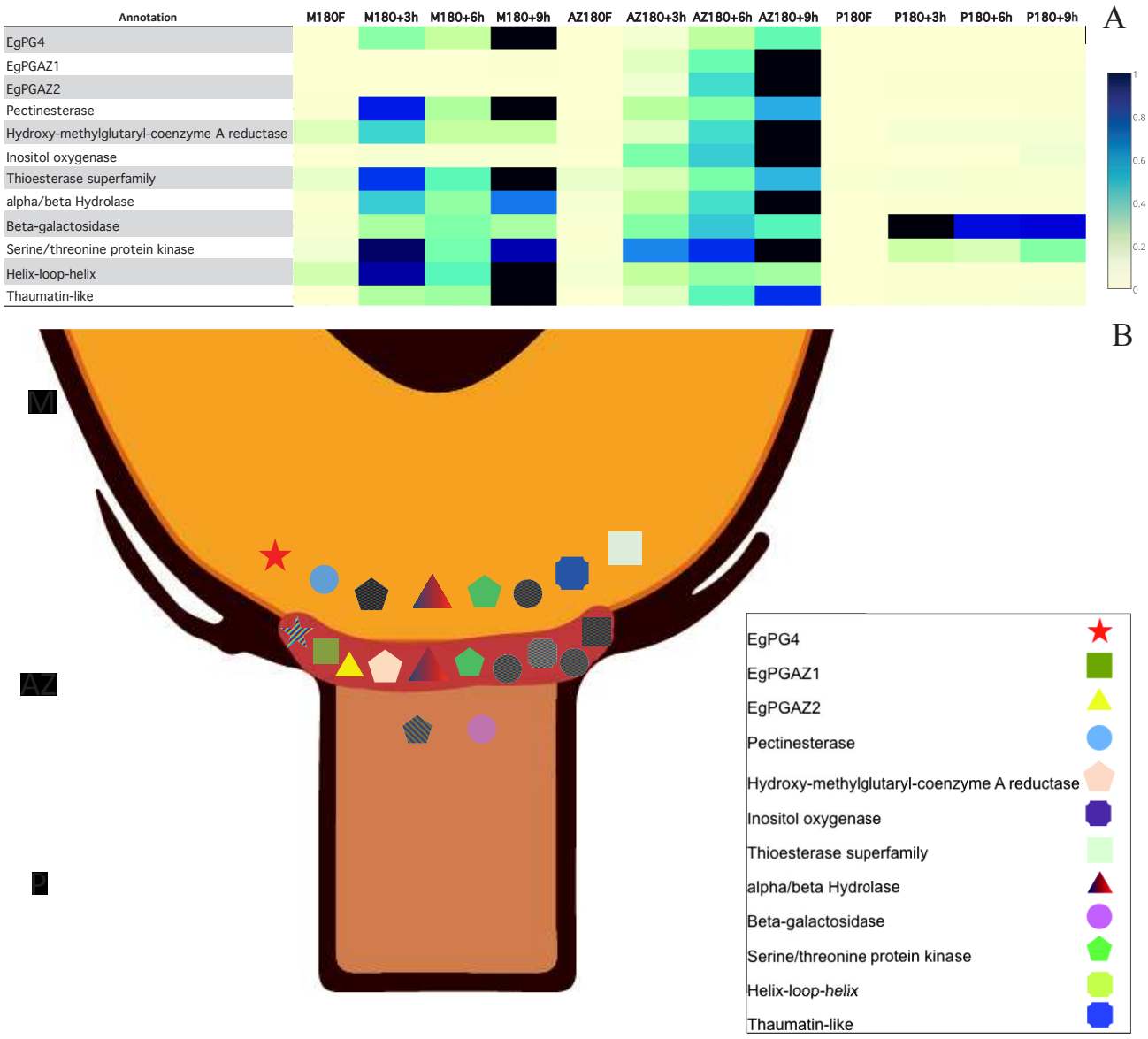

Figure 6. **A**. qPCR analysis of selected candidates in adjacent tissues (M, Mesocarp, AZ and P, pedicel) treated with ethylene. Results are shown as the relative expression calculated by using the maximum of each candidate and assigned as 1. **B**. Schematic model of the oil palm fruit base summarizes tissue expression localization of the most robust candidates (symbols) in the M (mesocarp) AZ (abscission zone) and P (pedicel).

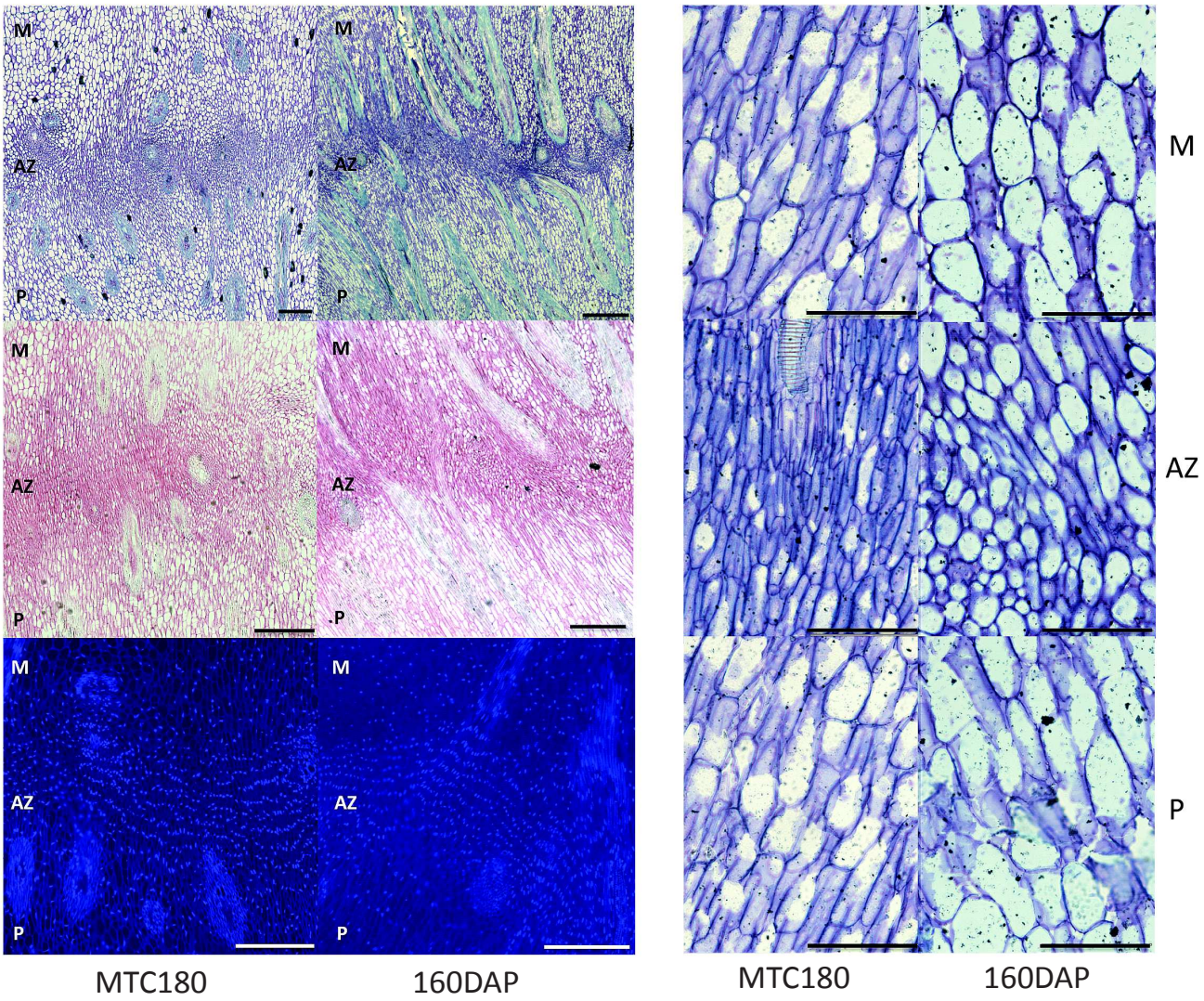

Figure 7. A comparison between the non-shedding MTC180 A and C and 160DAP B and D fruit reveals fully differentiation AZ cell characteristics. Shows the 3 different tissues; M, AZ and P. Scale bar, 100 µm for A and B. Scale bar, 1000 µm for C and D.

The candidate analysis expression in a tree that does not undergo fruit abscission provides evidence for roles in the AZ during abscission, and that a perturbation of gene expression is part of the basis for the non-shedding character. Importantly, 8 of our statistically significant candidates were validated during both natural ripening induced abscission and in the non-shedding backcross tree and comprise the list of the most robust candidates for important roles in abscission. These include all the pectin related candidates (EgPG4, two other PGs and the pectinesterase), a beta-ureidopropionase, a serine/threonine protein kinase, an alpha/beta hydrolase and an ankyrin Zinc finger TF. In addition, 6 other statistically significant candidates were validated by at least one of the approaches, including expansin, calmodulin and a LOB domain protein TF. Finally, 8 other candidates were validated by both approaches, 21 were validated by one of the two approaches, and only 5 were not validated by either approach.

Proteomic analysis identifies early abundant proteins during the ethylene induced abscission process

As a compliment to the transcriptome analyses described above, an analysis of the proteome changes that occur during the ethylene induced abscission process was performed. The experiment compared the field (0h time 150DAP AZ), the ethylene controls (no ethylene, air treatments of 150DAP AZ for 3h, 6h and 9h in the presence of ethylene absorbing material) with the fruit treated with ethylene for 3h, 6h and 9h. The same samples for the transcriptome were used for the proteome analysis, except that the transcriptome analysis did not examine the untreated air controls, but rather compared the non-functional 30 DAP AZ and the ripe fruit pedicel with the ripe fruit AZ 150 DAP samples. The proteome analysis identified 879 peptides with differential abundance during at least one time point of the experiment when compared to the air controls (Table S5). A contig from our transcriptome data was found for all peptides identified, and corresponding CDS were then identified from the oil palm genome. A comparison of the three global approaches (the ethylene induced abscission transcriptome, the Illumina natural abscission transcriptome and proteome) revealed 114 common contigs amongst the three approaches (Figure 8A, appendix Table S3). All but three of the predicted proteins derived from the differentially abundant peptides were found in the Illumina data. To examine the changes to the proteome at the early stages of abscission (3h), we examined the differentially abundant peptides that occur during the ethylene induced abscission process at the 3h time point. We then compared that the natural abscission trend line from the Illumina data to assess the expression of these candidates in the AZ at 30, 120 and 160 DAP during abscission (Figure 8B). We found 4 transcripts conformed to our prediction with highest expression in the AZ of ripe fruit, 8

with highest expression at 120 DAP, and 5 with highest expression at 30 DAP. The four candidates with high expression in ripe fruit included transcripts for a UDP-xylose synthase involved in cell wall biosynthesis, 3-ketoacyl-coenzyme thiolase involved in jasmonic acid biosynthesis, ubiquitin/activating enzyme involved in the proteosome pathway, and adenyly-sulfate kinase involved in sulfate assimilation. While we did not find the same gene candidates as with the transcriptome approaches, we observe similar functional categories represented in this group included those related to transcription, cell wall modifications, sulfate metabolism and changes in the 26S proteosome pathway, in addition to other categories such as hormone (JA and auxin), the redox system, vesicle cycling and proteolysis. This analysis provides insight into the proteomic changes that occur within 3h of ethylene treatment and prior to cell separation in the primary AZ.

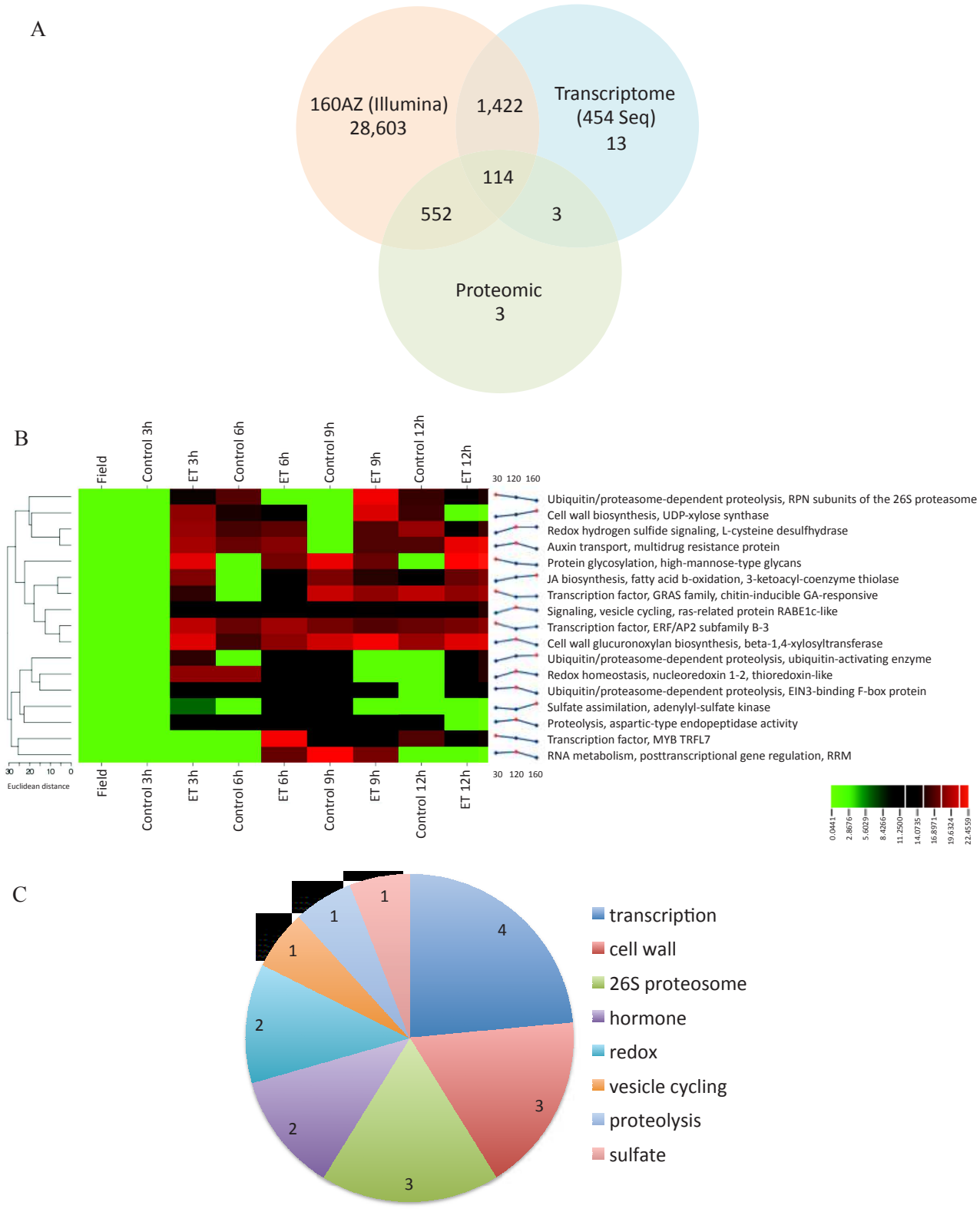

Figure 8. Proteome analysis identifies early abundant proteins in the ripe fruit AZ. A, The three global approaches compared results in 114 common contigs. B, Heat map analysis of the peptides that increase within 3h after ethylene treatment, in comparison to field (0h time) and control (3h air treatment). The 30, 120 and 160 column are Illumina profiles during ripe fruit abscission that occurs naturally in the field (calculated as RPKM, see Methods and Materials). C, Annotation overview of 3h and 6h induced peptides, numbers of contigs are indicated and the size of the slice is relative to the total %.

DISCUSSION

Conservation of genes and processes involved in organ abscission of dicots and the phylogenetically distinct monocot palm species

Abscission is a critical process in plants for both monocot and eudicots and can be regulated by different mechanisms at the different stages of the process (Estornell et al., 2013). In current study, we combined the Next Generation Sequencing (NGS) platforms 454 Pyrosequencing and Illumina, in combination with qPCR analysis of the AZ of material that does not undergo abscission to screen for gene candidates with expression profiles that correlate to the position and timing of abscission. In addition, a complementary LC-MS/MS proteome approach was conducted in parallel with the AZ from the same ethylene treated fruit samples. This is the first study for a monocot that uses a combination of large-scale transcriptome/proteome approaches combined with validation studies with a tree with a non-shedding phenotype. In the current study we use the combination of different approaches with different biological material (ethylene treated samples versus natural abscission samples versus non-shedding material) to identify a robust list of genes and processes that function in the AZ during ripe fruit abscission.

The mechanisms underlying the abscission process in plants have been studied broadly using physiological and genetic approaches in dicots but very little in monocots such as crop species like oil palm. Most studies of organ abscission and AZ development of monocots has been with seed abscission or shattering, with only a few on other organs including floral organs and leaves, and very little is known about fruit abscission (VAN DOORN, 2002; Lin et al., 2007; Nowak et al., 2007; Zhou et al., 2012). The abscission of the oil palm fruit occurs in the cell layers of the AZ at the base of fruit placed between the pedicel and mesocarp; separation always occurs first in the large multilayer primary AZ then in adjacent AZs that are less distinguishable (Henderson and Osborne, 1990; Roongsattham et al., 2012). This characteristic makes the oil palm fruit AZ a boundary type AZ comparable to Arabidopsis floral organ AZs, in contrast to the tomato fruit AZ which is within the pedicel tissue, not at the boundary between different tissues. The number of the AZ cell layers varies in plant species; Arabidopsis floral organ AZs consist of 1-2 layers, tomato flower/fruit pedicel AZ are 5-10 layers, while the AZ in the leaflet rachis of *Sambucus nigra* (common elder) consists of 50 layers (Taylor et al., 1994; Bleecker and Patterson, 1997). The oil palm primary AZ in fruit can have as many as 10 layers that were characterized to have high amounts of unmethylated pectin and PG activity (Henderson refs plus Peerapat manuscript in preparation). This characteristic makes the oil palm fruit AZ comparable to tomato with a multi cell-layer AZ. Therefore, the oil palm

fruit AZ shares similarities and differences with the two model dicots; a boundary AZ as with Arabidopsis floral organs, and a large multilayer AZ like the tomato pedicel AZ, and provides a valuable model to explore the mechanisms of fruit abscission in a monocot.

To determine whether genes identified in dicot organ abscission model systems, namely Arabidopsis and tomato, in addition to monocot cereal seed abscission models, are conserved and function in the oil palm AZ during fruit abscission, an initial analysis was made with a list of candidates selected from the literature. This biased approach provided an initial analysis of the ethylene induced abscission transcriptome, and the abundance of certain literature candidates in the three different sample groups; immature fruit AZ (AZ30), ripe fruit AZ (AZ150) and ripe fruit pedicel (P150). Firstly, the abscission related expression of *EgPG4* was corroborated by its relative abundance in the ripe fruit AZ (Roongsattham et al., 2012). In addition, at least two other PGs with similarity to the Arabidopsis ADPG1 and ADPG2 involved in seed abscission and floral organ abscission respectively, and silique dehiscence together were identified as highly expressed in the ripe fruit AZ (Ogawa et al., 2009). Notably, transcripts for *ACO* were the more abundant and *ACS* and *ERF1* were also enriched in the ripe fruit AZ, which suggests preferential expression and a higher ethylene biosynthesis and response capacity in the ripe fruit AZ compared with the other samples. Several transcripts with sequences similar for MADS-box proteins including MACROCALYX, SHATTERPROOF and AGL15 were also preferentially found in the ripe fruit AZ. AGL15 is a negative regulator of abscission when expressed ectopically in Arabidopsis, and appears to be independent of ethylene (Fernandez et al., 2000). In our study, we find AGL15 more highly expressed in the ripe fruit AZ, but at a relative low level compared to the *ACO* transcripts. In contrast, a MADS-box protein similar to JOINTLESS was found to be highest in the ripe pedicel sample. Finally, transcripts similar to the shattering genes from cereals were found to be not AZ specific, but more expressed in the ripe fruit pedicel samples. Overall, the results suggest conservation of function for certain genes involved in abscission may exist between dicots and monocots.

Gene expression profiles during ethylene induced and natural abscission suggest similar hormone related mechanisms in the oil palm AZ

Ethylene is well known to promote abscission in several fruit crop species, and has been used as an experimental tool to study abscission (Ruperti et al., 1998 Iannetta, 2000 ; Hilt and Bessis, 2003; Butenko et al., 2006; Barry and Giovannoni, 2007; Agusti et al., 2008 ; 2009; Bapat et al., 2010; Cheng et al., 2015 ; Hilt and Bessis, 2015; Zhang et al., 2015). However, a limitation with the

use of ethylene to induce abscission may lead to a large number of ethylene induced candidates that are not necessarily involved in abscission. Indeed, we identified a large number (1,957) of potential candidates differentially expressed in the ripe fruit AZ. This number is in the range of numbers found in the literature during studies with tomato (flower removal or 1-MCP pretreatment and flower removal, 1,789 differentially expressed), citrus (1313 and 1044 differentially expressed in AZ-C treated with ethylene for 4 and 24 h, respectively), litchi (2,771 differentially expressed after girdling plus defoliation), while less than that observed in olive (4,728 differentially expressed in AZ mature fruit AZ) and melon (4,801 differentially expressed in AZ of ripe fruit) (Meir et al., 2010; Corbacho et al., 2013; Gil-Amado and Gomez-Jimenez, 2013; Cheng et al., 2015; Li et al., 2015). Or next objective was to screen this differentially expressed population of transcripts to identify the most AZ enriched expression and robust abscission gene candidates.

During oil palm fruit development and ripening, changes in plant hormone quantities occur in the fruit mesocarp (Tranbarger et al., 2011). In particular, ethylene gas release increases along with transcript profiles for transcripts related to ethylene biosynthesis, perception and response. Indeed, these characteristics suggest that oil palm fruit is a climacteric fruit with regards to ethylene. Ethylene also induces oil palm fruit abscission and is known to be a key coordinator of cell separation during abscission and the ripening of climacteric fruits (Henderson and Osborne, 1994; Roberts and Gonzalez-Carranza, 2007; Roongsattham et al., 2012). In previous studies, it was proposed that ethylene is the primary signal separation in the primary AZ, while other signals are required for separation in the adjacent AZs, and that ethylene quickly induced cell separation in the primary AZ within 9h of treatment (Henderson and Osborne, 1994; Roongsattham et al., 2012). In this context, we focused our attention on changes in gene expression up to 9h after ethylene treatment. However, to minimize the false identification of genes induced by ethylene, but not involved in abscission, we compared the ripe fruit AZ expression with that found in immature fruit AZ (AZ30) and the ripe fruit pedicel (P150), and used these criteria to screen for differential gene expression predominantly in the ripe fruit AZ. This approach identified 45 annotated candidates, which suggested our screen was quite stringent. To expand the candidate list beyond those identified by this initial screen, we selected 34 additional highly abundant annotated transcripts in the ripe fruit AZ that were eliminated by our criteria. With this select group (79) of candidates, we then asked the question whether transcripts found during ethylene-induced abscission are also expressed in the ripe fruit AZ undergoing abscission in the field. The objectives were to compare the two processes to determine whether they have similar underlying transcriptional activity and to validate the role of our candidates during natural abscission.

Evidence from many different abscission model systems such as in tomato (Roberts et al., 1984; delCampillo and Bennett, 1996; Kalaitzis et al., 1997) and Arabidopsis (Grbić and Bleecker, 1995; Bleecker and Patterson, 1997; Butenko et al., 2006; Patterson et al., 2007; Cho et al., 2008; Li et al., 2015), supports that ethylene promotes abscission in dicots and is at least partially required for abscission, while there are also ethylene independent controls (Patterson and Bleecker, 2004; Butenko et al., 2006). Indeed, auxin is thought to counteract ethylene as an inhibitor of abscission, although a functional IAA signaling pathway is necessary for abscission to occur (Basu et al., 2013). In tomato, increased sensitivity to ethylene is thought to occur as auxin flow is reduced due to decrease biosynthesis and/or polar auxin transport from the distal organ, and resulting altered expression of auxin-regulated genes (Meir et al., 2006; Meir et al., 2010; Couzigou et al., 2015; Meir et al., 2015). The oil palm ripe fruit AZ responds to ethylene treatment with a massive increase in transcripts for ACO. During natural abscission, a similar increase is observed in the AZ of 120 DAP fruit, and remains high in fruit undergoing natural abscission. We also observed a consistent downward trend of expression for three auxin responsive proteins during both ethylene and naturally induced abscission, which parallels the decrease in IAA observed in the fruit mesocarp (Tranbarger et al., 2011). Furthermore, an auxin efflux protein and an IAA-amino acid hydrolase are ethylene induced by 3h, and have high expression in the ripe fruit AZ during natural abscission. The similar expression profiles for these two genes suggests both ethylene treatment or ethylene produced during natural ripening results in transcriptional changes to mobilize both local free IAA and amino acid conjugated IAA pools via efflux transport and IAA-amino acid hydrolysis respectively. Together, these observations are consistent with the idea that ethylene promotion and auxin inhibition of abscission are also accompanied by changes in auxin homeostasis through ethylene regulated transcriptional changes in this monocot AZ, analogous to the emerging model from dicots (Meir et al., 2010; Basu et al., 2013).

Ethylene induced and natural abscission involves the transcriptional coordination of pectin modifying and hydrolyzing enzymes

Earlier work on oil palm abscission suggested that pectin with a low methylation status and high ethylene inducible PG activity in the AZ are key mechanisms for oil palm fruit abscission (Henderson and Osborne, 1994; Henderson et al., 2001). Our initial molecular studies corroborated this previous work with the identification *EgPG4*; a highly ethylene induced *PG* in the AZ (Roongsattham et al., 2012). The current study provides more evidence for the importance of pectin by the identification of two additional PGs (renamed *EgPGAZ1* and *EgPGAZ2*) with similarity to the

Arabidopsis *ADPG1* and *ADPG2* involved in seed abscission and floral organ abscission respectively (Ogawa et al., 2009). In addition, a transcript for a pectinesterase (renamed *EgPME*) has similar profiles to the three PGs in the AZ during ethylene and naturally induced abscission, with a consistent increase of transcript with a peak at 9h or in ripe fruit. Collectively, it appears that these enzymes are highly coordinated transcriptionally in the AZ by either ethylene treatment or during natural ripening. Indeed, PG transcripts and activity increase in various species during the abscission process, and can be induced by ethylene or inhibited by auxin (Taylor et al., 1991; Bonghi et al., 1992; Taylor et al., 1993; Kalaitzis et al., 1995; Kalaitzis, 1997 ; Burns et al., 1998). In tomato, there is a single PG transcript, pTOM6, expressed during fruit ripening (Grierson et al., 1986; Sheehy et al., 1988 ; Smith et al., 1988), while four other PGs (TAPG1, TAPG2, TAPG4, and TAPG5) are expressed in the flower and leaf AZ (Kalaitzis et al., 1995; Kalaitzis et al., 1997 ; Hong and Tucker, 1998). In oil palm, *EgPG4* is highly expressed in the mesocarp during ripening and induced in the AZ in response to ethylene (Roongsattham et al., 2012). In contrast, *EgAZPG1* and *2* are very specific to the AZ based on a search of our mesocarp transcriptome database and qPCR analysis (Figure S5). Like *EgPG4*, *EgPME* is also expressed in the mesocarp so may also function during mesocarp ripening.

The main type of pectin in primary walls and the main constituent of the middle lamella is homogalacturonan (HG), a galacturonic acid polymer that exists in both methylesterified, less methylesterified and unmethylesterified forms (Mohnen, 2008). The consequence of PME activity includes not only the demethylesterification of HG, but also the generation of methanol and a decrease in pH (Wolf and Greiner, 2012). Complete demethylesterified HG can become stiff due to calcium cross-linking of adjacent HG molecules, while a pH decrease can provide more optimal conditions for hydrolysis by PG. In addition, an increase in demethylesterified HG may be more easily hydrated and lead to cell wall loosening (Wolf and Greiner, 2012). Indeed, the current model is that PME demethylesterifies HG, which subsequently is more susceptible to PG hydrolysis that could result in cell wall loosening (Verlent et al., 2005). Finally, combined PME and PG activities could release specific signaling oligogalacturonides, and in the case of the oil palm, could be a potential signal for activation of cell separation in the adjacent AZs as previously proposed (Henderson and Osborne, 1994).

Transcript profiles of a non-shedding oil palm tree substantiate processes and key genes required for oil palm fruit abscission

For further validation of the candidates identified during ethylene treatment and natural abscission, we examined gene expression the AZ of a tree that does not abscise its fruit. The AZ in this tree appears to develop normally and the non-abscission character does not appear to be due to a mutation in a gene such as in the tomato *JOINTLESS* tomato or Arabidopsis *BLADE-ON-PETIOLE1/2* (Mao et al., 2002; McKim et al., 2008). Our transcript profiling results support the hypothesis that the cause of the non-shedding character is a change in the regulation upstream of key genes involved in the process. Notably, abundance of all the pectin related transcripts, which are characterized in having coordinated expression profiles during abscission, are all very low in the AZ in these trees, corroborating their importance for the abscission process. Furthermore, our results point to the importance of gene expression of transcripts encoding other cell wall related functions including expansin, thaumatin-like, beta-1,3-glucanase 2, inositol oxygenase and beta-galactosidase are also expressed in very low amounts in the AZ of the non-shedding trees. Expansins are proteins that directly induce the extension of isolated plant cell walls (McQueen-Mason et al., 1992).

Expansin activity and gene expression were also reported during ethylene-promoted leaflet abscission in *Sambucus nigra*, and overexpression enhanced while reduced expression of expansin attenuated abscission at the base of the leaf pedicel in Arabidopsis (Cho and Cosgrove, 2000; Belfield et al., 2005). While expansins appear to function by disrupting hydrogen bonds between cellulose microfibrils and xyloglucans that tether them to one another in plant cell walls their specific roles during the cell separation process during abscission is unclear (McQueen-Mason and Cosgrove, 1994; McQueen-Mason and Cosgrove, 1995). Our data support a role of expansins in the AZ of mature fruit during abscission, and may be important to initiate cell wall loosening (Lashbrook and Cai, 2008).

Thaumatin-like proteins are pathogenesis-related (PR) proteins with antifungal activity involved in systematically acquired resistance and stress response in plants (Hejgaard et al., 1991; Vigers et al., 1992). Transcripts for thaumatin-like proteins were also found highly expression in the AZ of bean and in the AZ of peach after induction by ethylene (del Campillo and Lewis, 1992; Ruperti et al., 2002). Thaumatin-like proteins may be part of a defensive response by the plant against possible pathogen attack when the separated AZ tissue is exposed to the environment. However, it is unclear whether these proteins may also play an active role in the abscission process. While thaumatin transcripts increase in the mature fruit AZ during both ethylene and natural induced abscission and is low in the non-shedding AZ, an increase is observed in the ripe fruit pedicel,

mesocarp (data not shown) and in immature fruit AZ, so our evidence does not suggest a specific role during abscission.

Another PR protein are the *β*-1,3-glucanases that hydrolyse the *β*-1,3-glucans of the cell wall of fungi (Söderháll, 1981). As with thaumatin, increases in other tissues suggests a general role during ethylene induction related to defense, however the overexpression of *β*-1,3-glucanase was shown recently to increase pectin content and composition and we cannot rule out a direct role in abscission (Wojtasik et al., 2013).

β-galactosidase hydrolyze terminal non-reducing *β*-D-galactosyl residues from *β*-D-galactosides and are found in a wide range of plants (Smith et al., 1998). A study on mature fruit abscission of Valencia orange revealed an increase in expression of a *β*-galactosidase in the AZ in response to ethylene (Wu and Burns, 2004). Interestingly, a *β*-galactosidase the Arabidopsis mutant *bgal10* results in changes in xyloglucan composition associated with a decrease in cell elongation and shorter siliques and sepals (Sampedro et al., 2012). Furthermore, expression analysis revealed that *AtBGAL10* was high in many cell types undergoing wall extension or remodeling, including AZs. Our results suggest a potential role in the ripe fruit AZ, possible as with expansin for cell wall loosening. Finally, inositol oxygenase is an enzyme of one pathway to synthesize UDP-glucuronic acid, a precursor for plant cell wall polysaccharides including pectin (Loewus and Murthy, 2000; Kanter et al., 2005). While no specific role in abscission has been proposed, it suggests the metabolism of the AZ cells treated with ethylene respond to provide precursors for cell wall *de novo* biosynthesis.

Along cell wall biosynthesis, modification and disassembly, we observed genes with functions not typically associated with abscission but that were nonetheless expressed strongly associated with ethylene and natural induced abscission, and with opposite expression in the non-shedding AZ. *β*-ureidopropionase is an enzyme involved in the final step of the reductive catabolism of pyrimidine nucleotides that results in *β*-alanine production and a remobilized source of nitrogen (Walsh et al., 2001; Zrenner et al., 2009). In relation to development, *β*-ureidopropionase activity is important for tomato pollen germination, but the exact role is unknown (Shen et al., 2014). The oil palm transcript increases during both ethylene and natural induced abscission, and is expressed lowest in the non-shedding tree AZ, which makes this enzyme a robust candidate for a role during abscission. Similarly, a serine/threonine protein kinase is also highly associated to have a role during oil palm fruit abscission. This very large super family of proteins makes it difficult to predict specific functions from similarities, but our data support a role in signal transduction in the AZ during abscission. An alpha/beta hydrolase was also highly induced in the AZ during ethylene and natural abscission, and the most similar Arabidopsis protein was associated to the endoplasmic reticulum

(Nikolovski et al., 2012). Finally an ankyrin Zinc finger TF decrease in abundance in the AZ during ethylene and natural abscission, and was highly expressed in the AZ of the non-shedding tree. The most similar Arabidopsis proteins are related to confers resistance to *Xanthomonas oryzae* pv *oryzae* through a JA-dependent pathway, and the regulation of plant innate immunity (Deng et al., 2012; Maldonado-Bonilla, 2014). A decrease in abundance during the ethylene and natural abscission, in addition to a high expression in the non-shedding AZ supports a functional role for this TF during abscission.

The identification of robust gene candidates and the key processes in the AZ during oil palm fruit abscission

The major objective of the current study was to identify AZ specific expression related to the abscission process. Surprisingly, we did not find a large number of AZ specific expression as found by other transciptome studies such as in citrus fruit (Cheng et al., 2015), in olive (Gil-Amado and Gomez-Jimenez, 2013). However, we found a small number of candidates with highly coordinated expression during ethylene and natural abscission, and with opposite expression in the non-shedding tree AZ, hence, with profiles consistently associated with the cell separation process in the AZ. Furthermore, to the best of our knowledge we present the first large-scale proteomics study of monocot AZ during abscission. Interestingly, while we did not find the same candidates as with the transcriptome approach, we identified similar keys processes that are activated at both the transcriptional and proteome levels, such as cell wall biosynthesis, transcription and hormone homeostasis. Finally, both approaches also point to changes in components for the 26S proteasome pathway, which suggests degradation of targets may be a possible reason for the short time period (9h) for cell separation to take place.

METHODS

Plant material sampling and preparation

For the ethylene-induced abscission transcriptome analysis, oil palm (*Elaeis guineensis*) fruit bunches at 30 and 150 Days After Pollination (DAP) from a *tenera* clone (clone C) produced in Thailand were collected at the Golden Tenera Partnership Limited Krabi province as previously reported (Roongsattham et al., 2012). For the *E. guineensis* natural abscission and gene candidate validation experiments, pedicel, AZ and mesocarp tissue from fruit bunches at 120 DAP (unripe and no abscission observed in field) and 160 DAP (ripe fruit bunches observed to shed fruit in the field) were collected. For Illumina sequencing, AZ samples at 30, 120 and 160 were collected. The backcross [hybrid palm LM10986D (*E. oleifera* H833D x *E. guineensis* LM3261D) x *E. guineensis* LM2509D] AZ samples for the gene candidate validation experiments were sampled from the clone MTC95, which retained fruit at 177 DAP and shed fruit at 198 DAP, in addition to the clone MTC180, which retained fruit at 274 and 283 DAP, collected from Palmeras de los Andes (PDA)/Murrin Corporation, Quinindé, Ecuador. The non-shedding backcross phenotype of the material from Ecuador was identified and analyzed by the phenotypic test previously described (Fooyontphanich et al, 2015). All fruit bunches, fruit and tissues were sampled as previously reported (Roongsattham et al., 2012).

Sample preparation for RNA extraction, histology and microscopy analysis

For RNA extractions, the natural abscission fruit bunches at 120 DAP (no abscission) and 160 DAP (fruit abscission observed) from Thailand were collected and the base of fruits containing AZ were sampled as follows: the spikelets were removed from the bunches, rinsed in water, then individual fruit containing the base of the fruit which containing the AZ (approximately 50 AZ pieces were collected) and a slice of the spikelet stalk were removed with scalpel, then the base of the fruits were cut at different position (M, AZ and P) and weighed at approximately 3 grams then frozen immediately in liquid nitrogen. Material of MTC backcross from Ecuador were cleaned and processed with the same procedure as in Thailand but the fruits were cut only to collect the AZ and total weights were approximately 3-6 grams. The AZ samples that were sequenced were enriched in the primary AZ, but also contain portions of mesocarp and pedicel tissues. An approximation of AZ in the samples was performed based on the areas measured under a stereoscope and resulted in estimations of mesocarp. Both of materials from the two sources were shipped back to France by air

cargo. In Montpellier total RNA from samples were extracted as described previously by using Cesium Chloride method (Morcillo *et al*., 2006). RNA quality was gel verified and quantified spectrophotometrically (NanoDrop, ThermoScientific). For cDNA synthesis were processed as describe previously (Roongsattham et al., 2012). From measurements of the area of the samples, the size of the M, AZ and pedicel tissues are approximately 46, 12 and 42% respectively (Supplemental Figure S6).

Histology and microscopy analysis

For histology analysis, the base of the fruits containing the AZ were collected and processed as previously described (Fooyontphanich et al, 2015). In Montpellier, fixed samples were also processed as previously described (Fooyontphanich et al, 2015) and stained with the following dyes; Toluidine Blue, Ruthidium Red and DAPI for comparison. Samples were then mounted on slides with Mowiol and observed with a bright-field microscope (Leica DM6000) using different numeric apertures. To visualize the AZ, tissue sections were also observed and photographs were taken with a Retiga 2000R camera (Qimaging).

454 Sequencing data analysis and data mining

AZ (30 DAP and 150 DAP) and pedicel (30 DAP) samples selected for 454 pyrosequencing were obtained by treating spikelets of fruit at 30 DAP and 150 DAP with ethylene at 0h, 3h, 6h and 9h as previously described (Roongsattham et al., 2012). Total RNA from AZ and pedicel tissue samples described above was extracted as previously (Morcillo *et al*., 2006). The titanium kit (Roche) was used and cDNAs derived from the different tissues and different ethylene treatment time points were tagged independently and then mixed together in one sample for 454 pyrosequencing carried out by Biotech, Thailand. The 454 pyrosequence analysis, *de novo* assembly, and contig annotation were performed following the methods described previously (Tranbarger et al., 2011). The reads were processed and assembled using an automated pipeline previously described (Argout et al., 2008; Tranbarger et al., 2011). After assembled contigs were annotated and cleaned, we applied a candidate and a statistical approach to analyze the transcriptome. The candidate approach was based on a review of publications related to organ abscission including several recent reviews of the subject in addition to studies carried out previously by our lab group (Estornell et al. 2013, Acosta and Farmer 2009). The nucleotide sequences of each gene candidate selected from the literature were collected from NCBI database (http://blast.ncbi.nlm.nih.gov) in FASTA format and

compared by tblastx against the ethylene induced abscission transcriptome database (originating from the 454 pyrosequencing of AZ 30 and 150 DAP and P 150DAP) with an E-value cutoff of 1E-15. The most similar contigs identified from this analysis were then compared by blastn against the tomato (*Solanum lycopersicum*) and Arabidopsis (*Arabidopsis thaliana*) non-redundant nucleotide collections at NCBI and only first five hits (lowest E values) were kept. The contigs identified from this blast step were then compared by blastn with previous transcriptome data to provide information on read abundance in the mesocarp tissue during ripening (Tranbarger et al., 2011). The annotation of the sequences was done as previously described (Tranbarger et al., 2011). All of this information was put together and the read numbers in each tissue were used to create an overview of the presence and relative abundance of each candidate in each tissue (see appendix Table S5 for raw data used to generate Figure 2).

The statistical approach was performed as previously with some modifications (Tranbarger et al., 2011). Statistical differences in read abundances between the AZ150 DAP (ripe fruit) untreated ethylene field samples (0h) and each ethylene treatment time point (0h compared with 3h, 6h and 9h) were identified by Audic and Claverie statistics (Audic and Claverie, 1997). A contig was considered differentially expressed during the ethylene treatment time course when it exhibited a highly significant (P = 0.05) difference in read abundance when compared to the untreated 0h sample. P values obtained by the Audic and Claverie test were then transformed using the Bonferroni correction to control FDRs. The HCA was performed to group the differentially abundant contigs according to their transcription profile with the tool developed by Eisen et al. 1998 (http://rana.lbl.gov/eisen/). Differentially abundant contigs were then statistically (P = 0.05) compared using Audic and Claverie statistics to the P150 DAP and AZ30 DAP samples to identify ripe fruit (AZ150 DAP) specific or enriched gene expression. Each differentially abundant contig was compared by blastn against the mesocarp database with the E-value cutoff of 0 to identify the exact sequence and determine presence and abundance during mesocarp development and ripening (Tranbarger et al., 2011).

Illumina data analysis

Sequencing of the three samples (AZ30, AZ120 and AZ160) was complete by the company GATC Biotech (www.gatc-biotech.com). Low quality reads were removed using Cutadapt. Trimmed reads were mapped using the BWA-MEM package with default parameters (Li, 2013). Samtools was used to count mapped reads and the number of reads per kilobase and million reads (RPKM) were then calculated (Li et al., 2009). The oil palm predicted CDS used for mapping was downloaded

from the NCBI website (http://www.ncbi.nlm.nih.gov/, GCF_000442705.1_EG5_rna.fna; January 2015).

Gene Ontology (GO) annotations

GO annotation analysis was performed to annotate and classify the differentially abundant contigs based on BLASTX alignment against the Uniprot database. The 1,957 differentially abundant contigs were analyzed with the Blast2Go desktop platform version (https://www.blast2go.com). The sequences were aligned by Blast2GO program and their annotations were predicted based on the UniProt Knowledgebase (UniProtKB). The different GO annotations for the sequences in the 4 clusters were searched and assigned. The GO categories; Biological Process, Molecular Function and Cellular Component were analyzed separately by Blast2Go. GO term enrichment of each cluster compared to all 1,957 differentially abundant contigs was tested with the Blast2GO enrichment Fisher's exact test with Benjamini Hochberg correction for multiple testing.

Primer design and qPCR data analysis

Primer pairs for the statistically significant contig gene candidates were designed using Primer3 and Primer3plus. The designed primers were tested with Amplify application (http://engels.genetics.wisc.edu/amplify) to check primer pair specificity and primer dimer formation. Primers used for this study are listed on (appendix Table S4). Primer pairs were tested to estimate the efficiency values based on a standard curve generated from a serial dilution of pooled cDNA (1, 10, 100, and 1000 fold dilutions). Only primers with efficiency values that ranged between 1.95 and 2.0 were retained for qPCR analysis. Total RNA was isolated as previously described (Morcillo *et al*., 2006). qPCR was conducted as previous described (Fooyontphanich et al. 2015).

To validate the expression of gene candidates during natural abscission, *E. guineensis* AZ samples AZ120 (unripe fruit, no abscission) and AZ160 (ripe fruit undergoing abscission) and the backcross MTC95 at 177 DAP (R1) (unripe fruit, no abscission) and MTC95 at 198 DAP (R2) (ripe fruit undergoing abscission) were examined and compared with the backcross MTC180 at 274 DAP (R3) and 283 DAP (R4) with ripe fruit that do not undergo abscission (Fooyontphanich et al, 2015). *EgEf1α* (accession number: AY550990) transcript accumulation was relatively constant in all tissues examined and used for normalization. A control using RNA matrices was also conducted to validate the absence of DNA in each sample. Each time point was replicated three times and all amplified

cDNA fragments were sequenced by Beckman-Cogenics to verify the specificity of amplification products. Each individual sample comprised of 3-5 pooled biological repetitions submitted to qPCR analysis with three technical replicates. Relative expression of numbers of copies was calculated by the ΔΔCt method (Livak and Schmittgen, 2001). Results from the relative expression of the qPCR were calculated by using the maximum of each candidate and calculate as 1. Gene expressed is reported as the mean and standard error bars were calculated from the technical replicates. Results from qPCR analysis were exported and recorded in excel format then analyzed to create graphs of expression profiles with comparison with the reference gene *Ef1α*. The highest relative expression of each gene was calculated as 100% and decrease follow the real ratio. The percentage of each gene was then compared with the other genes.

Proteome analysis of the AZ soluble protein fraction during ethylene treatment

Samples of the fruit AZ at 180 DAP prior to treatment (0h) and treated or not with ethylene at 3h, 6h, 9h and 12h were prepared for the proteomic study as follows. AZ region of the oil palm fruits were ground with a mortar and pestle using liquid nitrogen. Fine powder was dissolved in 0.1% SDS. Two volumes of cold acetone was added and the mixture was mixed thoroughly by vortex; afterward, proteins were allowed to precipitate at -20°C for overnight. After centrifugation at 10,000*g* for 15 min, the pellet was dissolved in 0.15% Sodium Deoxycholate and mixed well with two volumes of chloroform. Phases were separated by centrifugation at 10,000*g* for 15 min. The upper aqueous phase was transferred to a new microtube and stored at -80^{o}C prior to use.

The pellets were resuspended in 0.01% SDS and determined protein concentration by Lowry method (Lowry et al., 1951). The absorbance at 750 nm (OD_{750}) was measured and the protein concentration was calculated using the standard curve, plotted between OD_{750} on Y-axis and BSA concentration (μg/ml) on X-axis.

Proteins were fractionated on SDS-PAGE mini slab gel (8 x 9 x 0.1 cm, Hoefer miniVE, Amersham Biosciences, UK). The polyacrylamide gel was prepared according to the standard method described by Laemmli (1970). The separating gel used for the fractionation of soluble proteins from the AZ region of the oil palm fruits contained 12.5% acrylamide. The equal volume of protein samples were mixed with 5 μl of 5X sample buffer (0.125M Tris-HCl pH 6.8, 20% glycerol, 4% SDS, 0.2M DTT, 0.02% bromophenol blue), boiled at 95^{o}C (WB-710M, Optima, Japan) for 5 min before loading onto the 12.5% SDS-PAGE. To estimate size of polypeptides, low molecular weight protein standard marker (Amersham Biosciences, UK) was used. Electrophoresis was

performed in SDS electrophoresis buffer (25mM Tris-HCl pH 8.3, 192mM glycine, 0.1% SDS) until the tracking dye reached the bottom of the gel. After the electrophoresis finished, gels were silver stained according to Blum et al (1987).

After protein spots were excised, the gel pieces were subjected to in-gel digestion using an in-house method developed by Proteomics Laboratory, Genome Institute, National Center for Genetic Engineering and Biotechnology (BIOTEC), National Science and Technology Development Agency (NSTDA), Thailand (Jaresitthikunchai et al., 2009). The gel plugs were dehydrated with 100% acetonitrile (ACN), reduced with 10mM DTT in 10mM ammonium bicarbonate at room temperature for 1 h and alkylated at room temperature for 1 h in the dark in the presence of 100mM iodoacetamide (IAA) in 10mM ammonium bicarbonate. After alkylation, the gel pieces were dehydrated twice with 100% ACN for 5 min. To perform in-gel digestion of proteins, 10 µl of trypsin solution (10 ng/µl trypsin in 50% ACN/10mM ammonium bicarbonate) was added to the gels followed by incubation at room temperature for 20 min, and then 20 µl of 30% ACN was added to keep the gels immersed throughout digestion. The gels were incubated at 37°C for a few hours or overnight. To extract peptide digestion products, 30 µl of 50% ACN in 0.1% formic acid (FA) was added into the gels, and then the gels were incubated at room temperature for 10 min in a shaker. Peptides extracted were collected and pooled together in the new tube. The pool extracted peptides were dried by vacuum centrifuge and kept at -80°C for further mass spectrometric analysis. The protein digest was injected into Ultimate 3000 LC System (Dionex, USA) coupled to ESI-Ion Trap MS (HCT Ultra PTM Discovery System, Bruker, Germany) with electrospray at a flow rate of 300 nl/min to a nanocolumn (Acclaim PepMap 100 C18, 3 mm, 100A, 75 mm id x 150 mm). A solvent gradient (solvent A: 0.1% formic acid in water; solvent B: 80% 0.1% formic acid in 80% acetonitrile was run in 40 min.

For proteins quantitation, DeCyder MS Differential Analaysis software (DeCyderMS, GE Healthcare (Johansson et al., 2006; Thorsell et al., 2007) was used. Acquired LC-MS raw data were converted and the PepDetect module was used for automated peptide detection, charge state assignments, and quantitation based on the peptide ions signal intensities in MS mode. The analyzed MS/MS data from DeCyderMS were submitted to database search using the Mascot software (Matrix Science, London, UK, Perkins et al., 1999) against database for protein identification. Database interrogation was; enzyme (trypsin); variable modifications (carbamidomethyl, oxidation of methionine residues); mass values (monoisotopic); protein mass (unrestricted); peptide mass tolerance (1 Da); fragment mass tolerance (±0.4 Da), peptide charge state (1+, 2+ and 3+) and max

missed cleavages (1). Proteins considered as identified proteins had at least two peptides with an individual mascot score corresponding to $p<0.05$ and $p<0.1$, respectively.

SUPPLEMENTARY DATA

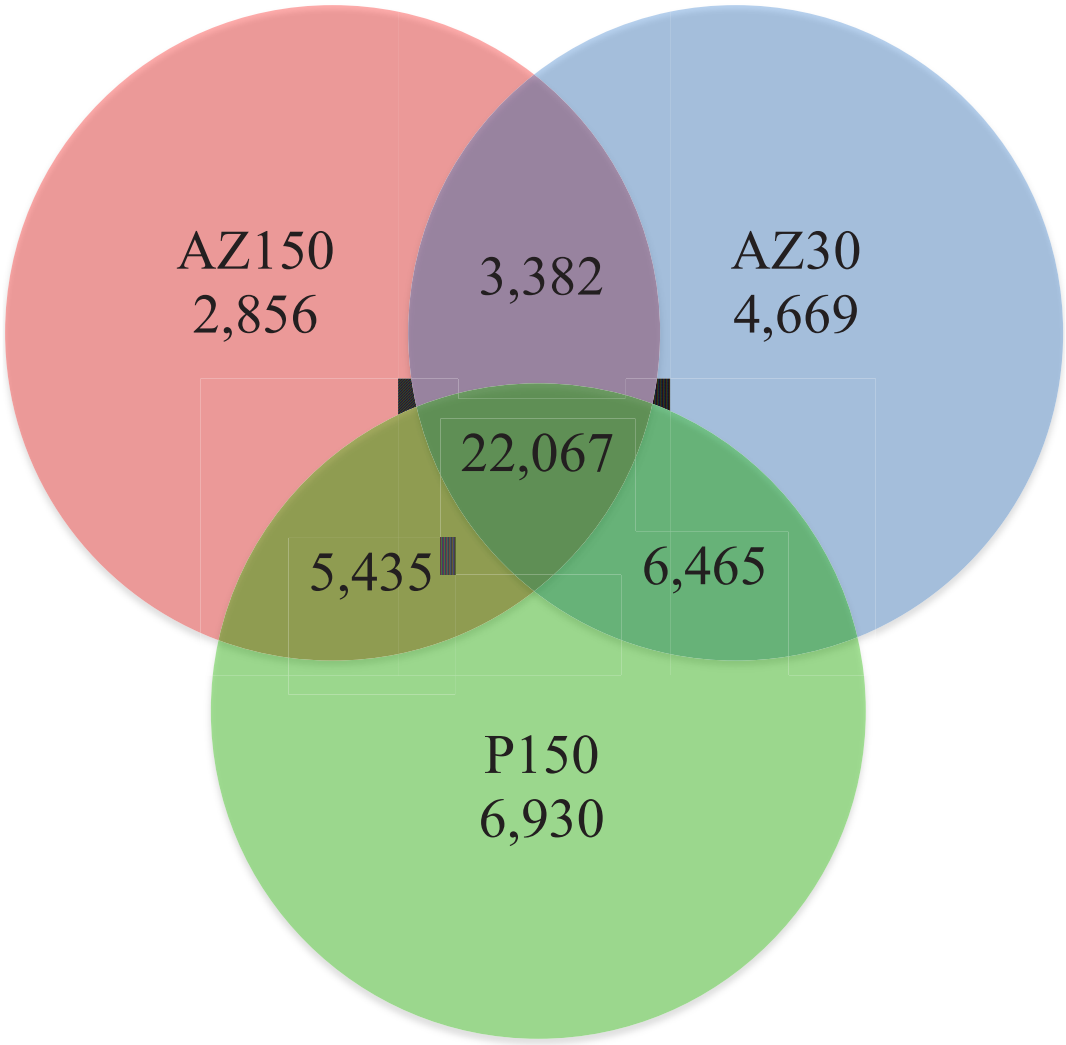

Figure S1. Venn diagram overview of 454 sequencing and numbers of unique and common contigs assembled between in each sample (AZ150, AZ30 and P150).

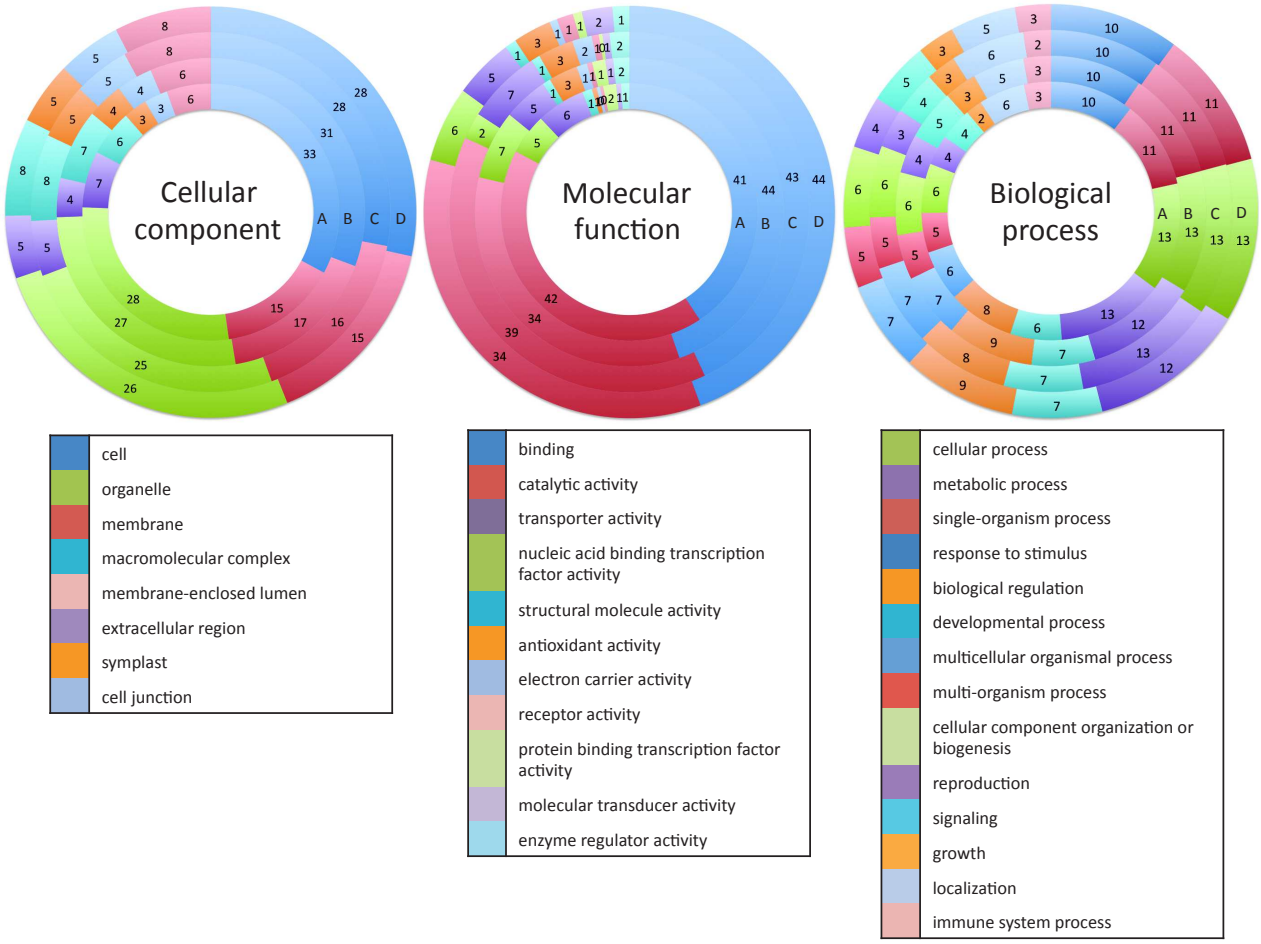

Figure S2. GO analysis shows the Cellular Component, Molecular Function and Biological Process annotation percentages for each cluster (A, B, C and D) of the 1,957 differentially abundant contigs identified.

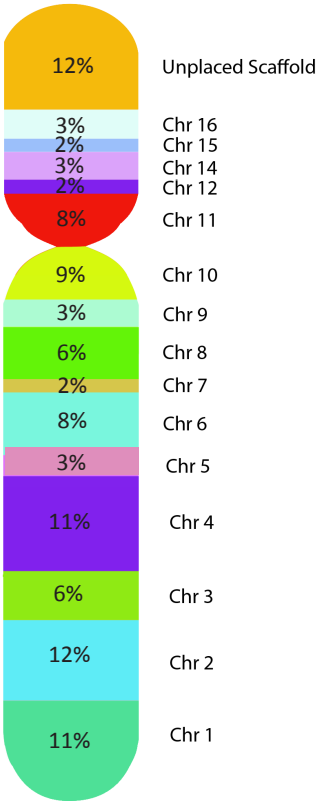

Figure S3. An overview of the chromosomal location of the candidates (in percentages for each chromosome) aligned to the oil palm genome.

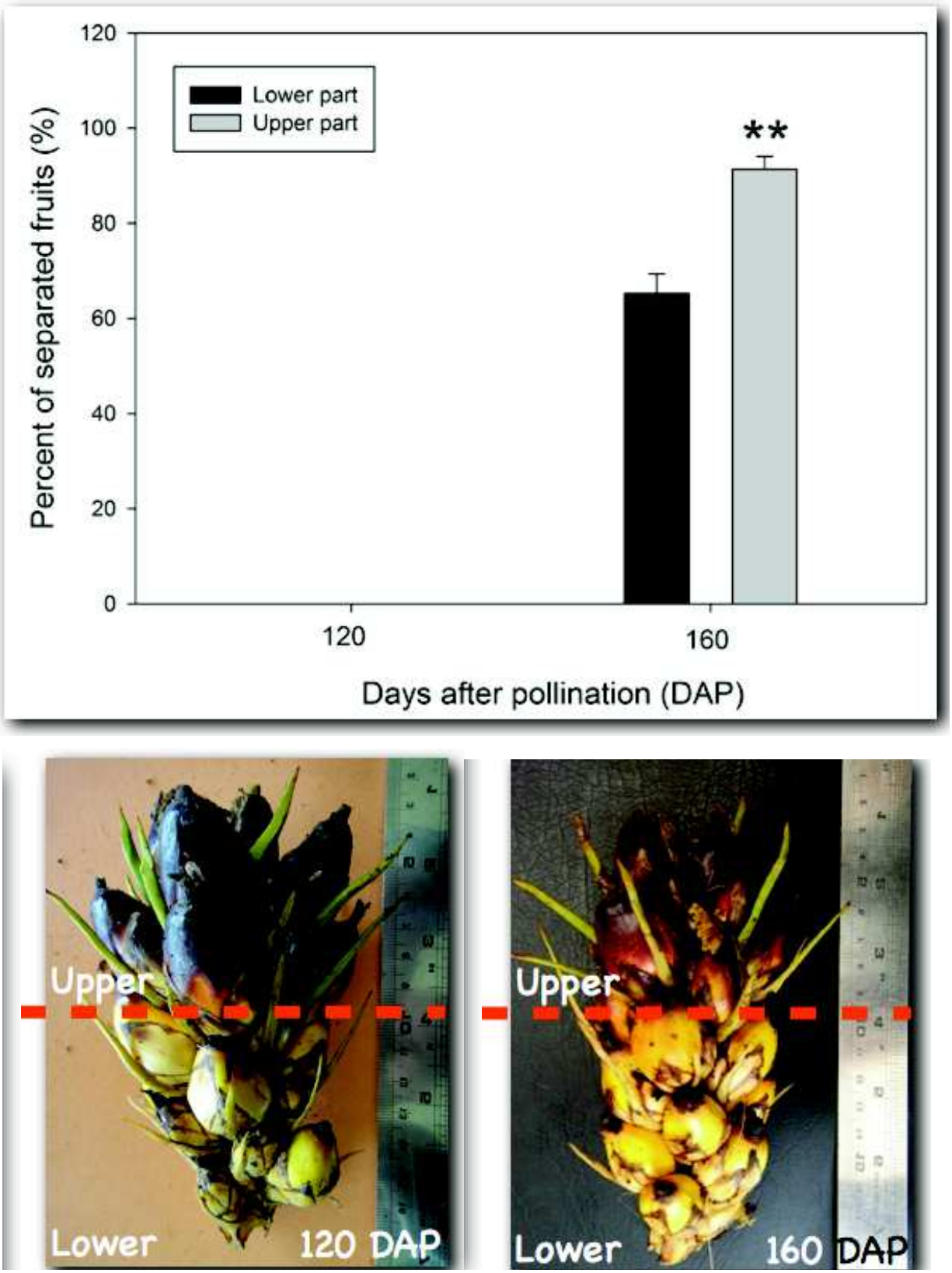

Figure S4. Fruit pull test with 120 and 160 DAP fruit.

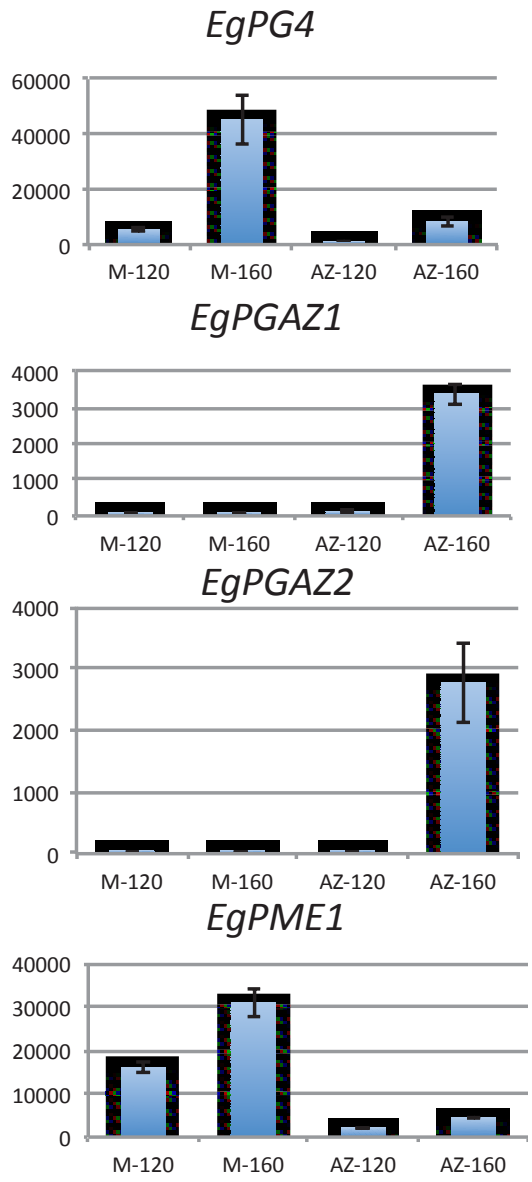

(RPKM)

Gene	XM	M-100	M-120	M-140	M-160	AZ 30	AZ 120	AZ 160
EgPG4	XM_010910254.1	0	1	13	2740	5	36	1938
EgPGAZ1	XM_010939219.1	0	0	0	0	1	5	201
EgPGAZ2	XM_010939232.1	0	0	0	2	1	12	697
EgPME	XM_010917893.1	0	0	12	54	3	110	1259

Figure S5. Tissue expression of the *EgPG4, EgPGAZ1, EgPGAZ2* and *EgPME1* by the qPCR.

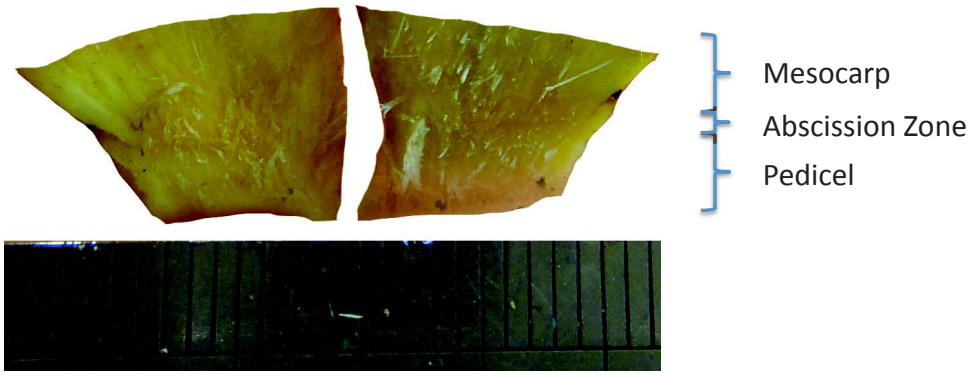

Tissue	Area (%)						mean	SD
Mesocarp	39	40.73	55.6	39.06	49.58	53.53	46.32	7.56
Abscission Zone	8.49	6.55	9.176	18.3	14.71	16.36	12.26	4.80
Pedicel	52.51	52.73	35.22	42.63	35.71	30.11	41.48	9.50

Figure S6. The measurements of the area of the fruit samples that were used in sample for RNA extraction.

ACKNOWLEDGEMENTS

This work was supported by Franco-Thai and Thailand Graduate Institute of Science and Technology (TGIST) scholarships to KF. Financial support for the project also came from PalmElit and IRD/CIRAD to KF, FM and TJT, and from the Kasetsart University Research and Development Institute (KURDI) to CJ. We especially thank Anek Limsrivilai and the staff at GoldenTenera Oil Palm Plantation in Thailand, Roberto Poveda and staff at the PDA/Murrin Companies (DANEC group) and Claude Louise of PalmElit in Quinindé, Ecuador for the excellent plant material and logistical support for the study.

REFERENCES

Agusti J, Merelo P, Cercos M, Tadeo FR, Talon M (2008) Ethylene-induced differential gene expression during abscission of citrus leaves. J Exp Bot **59:** 2717-2733

Agusti J, Merelo P, Cercos M, Tadeo FR, Talon M (2009) Comparative transcriptional survey between laser-microdissected cells from laminar abscission zone and petiolar cortical tissue during ethylene-promoted abscission in citrus leaves. Bmc Plant Biology **9**

Argout X, Fouet O, Wincker P, Gramacho K, Legavre T, Sabau X, Risterucci AM, Da Silva C, Cascardo J, Allegre M (2008) Towards the understanding of the cocoa transcriptome: Production and analysis of an exhaustive dataset of ESTs of Theobroma cacao L. generated from various tissues and under various conditions. BMC genomics **9:** 512

Bapat VA, Trivedi PK, Ghosh A, Sane VA, Ganapathi TR, Nath P (2010) Ripening of fleshy fruit: molecular insight and the role of ethylene. Biotechnology advances **28:** 94-107

Barry CS, Giovannoni JJ (2007) Ethylene and fruit ripening. Journal of Plant Growth Regulation **26:** 143-159

Basu MM, Gonzalez-Carranza ZH, Azam-Ali S, Tang S, Shahid AA, Roberts JA (2013) The manipulation of auxin in the abscission zone cells of Arabidopsis flowers reveals that indoleacetic acid signaling is a prerequisite for organ shedding. Plant Physiol **162:** 96-106

Belfield EJ, Ruperti B, Roberts JA, McQueen-Mason S (2005) Changes in expansin activity and gene expression during ethylene-promoted leaflet abscission in Sambucus nigra. Journal of Experimental Botany **56:** 817-823

Bleecker AB, Patterson SE (1997) Last exit: senescence, abscission, and meristem arrest in Arabidopsis. The Plant cell **9:** 1169-1179

Bonghi C, Rascio N, Ramina A, Casadoro G (1992) Cellulase and Polygalacturonase Involvement in the Abscission of Leaf and Fruit Explants of Peach. Plant Molecular Biology **20:** 839-848

Burns JK, Lewandowski DJ, Nairn CJ, Brown GE (1998) Endo-1,4-beta-glucanase gene expression and cell wall hydrolase activities during abscission in Valencia orange. Physiologia Plantarum **102:** 217-225

Burr CA, Leslie ME, Orlowski SK, Chen I, Wright CE, Daniels MJ, Liljegren SJ (2011) CAST AWAY, a Membrane-Associated Receptor-Like Kinase, Inhibits Organ Abscission in Arabidopsis. Plant Physiology **156:** 1837-1850

Butenko MA, Stenvik GE, Alm V, Saether B, Patterson SE, Aalen RB (2006) Ethylene-dependent and -independent pathways controlling floral abscission are revealed to converge using promoter::reporter gene constructs in the ida abscission mutant. J Exp Bot **57:** 3627-3637

Cheng C, Zhang L, Yang X, Zhong G (2015) Profiling gene expression in citrus fruit calyx abscission zone (AZ-C) treated with ethylene. Molecular Genetics and Genomics**:** 1-16

Cho H-T, Cosgrove DJ (2000) Altered expression of expansin modulates leaf growth and pedicel abscission in Arabidopsis thaliana. Proceedings of the National Academy of Sciences **97:** 9783-9788

Cho SK, Larue CT, Chevalier D, Wang H, Jinn T-L, Zhang S, Walker JC (2008) Regulation of floral organ abscission in Arabidopsis thaliana. Proceedings of the National Academy of Sciences **105:** 15629-15634

Corbacho J, Romojaro F, Pech JC, Latche A, Gomez-Jimenez MC (2013) Transcriptomic events involved in melon mature-fruit abscission comprise the sequential induction of cell-wall degrading genes coupled to a stimulation of endo and exocytosis. PLoS One **8:** e58363

Couzigou JM, Magne K, Mondy S, Cosson V, Clements J, Ratet P (2015) The legume NOOT−BOP−COCH−LIKE genes are conserved regulators of abscission, a major agronomical trait in cultivated crops. New Phytologist

del Campillo E, Lewis LN (1992) Identification and kinetics of accumulation of proteins induced by ethylene in bean abscission zones. Plant Physiology **98:** 955-961

delCampillo E, Bennett AB (1996) Pedicel breakstrength and cellulase gene expression during tomato flower abscission. Plant Physiology **111:** 813-820

Deng W, Yang Y, Ren Z, Audran-Delalande C, Mila I, Wang X, Song H, Hu Y, Bouzayen M, Li Z (2012) The tomato SlIAA15 is involved in trichome formation and axillary shoot development. The New phytologist **194:** 379-390

Estornell LH, Agusti J, Merelo P, Talon M, Tadeo FR (2013) Elucidating mechanisms underlying organ abscission. Plant Sci **199-200:** 48-60

Fernandez DE, Heck GR, Perry SE, Patterson SE, Bleecker AB, Fang SC (2000) The embryo MADS domain factor AGL15 acts postembryonically: Inhibition of perianth senescence and abscission via constitutive expression. Plant Cell **12:** 183-197

Gil-Amado JA, Gomez-Jimenez MC (2013) Transcriptome analysis of mature fruit abscission control in olive. Plant Cell Physiol **54:** 244-269

Grbić V, Bleecker AB (1995) Ethylene regulates the timing of leaf senescence in Arabidopsis. The Plant Journal **8:** 595-602

Grierson D, Maunders M, Slater A, Ray J, Bird C, Schuch W, Holdsworth M, Tucker G, Knapp J (1986) Gene expression during tomato ripening. Philosophical Transactions of the Royal Society B: Biological Sciences **314:** 399-410

Hejgaard J, Jacobsen S, Svendsen I (1991) Two antifungal thaumatin-like proteins from barley grain. FEBS letters **291:** 127-131

Henderson J, Davies HA, Heyes SJ, Osborne DJ (2001) The study of a monocotyledon abscission zone using microscopic, chemical, enzymatic and solid state C-13 CP/MAS NMR analyses. Phytochemistry **56:** 131-139

Henderson J, Osborne DJ (1990) Cell Separation and Anatomy of Abscission in the Oil Palm, Elaeis guineensis Jacq. Journal of Experimental Botany **41:** 203-210

Henderson J, Osborne DJ (1990) Cell-Separation and Anatomy of Abscission in the Oil Palm, Elaeis-Guineensis Jacq. Journal of Experimental Botany **41:** 203-210

Henderson J, Osborne DJ (1994) Intertissue Signaling during the 2-Phase Abscission in Oil Palm Fruit. Journal of Experimental Botany **45:** 943-951

Hilt C, Bessis R (2003) Abscission of grapevine fruitlets in relation to ethylene
biosynthesis. Vitis **42:** 1-3

Hilt C, Bessis R (2015) Abscission of grapevine fruitlets in relation to ethylene biosynthesis. VITIS-Journal of Grapevine Research **42:** 1

Hong SB, Tucker ML (1998) Genomic organization of six tomato polygalacturonases and 5 ' upstream sequence identity with tap1 and win2 genes. Molecular and General Genetics **258:** 479-487

Kalaitzis P, Koehler SM, Tucker ML (1995) Cloning of a Tomato Polygalacturonase Expressed in Abscission. Plant Molecular Biology **28:** 647-656

Kalaitzis P, Solomos T, Tucker ML (1997) Three different polygalacturonases are expressed in tomato leaf and flower abscission, each with a different temporal expression pattern. Plant Physiology **113:** 1303-1308

Kanter U, Usadel B, Guerineau F, Li Y, Pauly M, Tenhaken R (2005) The inositol oxygenase gene family of Arabidopsis is involved in the biosynthesis of nucleotide sugar precursors for cell-wall matrix polysaccharides. Planta **221:** 243-254

Lashbrook CC, Cai S (2008) Cell wall remodeling in Arabidopsis stamen abscission zones: temporal aspects of control inferred from transcriptional profiling. Plant signaling & behavior **3:** 733-736

Li C, Wang Y, Huang X, Li J, Wang H, Li J (2015) An improved fruit transcriptome and the identification of the candidate genes involved in fruit abscission induced by carbohydrate stress in litchi. Name: Frontiers in Plant Science **6:** 439

Li H (2013) Aligning sequence reads, clone sequences and assembly contigs with BWA-MEM. arXiv preprint arXiv:1303.3997

Li H, Handsaker B, Wysoker A, Fennell T, Ruan J, Homer N, Marth G, Abecasis G, Durbin R (2009) The sequence alignment/map format and SAMtools. Bioinformatics **25:** 2078-2079

Liljegren SJ, Leslie ME, Darnielle L, Lewis MW, Taylor SM, Luo RB, Geldner N, Chory J, Randazzo PA, Yanofsky MF, Ecker JR (2009) Regulation of membrane trafficking and organ separation by the NEVERSHED ARF-GAP protein. Development **136:** 1909-1918

Lin Z, Griffith ME, Li X, Zhu Z, Tan L, Fu Y, Zhang W, Wang X, Xie D, Sun C (2007) Origin of seed shattering in rice (Oryza sativa L.). Planta **226:** 11-20

Livak KJ, Schmittgen TD (2001) Analysis of relative gene expression data using real-time quantitative PCR and the 2− ΔΔCT method. methods **25:** 402-408

Loewus FA, Murthy PP (2000) Myo-inositol: its biosynthesis and metabolism. Plant Science **150:** 1-19

Maldonado-Bonilla LD (2014) Composition and function of P bodies in Arabidopsis thaliana. Frontiers in plant science **5**

Mao ZC, Yu QJ, Zhen W, Guo JY, Hu YL, Gao Y, Lin ZP (2002) Expression of ipt gene driven by tomato fruit specific promoter and its effects on fruit development of tomato. Chinese Science Bulletin **47:** 928-+

McKim SM, Stenvik GE, Butenko MA, Kristiansen W, Cho SK, Hepworth SR, Aalen RB, Haughn GW (2008) The BLADE-ON-PETIOLE genes are essential for abscission zone formation in Arabidopsis. Development **135:** 1537-1546

McQueen-Mason S, Cosgrove DJ (1994) Disruption of hydrogen bonding between plant cell wall polymers by proteins that induce wall extension. Proceedings of the National Academy of Sciences **91:** 6574-6578

McQueen-Mason S, Durachko DM, Cosgrove DJ (1992) Two endogenous proteins that induce cell wall extension in plants. The Plant Cell **4:** 1425-1433

McQueen-Mason SJ, Cosgrove DJ (1995) Expansin mode of action on cell walls (analysis of wall hydrolysis, stress relaxation, and binding). Plant Physiology **107:** 87-100

Meir S, Hunter DA, Chen JC, Halaly V, Reid MS (2006) Molecular changes occurring during acquisition of abscission competence following auxin depletion in Mirabilis jalapa. Plant Physiol **141:** 1604-1616

Meir S, Philosoph-Hadas S, Sundaresan S, Selvaraj KS, Burd S, Ophir R, Kochanek B, Reid MS, Jiang CZ, Lers A (2010) Microarray analysis of the abscission-related transcriptome in the tomato flower abscission zone in response to auxin depletion. Plant Physiol **154:** 1929-1956

Meir S, Sundaresan S, Riov J, Agarwal I, Philosoph-Hadas S (2015) Role of auxin depletion in abscission control. Stewart Postharvest Review **11:** 1-15

Mohnen D (2008) Pectin structure and biosynthesis. Current opinion in plant biology **11:** 266-277

Nikolovski N, Rubtsov D, Segura MP, Miles GP, Stevens TJ, Dunkley TP, Munro S, Lilley KS, Dupree P (2012) Putative glycosyltransferases and other plant Golgi apparatus proteins are revealed by LOPIT proteomics. Plant physiology **160:** 1037-1051

Nowak J, Dengler NG, Posluszny U (2007) The role of abscission during leaflet separation in Chamaedorea elegans (Arecaceae). International Journal of Plant Sciences **168:** 533-545

Ogawa M, Kay P, Wilson S, Swain SM (2009) ARABIDOPSIS DEHISCENCE ZONE POLYGALACTURONASE1 (ADPG1), ADPG2, and QUARTET2 are Polygalacturonases required for cell separation during reproductive development in Arabidopsis. Plant Cell **21:** 216-233

Patterson S, Butenko M, Kim J (2007) Ethylene responses in abscission and other processes of cell separation in Arabidopsis. *In* Advances in Plant Ethylene Research. Springer, pp 271-278

Patterson SE (2001) Cutting loose. Abscission and dehiscence in Arabidopsis. Plant Physiology **126:** 494-500

Patterson SE, Bleecker AB (2004) Ethylene-dependent and -independent processes associated with floral organ abscission in Arabidopsis. Plant Physiology **134:** 194-203

Roberts JA, Gonzalez-Carranza Z (2007) Cell Separation and Adhesion Processes in Plants *In* JA Roberts, Z Gonzalez-Carranza, eds, Plant Cell Separation and Adhesion, Annual Plant Reviews. Blackwell Publishing Ltd, pp 1-7

Roberts JA, Schindler CB, Tucker GA (1984) Ethylene-Promoted Tomato Flower Abscission and the Possible Involvement of an Inhibitor. Planta **160:** 159-163

Roongsattham P (2011) Cell separation processes that underlie fruit abscission and shedding in oil palm (Elaeis guineensis Jacq.). UNIVERSITÉ MONTPELLIER 2, Montpellier, France

Roongsattham P, Morcillo F, Jantasuriyarat C, Pizot M, Moussu S, Jayaweera D, Collin M, Gonzalez-Carranza Z, Amblard P, Tregear JW, Tragoonrung S, Verdeil JL, Tranbarger TJ (2012) Temporal and spatial expression of polygalacturonase gene family members reveals divergent regulation during fleshy fruit ripening and abscission in the monocot species oil palm. BMC Plant Biology **12:** 150

Ruperti B, Bonghi C, Tonutti P, Ramina A (1998) Ethylene biosynthesis in peach fruitlet abscission. Plant, Cell and Environment **21:** 731-737

Ruperti B, Cattivelli L, Pagni S, Ramina A (2002) Ethylene-responsive genes are differentially regulated during abscission, organ senescence and wounding in peach (Prunus persica). Journal of Experimental Botany **53:** 429-437

Sampedro J, Gianzo C, Iglesias N, Guitián E, Revilla G, Zarra I (2012) AtBGAL10 is the main xyloglucan β-galactosidase in Arabidopsis, and its absence results in unusual xyloglucan subunits and growth defects. Plant physiology **158:** 1146-1157

Sheehy RE, Kramer M, Hiatt WR (1988) Reduction of polygalacturonase activity in tomato fruit by antisense RNA. Proceedings of the National Academy of Sciences **85:** 8805-8809

Shen YH, Chen YH, Liu HY, Chiang FY, Wang YC, Hou LY, Lin JS, Lin CC, Lin HH, Lai HM (2014) Expression of a gene encoding β−ureidopropionase is critical for pollen germination in tomatoes. Physiologia plantarum **150:** 425-435

Singh R, Ong-Abdullah M, Low ETL, Manaf MAA, Rosli R, Nookiah R, Ooi LCL, Ooi SE, Chan KL, Halim MA, Azizi N, Nagappan J, Bacher B, Lakey N, Smith SW, He D, Hogan M, Budiman MA, Lee EK, DeSalle R, Kudrna D, Goicoechea JL, Wing RA, Wilson RK, Fulton RS, Ordway JM, Martienssen RA, Sambanthamurthi R (2013) Oil palm genome sequence reveals divergence of interfertile species in Old and New Worlds. Nature **500:** 335-339

Smith C, Watson C, Ray J, Bird C, Morris P, Schuch W, Grierson D (1988) Antisense RNA inhibition of polygalacturonase gene expression in transgenic tomatoes.

Smith DL, Starrett DA, Gross KC (1998) A Gene Coding for Tomato Fruit β-Galactosidase II Is Expressed during Fruit Ripening Cloning, Characterization, and Expression Pattern. Plant Physiology **117:** 417-423

Söderháll K (1981) Fungal cell wall β-1, 3-glucans induce clotting and phenoloxidase attachment to foreign surfaces of crayfish hemocyte lysate. Developmental & Comparative Immunology **5:** 565-573

Taylor JE, Coupe SA, Picton S, Roberts JA (1994) Characterization and Accumulation Pattern of an Messenger-Rna Encoding an Abscission-Related Beta-1,4-Glucanase from Leaflets of Sambucus-Nigra. Plant Molecular Biology **24:** 961-964

Taylor JE, Tucker GA, Lasslett Y, Smith CJS, Arnold CM, Watson CF, Schuch W, Grierson D, Roberts JA (1991) Polygalacturonase Expression during Leaf Abscission of Normal and Transgenic Tomato Plants. Planta **183:** 133-138

Taylor JE, Webb STJ, Coupe SA, Tucker GA, Roberts JA (1993) Changes in Polygalacturonase Activity and Solubility of Poluronides during Ethylene-Stimulated Leaf Abscission in Sambucus-Nigra. Journal of Experimental Botany **44:** 93-98

Taylor JE, Whitelaw CA (2001) Signals in abscission. New Phytologist **151:** 323-339

Tranbarger TJ, Dussert S, Joet T, Argout X, Summo M, Champion A, Cros D, Omore A, Nouy B, Morcillo F (2011) Regulatory mechanisms underlying oil palm fruit mesocarp maturation, ripening, and functional specialization in lipid and carotenoid metabolism. Plant Physiol **156:** 564-584

VAN DOORN WG (2002) Effect of ethylene on flower abscission: a survey. Annals of Botany **89:** 689-693

Verlent I, Smout C, Duvetter T, Hendrickx M, Van Loey A (2005) Effect of temperature and pressure on the activity of purified tomato polygalacturonase in the presence of pectins with different patterns of methyl esterification. Innovative food science & emerging technologies **6:** 293-303

Vigers AJ, Wiedemann S, Roberts WK, Legrand M, Selitrennikoff CP, Fritig B (1992) Thaumatin-like pathogenesis-related proteins are antifungal. Plant Science **83:** 155-161

Walsh TA, Green SB, Larrinua IM, Schmitzer PR (2001) Characterization of plant β-ureidopropionase and functional overexpression in Escherichia coli. Plant physiology **125:** 1001-1011

Wojtasik W, Kulma A, Dymińska L, Hanuza J, Żebrowski J, Szopa J (2013) Fibres from flax overproducing β-1, 3-glucanase show increased accumulation of pectin and phenolics and thus higher antioxidant capacity. BMC biotechnology **13:** 10

Wolf S, Greiner S (2012) Growth control by cell wall pectins. Protoplasma **249:** 169-175

Wu ZC, Burns JK (2004) A beta-galactosidase gene is expressed during mature fruit abscission of 'Valencia' orange (Citrus sinensis). Journal of Experimental Botany **55:** 1483-1490

Zhang X-l, Qi M-f, Xu T, Lu X-j, Li T-l (2015) Proteomics profiling of ethylene-induced tomato flower pedicel abscission. Journal of proteomics **121:** 67-87

Zhou Y, Lu D, Li C, Luo J, Zhu BF, Zhu J, Shangguan Y, Wang Z, Sang T, Zhou B, Han B (2012) Genetic control of seed shattering in rice by the APETALA2 transcription factor shattering abortion1. Plant Cell **24:** 1034-1048

Zrenner R, Riegler H, Marquard CR, Lange PR, Geserick C, Bartosz CE, Chen CT, Slocum RD (2009) A functional analysis of the pyrimidine catabolic pathway in Arabidopsis. New Phytologist **183:** 117-132

Appendix

Figure S1. Sub cluster averages (upper panel) in table format show the average of cluster and number of contig in the cluster. Graph information (lower panels) of each cluster present the pattern of the contig from A1 – D10. The X axes 1 as AZ_0_150DAP, 2 as AZ_3_150DAP, 3 as AZ_6_150DAP and 4 as AZ_9_150DAP.

AZ_0_150_std	AZ_3_150_std	AZ_6_150_std	AZ_9_150_std	Cluster	#Contigs
0.11	0.28	0.56	1.00	A1	86
0.07	0.14	0.19	1.00	A2	73
0.43	0.34	0.42	1.00	A3	14
0.09	0.62	0.20	1.00	A4	60
0.15	0.71	0.84	0.99	A5	29
0.23	0.69	0.48	1.00	A6	58
0.44	0.79	0.80	0.98	A7	43
0.17	0.49	1.00	0.23	B1	43
0.06	0.07	1.00	0.14	B2	67
0.10	0.52	1.00	0.61	B3	43
0.08	0.20	1.00	0.49	B4	49
0.13	0.32	0.96	0.94	B5	44
0.46	0.32	0.99	0.71	B6	63
0.24	1.00	0.52	0.73	C1	115
0.14	1.00	0.26	0.45	C2	94
0.05	1.00	0.10	0.11	C3	93
0.23	0.89	0.91	0.50	C4	70
0.48	1.00	0.62	0.26	C5	25
0.65	1.00	0.29	0.11	C6	41
0.97	0.80	0.12	0.25	C7	85
0.94	0.21	0.84	0.23	D1	52
0.99	0.17	0.71	0.76	**D2**	25
1.00	0.55	0.62	0.24	D3	86
0.96	0.94	0.60	0.25	D4	48
0.85	0.62	0.99	0.26	D5	42
1.00	0.17	0.26	0.46	D6	74
1.00	0.38	0.21	0.21	D7	153
1.00	0.05	0.07	0.06	D8	200
1.00	0.14	0.51	0.08	D9	67
0.94	0.64	0.14	0.91	D10	15
					1957

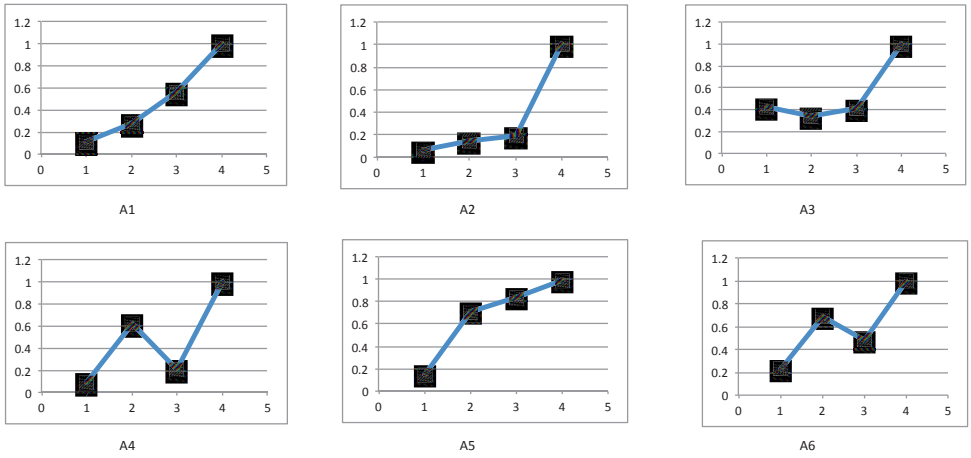

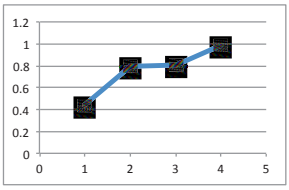

A7

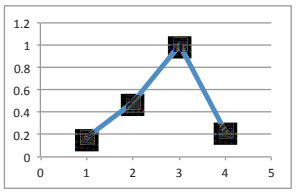

B1

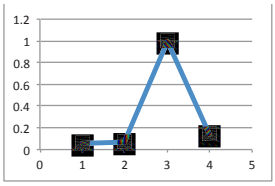

B2

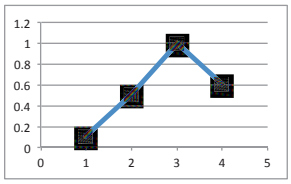

B3

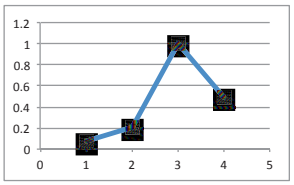

B4

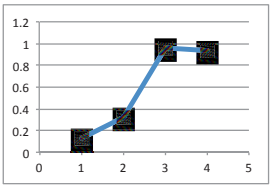

B5

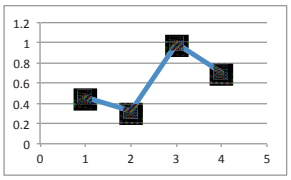

B6

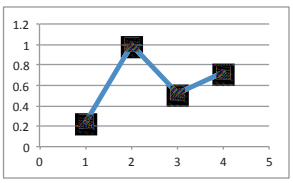

C1

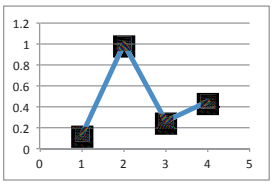

C2

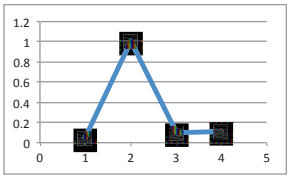

C3

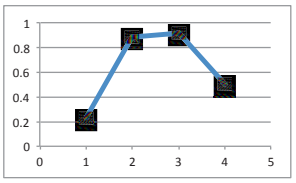

C4

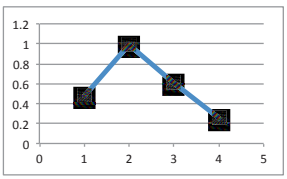

C5

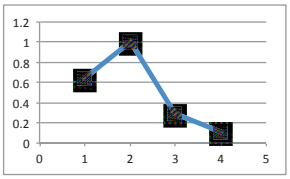

C6

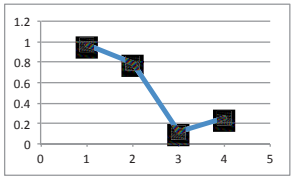

C7

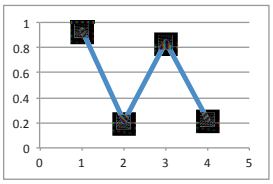

D1

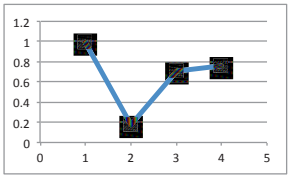

D2

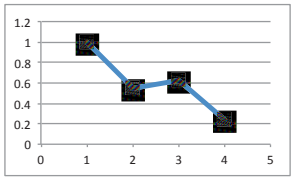

D3

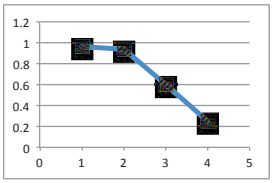

D4

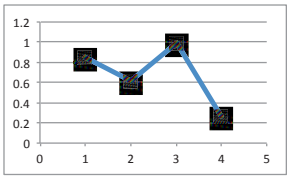

D5

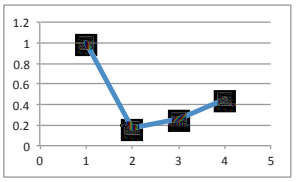

D6

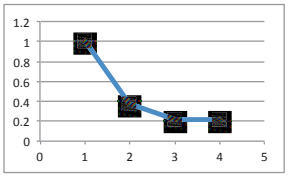

D7

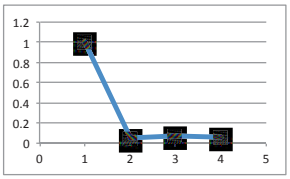

D8

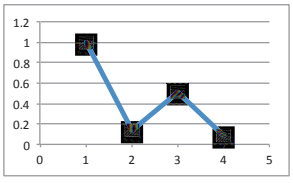

D9

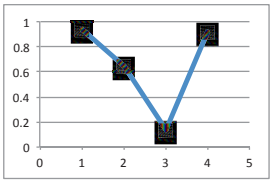

D10

Table S2. 64 candidates with their annotation, contig number, coding sequence (CDS) from the oil palm genome, position on the chromosome, % identity, NCBI annotation and corresponding tomato and Arabidopsis ID numbers.

Annotation	Gene	contig	CDS (V2)	Genome location	% identity	alignment length	mismatches	NCBI annotation	NCBI ID	Categories	Tomato ID	Arabidopsis ID
T-snare/myosin heavy chain-related protein	T-snare/myosin heavy chain-related protein	CL1Contig2725	p5_sc00015.V1.gene28	EG5_Chr10	100	192	0	paramyosin	105052244	Vesicle cycling	Solyc09g055760.1.1	AT5G59210.1
Armadillo-type fold (endocytosis)	-	CL1Contig16450	No cds found	EG5_Chr4	99.74	385	1	dnaJ homolog subfamily C (gravitropism defective 2, GRV2)	105044097	Vesicle cycling	Solyc08g021910.1.1	AT2G26890.2
Pathogenesis-related transcriptional factor and ERF, DNA-binding	Pathogenesis-related transcriptional factor and ERF	CL1Contig15917	p5_sc00024.V1.gene28	EG5_Chr12	99.27	1233	7	dehydration-responsive element-binding protein 1C-like	105054588	Transcription	Solyc03g026270.1.1	AT5G51990.1
LOB domain-containing protein	LOB domain protein 38	CL1Contig6183	p5_sc00155.V1.gene192	EG5_Chr15	99.72	709	2	LOB domain-containing protein 38-like	105058052	Transcription	Solyc02g092550.1.1	AT4G37540.1
methyl-CpG-binding domain-containing protein	methyl-CpG-binding domain-containing protein	CL1359Contig1	p5_sc00044.V1.gene567	p5_sc00044	99.84	1825	3	methyl-CpG-binding domain-containing protein 9-like	105060269	Transcription	Solyc05g005640.1.1	AT3G01460.1
Pathogenesis-related transcriptional factor and ERF	Ethylene-responsive transcription factor 2	CL1Contig5642	p5_sc00065.V1.gene49	EG5_Chr1	96.48	1618	25	pathogenesis-related genes transcriptional activator PTI5-like	105043213	Transcription	Solyc02g077370.1.1	AT5G47220.1
TFIIS/elongin A/CRSP70, N-terminal	TFIIS/elongin A/CRSP70, N-terminal	CL1Contig12354	p5_sc00120.V1.gene52	EG5_Chr2	100	786	0	probable mediator of RNA polymerase II transcription subunit 26c	105038352	Transcription	Solyc11g005450.1.1	AT5G09850.1
Transcription initiation factor IIB	Transcription initiation factor IIB	CL435Contig1	p5_sc00267.V1.gene102	p5_sc00566	98.69	381	3	uncharacterized LOC105034549	105034549	Transcription	Solyc02g085470.1.1	AT4G36650.1
Ankyrin	Ankyrin Zinc finger TF	CL1Contig14415	p5_sc00065.V1.gene164	EG5_Chr14	99.7	2310	7	zinc finger CCCH domain-containing protein 33-like	105057098	Transcription	Solyc06g082010.1.1	AT5G58620.1
Sulphate anion transporter	Sulphate anion transporter	CL1Contig9617	p5_sc00105.V1.gene28	EG5_Chr1	98.48	526	1	probable sulfate transporter 3.5	105043754	Sulphate Transporter	Solyc12g006950.1.1	AT1G78000.2
Chaperone protein ClpB 1	Chaperone protein ClpB 1	CL1Contig7865	p5_sc00046.V1.gene43	p5_sc00046	98.75	562	3	chaperone protein ClpD2, chloroplastic	105060334	Stress	Solyc03g117950.1.1	AT1G74310.1
Ped,Rubber elongation factor	REF-like stress related protein 1	CL1Contig14973	p5_sc00021.V1.gene686	p5_sc04128	99.37	788	5	stress-related protein-like	105036311	Stress	Solyc09g074930.1.1	AT3G05500.1
Harpin-induced protein/LEA	Harpin-induced protein/LEA	CL5804Contig1	p5_sc00300.V1.gene46	p5_sc00300	98.99	395	0	uncharacterized LOC105033113	105033113	Stress	Solyc01g087140.1.1	AT3G08490.1
Calmodulin	Calmodulin	CL1Contig4998	p5_sc00032.V1.gene439	EG5_Chr14	99.49	784	3	calmodulin-like protein 3	105057652	Signal Transduction	Solyc10g079420.1.1	AT3G10190.1
WD-40 repeat family protein	WD-40 repeat family protein	CL1Contig11551	p5_sc00182.V1.gene35	EG5_Chr9	99.23	910	3	lissencephaly-1 homolog 1-like	105052050	Signal Transduction	Solyc08g008490.1.1	AT5G54200.1
Leghaemoglobin	Leghaemoglobin	CL1Contig22867	p5_sc00366.V1.gene27	p5_sc00366	99.72	352	1	non-symbiotic hemoglobin 1-like	105033708	Signal Transduction	Solyc07g008240.1.1	AT2G16060.1
Serine/threonine protein kinase		CL4088Contig1	No cds found	p5_sc03018	99.85	647	0	phytosulfokine receptor 1-like	105036160	Signal Transduction	Solyc01g008140.1.1	AT2G02220.1
Serine/threonine protein kinase	Serine/threonine protein kinase	CL1Contig11148	p5_sc00002.V1.gene1532	EG5_Chr11	99.76	821	2	probable serine/threonine-protein kinase At1g01540	105054206	Signal Transduction	Solyc01g094940.1.1	AT4G01330.1
Serine/threonine protein kinase	Serine/threonine protein kinase	CL1Contig16304	p5_sc00009.V1.gene307	EG5_Chr10	99.55	673	3	RGS domain-containing serine/threonine-protein kinase A-like	105052602	Signal Transduction	Solyc01g059860.1.1	AT1G67890.2
Alpha/beta hydrolase fold-1 (lipid?)	alpha/beta Hydrolase	CL1Contig9601	p5_sc00012.V1.gene469	EG5_Chr2	98.82	593	7	uncharacterized LOC105038267	105038267	Signal Transduction	Solyc09g009500.1.1	AT3G48410.1
Translocon-associated protein (?)	Translocon-associated protein	CL1Contig8879	p5_sc00013.V1.gene695	EG5_Chr16	99.46	373	1	translocon-associated protein subunit alpha-like	105059612	Protein targeting	Solyc10g054880.1.1	AT2G21160.1
Armadillo-like helical	Armadillo-like helical	CL1Contig9095	p5_sc00069.V1.gene152	EG5_Chr5	99.74	1561	4	pumilio homolog 1-like	105044366	Post transcriptional regulation	Solyc06g076340.1.1	AT2G29140.1
Adenine nucleotide translocator 1	Adenine nucleotide translocator 1	CL1Contig10256	p5_sc00020.V1.gene683	EG5_Chr2	100	706	0	ADP,ATP carrier protein 1, mitochondrial	105038936	Nucleotide Metabolism	Solyc11g062190.1.1	AT5G13490.2
ATP-sulfurylase	ATP-sulfurylase	CL1Contig18558	p5_sc00083.V1.gene173	EG5_Chr4	99.37	794	4	ATP sulfurylase 2-like	105044163	Nucleotide Metabolism	Solyc03g005260.1.1	AT1G19920.1
ATP-sulfurylase	ATP-sulfurylase 2	CL1Contig2309	p5_sc00083.V1.gene173	EG5_Chr4	99.8	512	1	ATP sulfurylase 2-like	105044163	Nucleotide Metabolism	Solyc09g082860.1.1	AT4G14680.1
Nitrilase/cyanide hydratase and apolipoprotein N-acyltransferase	Nitrilase/cyanide hydratase	CL1Contig15784	p5_sc00002.V1.gene812	EG5_Chr11	99.5	794	4	beta-ureidopropionase	105054031	Nucleotide Metabolism	Solyc10g047630.1.1	AT5G64370.1
Cytidine deaminase	Cytidine deaminase	CL1Contig4249	p5_sc00018.V1.gene584	EG5_Chr1	99.29	1415	7	cytidine deaminase 1-like	105058482	Nucleotide Metabolism	Solyc07g021750.1.1	AT2G19570.1
Cytidine deaminase, homodimeric	Cytidine deaminase, homodimeric	CL1Contig10645	p5_sc00010.V1.gene87	EG5_Chr1	99.69	652	0	cytidine deaminase 1-like	105058482	Nucleotide Metabolism	Solyc07g021750.1.1	AT2G19570.1
Universal stress protein/adenine nucleotide alpha hydrolases-like	Universal stress protein/adenine nucleotide alpha hydrolase-like	CL1Contig16927	p5_sc00175.V1.gene141	EG5_Chr6	99.52	629	3	uncharacterized LOC105046969	105046969	Nucleotide Metabolism	Solyc02g079410.1.1	AT1G11360.1
Survival protein SurE-like phosphatase/nucleotidase	Survival protein SurE-like phosphatase/nucleotidase	CL1Contig11042	p5_sc00018.V1.gene529	EG5_Chr6	99.78	449	1	uncharacterized LOC105047656	105047656	Nucleotide Metabolism	Solyc03g121730.1.1	AT1G72880.2
Aldehyde dehydrogenase	Aldehyde dehydrogenase	CL1Contig6734	p5_sc00005.V1.gene555	EG5_Chr8	98.38	247	4	aldehyde dehydrogenase family 2 member B7, mitochondrial-like	105050327	Metabolism	Solyc03g114150.1.1	AT3G48000.1
Hexokinase	Hexokinase	CL1Contig8247	p5_sc00001.V1.gene519	EG5_Chr3	98.68	607	2	hexokinase-2-like	105040520	Metabolism	Solyc12g008510.1.1	AT2G19860.1
Ornithine cyclodeaminase/mu-crystallin	Ornithine cyclodeaminase/mu-crystallin	CL1Contig1362	p5_sc00002.V1.gene1542	EG5_Chr11	99.46	741	4	uncharacterized protein P11E10.01	105054210	Metabolism	Solyc06g036330.1.1	AT5G52810.1
Aromatic-ring hydroxylase-like	Aromatic-ring hydroxylase-like	CL1Contig11041	p5_sc00023.V1.gene458	EG5_Chr4	99.33	1048	3	zeaxanthin epoxidase, chloroplastic-like	105043756	Metabolism	Solyc06g060880.1.1	AT2G35660.1
PME,Pectinesterase inhibitor	Pectinesterase	CL1Contig10995	p5_sc00001.V1.gene2372	p5_sc04727	100	85	0	21 kDa protein	105041092	Cell wall	Solyc10g076730.1.1	AT1G14890.1
Leaf senescence protein-like	Leaf senescence protein-like	CL1Contig10496	p5_sc00005.V1.gene466	EG5_Chr8	100	676	0	ALTERED XYLOGLUCAN 4-like	105050308	Cell wall	Solyc02g087120.1.1	AT3G28150.1
Expansin 45, endoglucanase-like	Expansin 45, endoglucanase-like	CL1Contig11417	p5_sc00023.V1.gene313	EG5_Chr4	99.59	488	2	expansin-B5-like	105043690	Cell wall	Solyc01g090810.1.1	AT1G65680.1
Laccase	Laccase	CL1Contig10326	p5_sc00084.V1.gene301	EG5_Chr10	100	977	0	laccase-7-like	105052147	Cell wall	Solyc07g049460.1.1	AT2G40370.1
leucine-rich repeat extensin-like protein	leucine-rich repeat extensin-like protein	CL1Contig14135	p5_sc00018.V1.gene736	EG5_Chr7	99.81	1593	0	leucine-rich repeat extensin-like protein 3	105048039	Cell wall	Solyc12g006980.1.1	AT3G24480.1
Root cap/LEA uncharacterized protein	Root cap protein 1/LEA	CL1Contig11570	p5_sc00056.V1.gene298	EG5_Chr5	87.89	875	87	No hits found	-	Cell wall	Solyc02g078930.1.1	AT5G54370.1
EgPG4	EgPG4	CL1Contig10800	p5_sc00060.V1.gene171	EG5_Chr2	99.81	516	1	PG4 polygalacturonase-like	105034919	Cell wall	Solyc12g019120.1.1	AT3G59850.1
Polygalacturonase A	Polygalacturonase A	CL1Contig6920	p5_sc00072.V1.gene433	EG5_Chr1	98.46	583	5	polygalacturonase-like	105056882	Cell wall	Solyc10g080210.1.1	AT2G41850.1
ADPG1	ADPG1 and ADPG2	CL1Contig9409	p5_sc00072.V1.gene433	EG5_Chr1	99.39	329	2	polygalacturonase-like	105056874	Cell wall	Solyc04g015530.1.1	AT2G41850.1
Hydroxyproline-rich glycoprotein/Cotton fibre protein	Hydroxyproline-rich glycoprotein/Cotton fibre protein	CL1328Contig1	p5_sc00018.V1.gene608	EG5_Chr6	98.41	820	2	wiskott-Aldrich syndrome protein homolog 1-like	105047696	Cell wall	Solyc03g121890.1.1	AT1G72790.1
Ubiquitin subgroup	Ubiquitin subgroup	CL1Contig7802	p5_sc00004.V1.gene274	EG5_Chr6	86.93	597	76	polyubiquitin 11	105052028	26S proteosome	Solyc11g005670.1.1	AT4G05320.2
Ped,Protein of unknown function/Cotton fiber	Ped,Protein of unknown function/Cotton fiber	CL1Contig5278	p5_sc00154.V1.gene209	EG5_Chr9	100	827	0	beta-galactosidase 15?????	105051146	Unknown	Solyc07g063560.1.1	AT1G61260.1
Plant viral-response family protein (?)	Plant viral-response family protein	CL1Contig24634	p5_sc00004.V1.gene776	EG5_Chr10	100	851	0	transmembrane protein 45B-like ???	105053118	Unknown	Solyc01g006050.1.1	AT1G55230.1
Protein of unknown function/senescence/Ca2+	Protein of unknown function/senescence/Ca2+	CL32Contig3	p5_sc00020.V1.gene519	EG5_Chr8	99.85	668	1	uncharacterized LOC105050452	105050452	Unknown	Solyc07g017220.1.1	AT5G20700.1
Protein of unknown function	-	CL1Contig13232	No cds found	EG5_Chr4	99.71	1708	1	calcium uniporter protein 4, mitochondrial-like	105042854	Unknown	Solyc02g089850.1.1	AT2G23790.1
Unknown	Polyadenylate-binding protein-interacting protein 11-like	CL1Contig10757	p5_sc00081.V1.gene352	EG5_Chr16	98.18	603	4	polyadenylate-binding protein-interacting protein 11-like	105059294	No Hit		
chloroplast envelope membrane protein	Elaeis guineensis chloroplast envelope membrane protein-like	CL1Contig8232	p5_sc00020.V1.gene458	EG5_Chr8	100	507	0	chloroplast envelope membrane protein-like	105050429	No Hit	Solyc07g042800.1.1	AT4G31040.1
glycine dehydrogenase [decarboxylating]	Glycine dehydrogenase (decarboxylating)	CL3674Contig1	p5_sc00018.V1.gene573	EG5_Chr6	98.1	210	0	glycine dehydrogenase	105047677	No Hit		
ADP-ribosylation factor GTPase-activating protein		CL1Contig10949	p5_sc00032.V1.gene355	EG5_Chr10	95.58	498	22	No hits found	-	No Hit		
???		CL1Contig13768	No cds found	EG5_Chr6	99.46	743	1	No hits found	-	No Hit		
???		CL1Contig5953	No cds found	EG5_Chr3	94.99	639	5	classical arabinogalactan protein 10-like	105041432	No Hit		
???		CL1Contig21612	No cds found	EG5_Chr2	100	434	0	No hits found	-	No Hit		
???		CL1Contig23550	No cds found	EG5_Chr3	99.85	1373	0	No hits found	-	No Hit		
???		CL3716Contig1	No cds found	EG5_Chr10	97.76	850	13	No hits found	-	No Hit		
???		CL5318Contig1	No cds found	p5_sc02348	99.75	788	2	No hits found	-	No Hit		
???		CL5665Contig1	No cds found	EG5_Chr2	99.13	346	3	No hits found	-	No Hit		
???		CL5922Contig1	No cds found	EG5_Chr11	99.81	527	1	No hits found	-	No Hit		
???		CL6031Contig1	No cds found	EG5_Chr4	100	537	0	No hits found	-	No Hit		
???		CL6447Contig1	No cds found	EG5_Chr2	99.2	125	1	No hits found	-	No Hit		
???		CL731Contig1	No cds found	EG5_Chr11	98.17	3005	34	No hits found	-	No Hit		

Table S3. The 114 contigs common to the proteome and transcriptome studies with corresponding CDS and Annotation.

CDS	Annotation
p5_sc00001.V1.gene1871	Os01g0236700, putative
p5_sc00001.V1.gene2792	cysteine-rich receptor-like protein kinase 41-like, putative
p5_sc00001.V1.gene2906	non-specific lipid-transfer protein 2-like, putative
p5_sc00001.V1.gene3022	hypothetical protein SORBIDRAFT_01g010630
p5_sc00001.V1.gene3385	hypothetical protein SORBIDRAFT_02g039530
p5_sc00001.V1.gene881	14-3-3-like protein D-like, putative
p5_sc00002.V1.gene1	thaumatin-like protein-like, partial, putative
p5_sc00002.V1.gene1532	probable serine/threonine-protein kinase At1g01540-like, putative
p5_sc00002.V1.gene275	Os10g0575000, putative
p5_sc00002.V1.gene812	beta-ureidopropionase-like, putative
p5_sc00003.V1.gene1004	Os05g0476700, putative
p5_sc00003.V1.gene485	elongation factor 1-alpha, putative
p5_sc00004.V1.gene499	hypothetical protein SORBIDRAFT_04g019020
p5_sc00004.V1.gene841	hypothetical protein SORBIDRAFT_04g034650
p5_sc00005.V1.gene239	protein disulfide isomerase-like 2-3, putative
p5_sc00006.V1.gene677	predicted protein, putative
p5_sc00006.V1.gene978	ATP-dependent Clp protease ATP-binding subunit ClpX-like, putative
p5_sc00008.V1.gene1143	mitogen-activated protein kinase 10-like, putative
p5_sc00008.V1.gene775	uncharacterized LOC100273822, putative
p5_sc00008.V1.gene792	probable isoprenylcysteine alpha-carbonyl methylesterase ICME-like, putative
p5_sc00009.V1.gene180	ethylene receptor-like isoform X1, putative
p5_sc00011.V1.gene780	Aminotransferase ybdL, putative
p5_sc00011.V1.gene826	predicted protein, putative
p5_sc00012.V1.gene965	serine hydroxymethyltransferase 1-like, putative
p5_sc00013.V1.gene557	dynamin-related protein 1E, putative
p5_sc00015.V1.gene565	2,3-bisphosphoglycerate-independent phosphoglycerate mutase isoform 1, putative
p5_sc00017.V1.gene343	stem-specific protein TSJT1-like, putative
p5_sc00017.V1.gene45	hypothetical protein ARALYDRAFT_325786
p5_sc00017.V1.gene683	uncharacterized protein LOC100192501, putative
p5_sc00018.V1.gene557	transmembrane 9 superfamily member 4 isoform 1, putative
p5_sc00019.V1.gene247	apolipoprotein d, putative
p5_sc00020.V1.gene487	transcription factor GTE2-like, putative
p5_sc00020.V1.gene560	40S ribosomal protein S19, mitochondrial-like, putative
p5_sc00021.V1.gene286	putative chromatin-remodeling complex ATPase chain-like, putative
p5_sc00021.V1.gene579	hypothetical protein SORBIDRAFT_01g035540
p5_sc00023.V1.gene758	uncharacterized protein LOC100853100, putative
p5_sc00027.V1.gene402	Os12g0638700, putative
p5_sc00028.V1.gene36	aldehyde dehydrogenase family 2 member C4-like, putative
p5_sc00030.V1.gene436	Os01g0382400, putative
p5_sc00031.V1.gene191	hypothetical protein SORBIDRAFT_04g027660
p5_sc00031.V1.gene577	predicted protein, putative
p5_sc00032.V1.gene555	eukaryotic peptide chain release factor subunit 1-3-like isoform X2, putative
p5_sc00032.V1.gene603	inactive beta-amylase 9-like, putative
p5_sc00033.V1.gene191	gamma-interferon-inducible lysosomal thiol reductase isoform 1, putative
p5_sc00033.V1.gene233	hypothetical protein SORBIDRAFT_09g015940
p5_sc00033.V1.gene336	UDP-glucuronic acid/UDP-N-acetylgalactosamine transporter, putative
p5_sc00035.V1.gene126	multidrug resistance protein 1, 2, putative
p5_sc00035.V1.gene135	F-box/kelch-repeat protein At1g74510-like, putative
p5_sc00035.V1.gene670	probable nucleoredoxin 1-2-like, putative
p5_sc00039.V1.gene358	predicted protein, putative
p5_sc00041.V1.gene352	conserved hypothetical protein
p5_sc00041.V1.gene560	Os03g0161200, putative
p5_sc00042.V1.gene56	S-adenosylmethionine decarboxylase proenzyme-like, putative
p5_sc00043.V1.gene226	actin-101, putative
p5_sc00044.V1.gene433	transmembrane 9 superfamily member 4, putative
p5_sc00045.V1.gene322	amino acid permease 3-like isoform X1, putative
p5_sc00046.V1.gene43	hypothetical protein SORBIDRAFT_06g015220
p5_sc00050.V1.gene493	auxin-responsive protein IAA27-like isoform 1, putative
p5_sc00051.V1.gene173	probable methyltransferase PMT26-like, putative
p5_sc00053.V1.gene367	probable phenylalanyl-tRNA synthetase alpha chain-like, putative
p5_sc00053.V1.gene85	hypothetical protein SORBIDRAFT_02g030400
p5_sc00054.V1.gene369	sucrose transporter1, putative
p5_sc00057.V1.gene470	protein BONZAI 1-like, putative
p5_sc00062.V1.gene73	ATP binding protein, putative
p5_sc00068.V1.gene281	Os08g0481400, putative
p5_sc00070.V1.gene222	sucrose synthase 2, putative
p5_sc00070.V1.gene40	medium-chain-fatty-acid--CoA ligase-like, putative
p5_sc00071.V1.gene433	hypothetical protein SORBIDRAFT_01g017860
p5_sc00074.V1.gene13	Transmembrane BAX inhibitor motif-containing protein, putative
p5_sc00074.V1.gene60	hypothetical protein SORBIDRAFT_01g008450
p5_sc00075.V1.gene315	uncharacterized protein LOC100267615 isoform 1, putative
p5_sc00084.V1.gene255	alpha-glucan phosphorylase, H isozyme, putative
p5_sc00091.V1.gene240	uncharacterized protein At3g27210-like, putative
p5_sc00096.V1.gene106	uncharacterized protein LOC100263099, putative
p5_sc00099.V1.gene206	RNA and export factor-binding protein 2, putative
p5_sc00104.V1.gene167	uncharacterized protein LOC100262887 isoform 2, putative
p5_sc00113.V1.gene352	hypothetical protein SORBIDRAFT_01g032340
p5_sc00116.V1.gene49	mitochondrial-processing peptidase subunit alpha, putative
p5_sc00128.V1.gene64	2-dehydro-3-deoxyphosphoheptonate aldolase/ 3-deoxy-d-arabino-heptulosonate 7-phosphate synthetase, putative
p5_sc00158.V1.gene11	predicted protein, putative
p5_sc00158.V1.gene64	class I beta-1,3-glucanase precursor, putative
p5_sc00161.V1.gene68	high affinity cationic amino acid transporter 1-like isoform 1, putative
p5_sc00170.V1.gene181	E3 ubiquitin-protein ligase RHF2A, putative
p5_sc00175.V1.gene261	uncharacterized protein LOC101311253, putative
p5_sc00179.V1.gene136	guanine nucleotide-binding protein-like 3 homolog, putative
p5_sc00187.V1.gene111	luminal-binding protein 5-like, putative
p5_sc00193.V1.gene43	protein EIN4-like, putative
p5_sc00210.V1.gene57	calmodulin-related protein isoform 4, putative
p5_sc00213.V1.gene128	uncharacterized exonuclease domain-containing protein At3g15140-like, putative
p5_sc00217.V1.gene21	uncharacterized protein LOC100253534, putative
p5_sc00220.V1.gene58	EG45-like domain containing protein 2-like, putative
p5_sc00233.V1.gene63	sugar transport protein 13-like, putative
p5_sc00267.V1.gene102	uncharacterized protein LOC100256546, putative
p5_sc00307.V1.gene38	UDP-glucuronate 4-epimerase 6, putative
p5_sc00310.V1.gene53	dolichyl-diphosphooligosaccharide--protein glycosyltransferase subunit STT3, putative
p5_sc00324.V1.gene90	uncharacterized protein LOC100499887 precursor, putative
p5_sc00334.V1.gene22	protein TRIGALACTOSYLDIACYLGLYCEROL 3, chloroplastic-like, putative
p5_sc00341.V1.gene31	uncharacterized protein LOC100251901, putative
p5_sc00346.V1.gene19	cyclin-dependent kinase F-4-like, putative
p5_sc00349.V1.gene64	charged multivesicular body protein 1-like, putative
p5_sc00406.V1.gene59	f-box family protein, putative
p5_sc00467.V1.gene33	Os11g0516000, putative
p5_sc00495.V1.gene21	glyceraldehyde-3-phosphate dehydrogenase-like isoform 1, putative
p5_sc00529.V1.gene27	enolase 2-like isoform X2, putative
p5_sc00540.V1.gene20	early responsive to dehydration protein, putative
p5_sc00571.V1.gene6	amino acid transporter, putative
p5_sc00751.V1.gene16	Os03g0794500, putative
p5_sc00783.V1.gene44	5-methyltetrahydropteroyltriglutamate--homocysteine methyltransferase-like, putative
p5_sc00793.V1.gene5	histone deacetylase HDT1-like, putative
p5_sc02046.V1.gene4	Os07g0100200, putative
p5_sc03502.V1.gene1	hypothetical protein SORBIDRAFT_02g003490
p5_sc04128.V1.gene7	stress-related protein-like, putative
p5_sc17072.V1.gene1	Os05g0116100, putative
p5_sc34255.V1.gene1	heat shock cognate 70 kDa protein-like, putative

Table S4. qPCR primer sequences used in study.

Contig	Gene	Name of primer	Sequence
-	EgEF1α	EgEF1-Q-S4	TATCAAAGGATGGGCAGACC
		EgEF1-Q-AS4	TCCAAGGCAAGGTATGATGA
CL1Contig10800	EgPG4	EGPG4qS1	ACCTACGGAAACAAGCC
		EGPG4qAS1	AATCCTACATCACCCATTTCA
CL1Contig6920	EgPGAZ1	EgPGAZ1_S	GTGATCCCGTTGCCTTGC
		EgPGAZ1_AS	GATGAGAAGAGGGCCCAAA
CL1Contig9409	EgPGAZ2	EgPGAZ2_S	CCCACAAAAATTGCTTCTGC
		EgPGAZ2_AS	GATGGATATGCAGCCATGC
CL1Contig10326	Laccase	Laccase-S	GCTTTTGAGGTGGAGAATGG
		Laccase-AS	ACGTTCGGCCTTAATTTTCC
CL1Contig10326	Laccase2	Laccase-S2	GGCTTTTGAGGTGGAGAATG
		Laccase-AS2	CTTATGAAACGTTCGGCCTT
CL1Contig10326	Laccase3	Laccase3_S	TATGGATCATGCACTGCCAC
		Laccase3_AS	TCCTTGTTCCCAGCTGTCC
CL1Contig6183	LOB	LOB-S	GCCTCCTGAACCTCTTCGTT
		LOB-AS	TGGTGGTTACAAGAGGAAAAAT
CL1Contig22867	Leghaemoglobin	Leghaemoglobin-S	CACCATAAAGGAGGCAGTCC
		Leghaemoglobin-AS	CGACCATGATACAACCATCCT
CL1Contig9601	a/b Hydrolase	a/b Hydrolase-S	ATTGATGGTTGGGCTGACAC
		a/b Hydrolase-AS	AAAATGATGTTGCAGCTGAAGT
CL1Contig10995	PME	PME-S	TCATGCAGTTCACCAGCAAC
		PME-AS	CAAACCTTTGCTCTTTAACCAA
CL1Contig11148	Serine/threonine protein kinase	Se/Tr-S	TGACTTGCTATTTCGCGATG
		Se/Tr-AS	TGCAAATTGTCAGGCACCTA
CL1Contig11417	Expansin 45, endoglucanase-like	Expansin45-S	CCGTTCTCGATTCGATTGAC
		Expansin-AS	TGGAGACGCACAAATTCTCA
CL1Contig1362	Ornithine cyclodeaminase/mu-crystallin	Ornithine-S	TGTTTAAGTCGGTGGGAACG
		Ornithine-AS	CCATGTCCAGCAACAGATTG
CL1Contig15784	Nitrilase/cyanide hydratase	Ni/Cy-S	TGCAGCAATGCTTTCTGAGT
		Ni/Cy-AS	CTGCTTGCGAGAACATTCAA
CL1Contig18558	ATP-sulfurylase	ATP-Sulfurase-S	GCCCTCCAGATGGTTTTATG
		ATP-Sulfurase-AS	TGATTGGCATCATCGACTTG
CL1Contig4998	Calmodulin	Calmodulin-S	GAGGACTGCCGACGTATGAT
		Calmodulin-AS	CCACCGTCCATTCTTTGTTT
CL1Contig14135	Leucine-Rich Repeat extensin-like protein (LRR)	LRR-S	AGTACAGTGGTGGGCTGCTT
		LRR-AS	TATTAGTAGGCCGCGCAAAG
CL1Contig5642	Patho	PathoERF-S	CCGTTGGAATTCACCAAACT
		PathoERF-AS	AACATGCCCAAATACCCAAG

CL1Contig16927	Universal stress protein/adenine nucleotide alpha hydrolases-like(USP)	USP1-S	GAGTACCACGATGCCTCTGA
		USP1-AS	GGATACATAGCGGAGTCCCC
CL1Contig16818	EIL3	EIL3_S	CATTGATGATGACCTGCTGCGAG
		EIL3_AS	TGGAGACCAGATCACAATAGCA
CL1Contig11417	EXPB6	EXPB6_S	CACCGGCTTCCCTGAACAT
		EXPB6_AS	GAGCCTGCGGATATGGGAAT
CL1Contig24346	NR	NR_S	CACGAATTGCCATTTCTGCC
		NR_AS	TGAACTGGAGCTTGTGGAGG
CL1Contig24346	EgNR	EgNR_S	CCTCCACAAGCTCCAGTTCA
		EgNR_AS	GAAGTTGTTGCTGTCCGTGT
CL1Contig10844	MBP(Myrosinase binding protein)	MBP_S	AGCTGGAAAAGTTGTTGGCT
		MBP_AS	ACAACCACAAATAGAGCTTGGAG
CL1Contig605	BURP domain-containing protein	BURP_S	GCCCATCTGCCACTTCCT
		BURP_AS	ACAGGAATACACATACATCACCA
CL1Contig24608	HM-coA(Hydroxy-methylglutaryl-coenzymeA reductase)	HM-coA_S	TTCCCTCATGTCAGCTCTCG
		HM-coA_AS	TGATGGGCTACTTTGT
CL1Contig7452	Inositol oxygenase	Inositol_s	AGATGTAGAGAAAGTGAAGCC
		Inositol_As	AGCTGCTTGAAGATGGAC
CL1Contig13583	O-methyltransferase3	O-methyl3_S	TCCTTACTACGGGAAAAGAACGA
		O-methyl3_AS	ACAAGCCAATCACTGCACTTT
CL1Contig19474	Thioesterase superfamily	Thioesterase_S	CGGAGGATTCAGAAGGTTGT
		Thioesterase_AS	CACTCTCTTCAATCAGCCACT
CL1Contig9095	Armadillo-like helical (Armadillo)	Armadillo_S	CTCGTGTTTCCGGTTCCAAA
		Armadillo_AS	TCCCCATCAAAGGCCTCATT
CL1Contig12380	CL12380-ADP	CL12380-ADP_S	GCACTTGTGCGACCTCTG
		CL12380-ADP_AS	CAAACACCCACCGCAACT
CL1Contig18927	CL18927-ADP	CL18927-ADP_S	TCATGCAAGAACTCAACCAACA
		CL18927-ADP_AS	ACCCCAGTTAGCCAAGTAACA
CL1Contig16450	Armadillo-type fold (Endocytosis)	Endocytosis_S	ATGAGATAAGTGAACCAGAGGCA
		Endocytosis_AS	AACCATTTTCAATTTCGGAGGAC
CL1Contig15917	Pathogenesis-related transcriptional factor and ERF, DNA-binding (Pathogenesis)	Pathogenesis_S	TGGGATGAGGTGGAGAAT
		Pathogenesis_AS	AACCAGCGATCTCCTATGC
CL1Contig13232	Protein of unknown function(PUF)	PUF_S	CCTCTGCCTACTTCATGGC
		PUF_AS	CTCCTGAGCTCATTGAAGCG
CL1Contig9617	Sulphate anion transporter(Sul-AT)	Sul-AT_S	CTTGATTGGAGAGAATTGGGTGT
		Sul-AT_AS	TGACAGAGCGCATGTACTAATC
CL1Contig9026	Thaumatin-like protein(Thaumatin)	Thaumatin_S	ATCCACCAGTCCTTGCTCAC
		Thaumatin_AS	GCTTGAAAGTGATCCCTCCTC

CL1Contig16927	Universal stress protein/adenine nucleotide alpha hydrolases-like(USP)	USP_S	TGGAGAAGGAGGCAGAGTTG
		USP_AS	CCCTCCATTTGATTCGTGGC
CL1Contig11041	Aromatic-ring hydroxylase-like(Aro-hydroxy)	Aro-hydroxy_S	AGTCTCAAGAAGCACCCTCC
		Aro-hydroxy_AS	CGCTGACGCTTTCCAAGAAT
CL32Contig3	Protein of unknown function/senescence/ Ca2+ (PUF-CA2+)	PUF-Ca2+_S	TCGTTGGATTGCTCTGTGTC
		PUF-Ca2+_AS	TCACTCAGATGACCCTTCTCG
CL1Contig25900	Auxin efflux carrier1	Auxin1_S	TGGATGGATTTTGTTGTATTTGG
		Auxin1_AS	CTCTACCATCAAACCAGATCTCC
CL1Contig23162	Auxin efflux carrier2	Auxin2_S	ATGTTGGTCAGCAGGAGTG
		Auxin2_AS	TCTTCCACACAAGAACCC
CL1Contig22762	auxin Iaa-amino acid hydrolase	Aux-hydrolase_S	TGGTGCTGCTATTCATGCTG
		Aux-hydrolase_AS	GCATACCTTTCCCCTTATGC
CL1Contig4884	Auxin responsive protein1	Auxin-RP1_S	GCTTGTTGGTGATGTTCCGT
		Auxin-RP1_AS	CCCCTGCAGACATTAGAT
CL1Contig11618	Auxin responsive protein2	Auxin-RP2_S	AGACAAGGATGGAGACTGGATG
		Auxin-RP2_AS	GCACTTTCATTGAGGGTTGG
CL1Contig1153	Auxin responsive protein3	Auxin-RP3_S	AGGAGGCTAAGGATCATGAAGG
		Auxin-RP3_AS	GCTTTTGGTTTTGAGATGGTC
CL1Contig25316	Gibberellin 2-oxidase	Gib2-oxidase_S	GTTCACATGGTGGGAGTACAAG
		Gib2-oxidase_AS	ACTGCCTTTTTGACCAGTGC
CL1Contig20991	Aquaporin1	Aquaporin1_S	ATGTGGATCTTCTGGGTGGG
		Aquaporin1_AS	CACAGCAGGACAGGTTGGAT
CL1Contig1241	Aquaporin2	Aquaporin2_S	CATAGCCGCAGCTTATC
		Aquaporin2_AS	GCCCCATCAAAATTCCAC
CL1Contig3656	ABA8OX	ABA_S	AATTCAGTTCGGGCCTTTCG
		ABA_AS	TCACCATGCAAATTAAGTG
CL1Contig2846	Carotenoid (CCD)	CCD_S	GGATTCCATGCCTTCTTTGTGA
		CCD_AS	GCATGCCCAGAATACACTT
CL1Contig10378	Carotene beta-hydroxylase	Carotene_S	CGGAGGAGTTGCAGAAAGAG
		Carotene_AS	CGGAGTCTAATCGTCATCTGGT
CL1Contig10363	pyrophosphatase	Pyro_S	CCAATGTCACCCAAAGAAGC
		Pyro_AS	GCGCTAAAATGGTCCTTGA
CL1Contig13991	Gamma-tubulin	G-tubulin_S	TCAGAGTCTTGTGCCCATCT
		G-tubulin_AS	ACGTGAGGAAGAGAGTGACC
CL1Contig14415	Zinc finger TF	Zinc-TF_S	ATGAGCCGGACCTATCTTGG
		Zinc-TF_AS	TGAGTATTGGTTGATGGCGT
CL1Contig1715	Actin	Actin_S	AGTACATTCCAACAGATGTGGA
		Actin_AS	ACCGGAAAATAAGTCAGATAGCA
CL1Contig2278	Beta-xylosidase1	Beta-xylo1_S	CCTCCCCCTTCTATTTATACCC
		Beta-xylo1_AS	ACGAAGAGGAGCGATTTGG
CL1Contig2306	Beta-xylosidase2	Beta-xylo2_S	TCCAACATCCACGCCCGC
		Beta-xylo2_AS	CCCTGCCTGGCCGCCGTT

CL1Contig7306	Beta-1 3-glucanase1	Beta-1,3-glu1_S	TGCAACCAGTCTACCCAATC
		Beta-1,3-glu1_AS	AACCACACTCCATTGCTTCC
CL1Contig11610	Beta-1 3-glucanase2	Beta-1,3-glu2_S	TACCCTGATAAGCAGCCA
		Beta-1,3-glu2_AS	GGAAAACTTAGTCAGGTGC
CL1Contig1963	Thaumatin-like	Thaumatin-like_S	GGATGCGTACAGTTACCCCA
		Thaumatin-like_AS	CTCAGAGGCCTACAGAGCA
CL1Contig9735	Helix-loop-helix	Helix_S	TTGGGATATTGCTGGCTTG
		Helix_AS	ATCGGGACACATAACCTCCA
CL1Contig3577	Beta-galactosidase	Beta-galac_S	CCCGGCACTATGAAGAAGCT
		Beta-galac_AS	ACTGTCCACACTTGCAATGA
CL1Contig9720	Cellulose synthase	Cellulose_S	ACCATCGTCGTTGTTTGGTC
		Cellulose_AS	AACACCCATTTGCAACTCCC
CL1Contig8313	Mannan endo-1 4-beta-mannosidase	Mannos_S	GATCGACGATGCAAGGAAAC
		Mannos_AS	TTGGTCGTCACGAAACCT
CL1Contig11193	BZIP transcription factor	BZIP_S	ACCTGATCCAATCCTTAAGCCA
		BZIP_AS	AAGGATCATGCAGCAAACCC
CL1Contig18272	CHY zinc finger	CHY-zinc_S	TAACAAAATGGTCCGCATCC
		CHY-zinc_AS	CTCAGCATAACAAGGCCAA
CL1Contig10271	MYB transcription factor	MYB_S	GAGCAGAGCGGTATGATGTG
		MYB_AS	CTTCTTCTTCTTCGAAGACC
CL1Contig11813	Peptide transporter	Peptide-TP_S	TGTGGTCTACCTTTGGATCG
		Peptide-TP_AS	AGCCCAAATTTGCATGTCTC
CL1Contig22781	Xyloglucan endotransglucosylase	Xyloglucan_S	TCTACGACTACTGCACGGA
		Xyloglucan_AS	TTCAACACAACGTCCCAA
CL1Contig697	BHLH transcription factor	BHLH_S	TGACGGCCTCCGGGCCGCGC
		BHLH_AS	TCTATGAGAACAAGCTCTCC
CL1Contig15451	Homeobox-leucine zipper	Ho-leucine_S	GCCACCCTCAATTGGTACTATG
		Ho-leucine_AS	AAACCTCCCCTAACTCCTTCC

Table S5. Raw data for Figure 2 in Chapter 3 show the tissue with the highest number of reads.

Gene, Contig	Number of Reads	Tissue
AtACO1, *AtACO2*, CL1Contig2645	2990	AZ150
AtEIL1, AtEIL2, AtEIL3 CL1Contig6561	1301	P
ADPG1, ADPG2, CL1Contig6920	1048	AZ150
EgPG4, CL1Contig10800	582	AZ150
MACROCALYX, CL1Contig17616	561	AZ150
AtHSL1, AtHSL2 CL1Contig16961	519	P
AtARF1, *AtARF2* CL1Contig10518	446	AZ30
NEVER RIPE, *AtEIN1, AtETR1, ERS1* CL1Contig24346	414	P
AtSHP2 CL1Contig5234	404	AZ150
AtAGL18 CL1026Contig1	267	P
AtACS CL1Contig24959	251	AZ150
FRUITFULL, CL1Contig17616	211	P
AtERF1, CL1Contig24426	210	AZ150
NEVERSHED, CL1Contig19131	193	P
AGL15, CL1Contig12212	186	AZ150
OsSH1, CL1Contig25404	177	P
AtCEL5, CL1Contig9407	170	AZ30
JOINTLESS, CL1Contig17616	162	P
FOREVER YOUNG FLOWER, CL3087Contig1	155	AZ30
EVERSHED, CL1Contig10506	141	P
SpSH1, CL1Contig5234	136	AZ30
GA3OX1GIBBERELLIN3-OXIDASE1, CL468Contig1	134	AZ150
AtSHP1, CL1Contig5234	126	AZ30
AtEXPA1, CL2858Contig1	118	AZ30
LATERALSUPRESSOR, CL1Contig12384	103	AZ30
SHATTERING_ABBORTION, CL1Contig10291	93	AZ150
Blade on Petiole1, CL1621Contig2	92	AZ150
AtIND, CL18525Contig1	90	P
TaQ, CL1Contig6821	88	P
CASTAWAY, CL580Contig2	85	AZ30
AtCEL2, CL1Contig9407	83	AZ30
Blade on Petiole2, CL1621Contig2	80	P
AtNST1, CL21034Contig1	74	P
AtSERK1, CL1Contig9746	73	AZ30
AtEXPB6, CL1Contig11417	69	AZ150
AtPDH1, CL4000Contig1	64	P
QSH, CL5323Contig1	58	P
OsSH5, CL1Contig13941	58	P
SHATTERING, CL12134Contig1	52	P
SpWRKY1, CL1Contig9642	52	P
AtDOF, CL11530Contig1	48	P
AtACC1, *AtACC2*, CL1Contig6142	45	P
AtNST3, CL21034Contig1	38	AZ30

ALCATRAZ, CL426Contig3	32	P
FOREVER YOUNG, CL1Contig890	9	AZ150
GREEN RIPE, CL1Contig2856	3	AZ150

Chapter 4
On going experiments and future prospects

Introduction

In addition to the completed studies described in the previous chapters, complementary approaches were initiated and performed as a basis to examine further the cellular, molecular and biochemical mechanisms that occur during oil palm ripe fruit abscission. Indeed, transcriptional responses in the AZ must lead to biochemical and the cellular changes for organ abscission to occur. To complement the knowledge learned from the approaches presented in previous chapters, targeted transcriptome studies, bioinformatics, biochemical and the cellular studies have been performed in parallel and are described and discussed below. The current chapter includes sections that summarize work initiated and in progress, and will provide a number of starting points for future research.

Results and discussion

I. Are the Auxin, Jasmonic acid and ABA hormone biosynthesis and signaling pathways affected by ethylene treatment; evidence for involvement in the abscission process?

To complement the transcriptome studies presented in Chapter 3, a targeted analysis of the auxin, jasmonic acid and ABA hormone biosynthesis and signaling pathways was performed. For the auxin pathway (Figure 1) there were a total of 23 potential contigs identified, 8 of which were found to be differentially abundant (based on read abundance see Chapter 3 Methods) and clustered in the ripe fruit AZ (AZ150) during the ethylene treatments. The highest expression was found for an auxin hydrogen symporter (77 reads) at 3 h of ethylene treatment (AZ150DAP+3). The deduced protein shares some features with other auxin efflux carriers that are regulated by light and development but not affected by ethylene or auxin (Dal Cin et al., 2009). Another abundant (66 reads) contig was an indole-3-acetic acid amino synthase, involved in auxin homeostasis through conjugation of excess IAA to amino acids (Ding et al., 2008), at 9 h of ethylene treatment (AZ150DAP+9). In contrast, no change in abundance for a contig for YUC or YUCCA, involved in auxin biosynthesis, was observed. Ethylene treatment also induces the expression of several auxin signaling and response related genes including contigs for TIR1 and auxin response factors (ARFs). Interestingly, there was a second TIR1 contig with very few read numbers that decreased during the ethylene treatment. Overall, ethylene treatment appears to modulate transcription of genes related to auxin efflux, modification, signaling and response, with conjugation to amino acids and efflux transport the most affected.

For jasmonic acid (JA) biosynthesis (Figure 2), 22 potential contigs were found, 12 of which were differentially abundant and clustered (See Chapter 3 Methods). The highest expression was

found in AIM, involved in the *β*-Oxidation of JA in the peroxisome (Delker et al., 2007), at all time points of ethylene treatment. Contigs for other JA biosynthesis transcripts including lipoxygenase (LOX), AOS, AOC, OPR3, OPCL1, ACX1 and KAT were identified, which suggests a high capacity for JA biosynthesis in the ripe fruit AZ. Normally JA is present in low concentration in various plant parts including buds, shoots, leaves, flowers, fruits, and seeds and largest amount in fruits (Meyer et al., 1984). Although a high concentration of JA has been reported in fruit, the concentrations and accumulation patterns vary among species. JA accumulates at early stages of development, then decreases, and then increases again before the ripening in climacteric fruits (Fan and Mattheis, 1998; Kondo et al., 2000). Contigs for JA signal transduction and response including the JA receptor (COI1), JAZ proteins, JAR1 and MYC2 were also identified, which suggest there is a JA response capacity in the ripe fruit AZ.

The ABA (Figure 3) results show that the ABA8OX is highest (187 reads) in ripe fruit without ethylene treatment, and decreases during all ethylene treatment time points. In sweet orange the ABA8OX expression were found related to the fruit ripening (Zhang et al., 2014). In plant the ABA8OX catalyzes oxidation of ABA to 80-hydroxy ABA that is spontaneously converted to phaseic acid (PA), a largely inactive ABA catabolite (Steffens and Sauter, 2014). This gene is related to the plant stress response. The *OsABA8ox1* from rice was strongly induced upon submergence in deep-water rice (Saika et al., 2007). In drought stress of maize root the ABA8OX was shown to be the major transcript component for regulating ABA catabolism (Vallabhaneni and Wurtzel, 2010). In contrast, an ABAGT (involved in glycosylation of ABA) was found to increase at 3h of ethylene treatment, while CDD (involved in ABA biosynthesis) appears to increase slightly, but was not statistically differentially abundant (Chapter 3 Methods). Overall, ethylene treatment appears to have the strongest affect towards the inhibition of ABA8OX, which may result less ABA turnover and an increase in active ABA.

For ethylene, *ACO1* was used as a marker to monitor ethylene production in Chapter 2 and is the candidate with the highest expression found in the ripe fruit AZ, and highly induced by 3h of ethylene treatment (Figure 3). Increased expression of *ACO* genes, which encode the enzyme converting ACC to ethylene, as well as ACO activity have been reported in organs which undergo abscission (Ruperti et al., 2001; Dal Cin et al., 2005; Dal Cin et al., 2007; Dal Cin et al., 2009). Another contig with a large number of reads was also identified for *EIN3*, which suggests a capacity for ethylene response in the ripe fruit AZ. From the current results, the data is consistent with a role for ACO during oil palm ripe fruit abscission, possibly through an increase in ethylene production localized in the ripe fruit AZ, which results in the maintenance of the ethylene response as observed with the steady high expression of in *EIN3*.

Gene	Contig	Cluster	AZ_0_150	AZ_3_150	AZ_6_150	AZ_9_150
YUC	CL1566Contig1					
AFB2 LRF2 At3g26810	CL1Contig4537					
UIP2 At5g42190	CL1Contig2198					
Indole-3-acetic acid-amido synthetase	CL1Contig6277	A4				
Bicunctional nitrilase/nitrile hidratase	CL1Contig21601					
FBL3	CL1Contig4537					
F-box family protein FBL5	CL1Contig14478					
ARF	CL1Contig12930	D8				
ARF	CL1Contig16153					
ARF	CL1Contig8910					
Aux/IAA protein	CL1Contig11535					
Aux/IAA protein	CL1Contig11531					
TIR1	CL745Contig1	D8				
TIR1	CL1Contig12528	B2				
Auxin exflux	CL112Contig3					
Auxin hydrogen symporter	CL1Contig23162	C2				
Indole 3 Butyric Acid	CL1Contig16919	C1				
UDP-glucosyltransferase	CL1Contig9022					
UDP glucose: indole 3 acetate beta D glucosyltransferase	CL1Contig10176	C4				
IAA aminoacid hydrolase	CL5099Contig1					
Primary amine oxidase	CL1Contig10658	D1				
Amine oxidase	CL1Contig22725	C4				
Aldehyde dehydrogenase	CL1Contig16100					

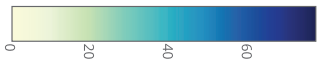

Figure 1. Auxin biosynthesis and signal transduction contigs identified and their relative expression profiles (relative read abundance) in the ripe fruit AZ (AZ150) during ethylene treatment. Clustered contigs were found to be statistically (P = 0.05) differentially abundant in the ripe fruit AZ (AZ150, see Chapter 3 Materials and Methods).

Gene	Contig	cluster	AZ_0_150	AZ_3_150	AZ_6_150	AZ_9_150
JMT	CL1623Contig1	-				
KAT5	CL1Contig25479	A7				
MFP2	CL1Contig8030	-				
AIM1	CL1Contig14113	D2				
JAR1	CL1Contig25238	C7				
AtJAZ10	CL1Contig7525	-				
AtJAZ9	CL1Contig8372	D5				
AtJAZ8	CL1Contig9900	-				
AtJAZ7	CL1Contig14212	C3				
AtJAZ6	CL1Contig7676	A1				
AtJAZ4	CL1Contig8362	D6				
JAZ3 (JAI3 = JAZ3)	CL1Contig8372	D5				
AtJAZ1	CL1Contig7676	A1				
MYC2	CL1Contig10500	-				
COI1	CL1Contig7284	-				
KAT2 (PKT3)	CL1Contig25479	A7				
ACX1	CL1Contig4771	-				
OPCL1	CL1Contig7905	-				
OPR3	CL1Contig11512	-				
AOC2	CL1Contig16267	C1				
AOS	CL1Contig12131	-				
LOX2	CL1Contig9110	C1				

Figure 2. Jasmonic acid biosynthesis and signal transduction contigs identified and their relative expression profiles (relative read abundance) in the ripe fruit AZ (AZ150) during ethylene treatment. Clustered contigs were found to be statistically (P = 0.05) differentially abundant in the ripe fruit AZ (AZ150, see Chapter 3 Materials and Methods).

Gene	Contig	cluster	AZ_0_150	AZ_3_150	AZ_6_150	AZ_9_150
ABAGT	CL1Contig10176	C4				
ABA8OX	CL1Contig3656	D8				
XO	CL1Contig16639					
CCD	CL1Contig2846	-				
NSY	CL1Contig9888	-				
ACO1 /ACO4	CL1Contig2645	A5				
ACS12	CL7292Contig1	-				
ACS7	CL7292Contig1	-				
ACO	CL1Contig8422	A4				
SAM1 /SAM2	CL1Contig23174	D7				
CTR1	CL1Contig2421	D7				
ERF/AP2	CL1Contig20149	C1				
RAP2.2	CL1Contig25825	-				
ERF/AP2	CL1Contig20149	-				
DREB2A	CL1Contig22465	-				
RAP2.4	CL1Contig12718	-				
RAP2.12	CL1Contig25825	-				
EIN3	CL1Contig6561	D3				
EIN2	CL1Contig5281	-				
EIN4	CL1Contig15440	A7				
ETR1	CL1Contig24346	C2				

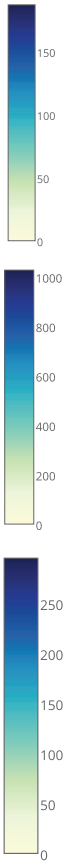

Figure 3. ABA (upper panel) and ethylene (lower panels) biosynthesis and signal transduction contigs identified and their relative expression profiles (relative read abundance) in the ripe fruit AZ (AZ150) during ethylene treatment. Clustered contigs were found to be statistically (P = 0.05) differentially abundant in the ripe fruit AZ (AZ150, see Chapter 3 Materials and Methods).

II. Immunohistochemistry approaches corroborate the accumulation of HG pectin along the edge of recently separated AZ and provide evidence for cell polarization

In the current study, the use of immunohistochemistry techniques were employed to characterize the pectin and other cell wall and cellular components in the AZ cells during separation at 160 DAP. Advantages of immunohistochemistry techniques over other methods such as chemical methods in structural analysis of pectin are the relatively small amounts of material required, the possibility to observe the localization of the components *in situ*, and to minimize the changes to pectin properties (Willats et al., 2000). In this study, antibodies raised against Extensin (LM1), homogalacturonan (HG) with different amounts of methyl-esterification (JIM5, LM19, LM20) and conformation (2F4 "eggbox"), FERULOYLATED-(1-4)-*β*-D-GALACTAN (LM9) and feruloylated polymer (LM12), and a marker for the golgi (ARF1) were tested on tissue samples taken from the base of ripe fruit at 160 DAP containing the AZ from oil palm (Knox et al., 1990; Clausen et al., 2003; Clausen et al., 2004; Verhertbruggen et al., 2009; Pedersen et al., 2012; Marais et al., 2015; Wang et al., 2015). The LM1, JIM5, LM19 and ARF1 antibodies revealed a difference between the signal observed in the control sample (controls consisted of incubating without the 1° antibody added, while 2° antibody was added) and test samples (1° antibody and 2° antibody added) (Table 4). Some of the antibodies have only been tested once and the signals are quite low, so the experiment needs to be repeated and corresponding controls need to be performed before a conclusion is made. Signals clearly above those observed in the controls were found for LM1, JIM5, LM19 and ARF1 (Table 4 and Figure 4). Previous results indicated that the JIM5 (and to a lesser extent JIM7) epitope was abundant on the surface of separated AZ cells suggesting a polarized accumulation or secretion of pectin from cells undergoing cell separation (Roongsattham 2015 submitted). Furthermore, the JIM5 signal, which detects partially methyl-esterified HG, increased in the AZ prior to separation in what appears to be the future sites of cell separation. To examine this phenomenon in more detail, the golgi marker ARF1 was used to determine the localization of golgi in the AZ cells in samples that have separated. The results indicate that the ARF1 epitope signal is similar to JIM5, the highest signal is in cells that have undergone cell separation, suggesting that indeed a high amount of transport activity via golgi is taking place in these cells during or after cell separation. In addition, LM19, a newer antibody that binds strongly to un-esterified HG, is also abundant at the tips of cells that have undergone cell separation (Figure 4). In contrast, the LM1 antibody that recognizes Extensin is localized more along the elongated sides and less at the tips of the AZ cells that have undergone cell separation. Overall, the results are consistent with the hypothesis that AZ cells that separated or have undergone separation are also elongating (LM1 signal

along sides of AZ cells) and are involved in a high amount of polarized golgi trafficking (ARF1 at tips), which may correspond to the high amount of pectin (JIM5 and LM19 at tips) accumulation or secretion observed.

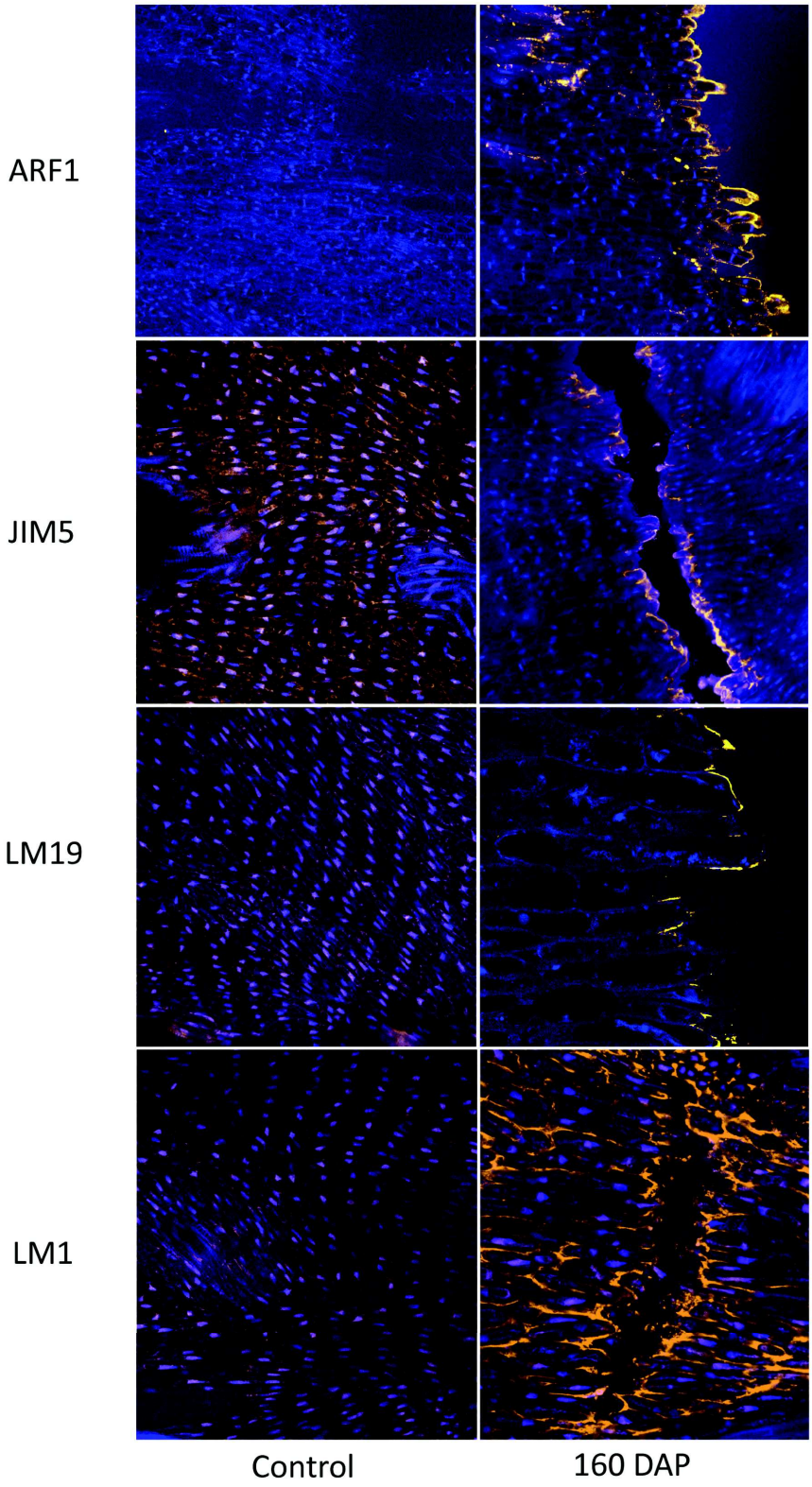

Figure 4 The different antibodies used included ARF1 (golgi marker), JIM5 (partial methyl-esterified HG), LM19 (un-esterified HG) and LM1 (extensin). Control (left panel, without 1° antibody with 2° antibody included) has only background signal, while the test samples (1° and 2° antibodies included) have signals in the AZ of 160 DAP fruit (right panels). The experiments were repeated at least twice and the results were consistent between the biological repetitions.

III. Is *IDA-HAE*/*HSL2* from Arabidopsis still involved in control of oil palm fruit abscission?

The following is an excerpt from work publish in collaboration with Professor Reidunn Aalen at the University of Oslo, Oslo, Norway. (IM Stø, R Orr, K Fooyontphanich, X Jin, JMB Knutsen, U Fischer, T J Tranbarger, I Nordal and R B Aalen. (2015) The evolutionary conservation of the abscission signaling peptide IDA in Angiosperms: withstanding numerous genome duplications. Frontiers in Plant Science doi: 10.3389/fpls.2015.00931.)

To test whether *IDA-HAE*/*HSL2* is involved in the control of fruit abscission in a monocot such as oil palm, a search for IDA sequences in the oil palm genome and in the Illumina data obtained during natural abscission was undertaken. Because the IDA peptides are quite small (alignments of approximately 59 aa), they may not be annotated in the genome or assembled de novo during transcriptome studies. In this study ten *IDA* sequences were identified from the oil palm genome using tBLASTn, and revealed that the oil palm genes come in five pairs encoding almost identical preproproteins (Figure 5) suggesting recent genome duplication (Stø et al., 2015). As known from the previous study, it takes about 160 days from pollination until the fruits are ripe and start separating from the bunches on the trees (Roongsattham, 2011). In our experiment mRNA was isolated from AZs of unripe and ripe fruit of trees that abscise their fruit (Shedding - Sh1, Sh2 and Sh3), and additionally from AZs of an unusual tree (Non-shedding, NSh1; See Chapter 2, MTC180) that fails to abscise its fruit. Expression of five of these genes (*EgIDA2* to *EgIDA6*) was detected in AZs of *E. guineensis* fruits using RT qPCR (Figure 6A). From the result showing fruit abscission *EgIDA2*, *EgIDA4* and the most abundant, *EgIDA5*, had highest expression levels when fruit are separating (Figure 6B), and *EgIDA2* and *EgIDA5* could also be induced by ethylene (Figure 6C and D). We identified two genes encoding HSL1 and HSL2 receptors; *HSL1* had a very low expression level that did not change over time (Figure 6E). *HSL2* on the other hand was low in unripe AZs of shedding trees, as well as AZs of ripe non-shedding (NSh1-R1 and R2) fruit, but increased strongly in AZs of ripe fruit of abscising trees (Sh1-R and Sh3-R). From about 145 DAP, ethylene treatment induce fruit abscission after 9 h. This treatment also induces increased *HSL2* expression (Figure 6F and G). Thus, *HSL2* expression was consistently associated with active fruit abscission. One interesting point was is that the *EgIDA* genes were not strictly associated with separation; as transcripts were present also in ripe AZs of the non-shedding tree (NSh1-R and NSh2-R; Figure 6B). Hence, *EgIDA* are expressed and induced in the non-shedding AZ although the receptor gene *HSL2* has a very low level of expression.

Overall, the results suggest that the IDA/HAE signaling pathway may function during oil palm ripe fruit abscission, a function that appears conserved between monocots and dicots.

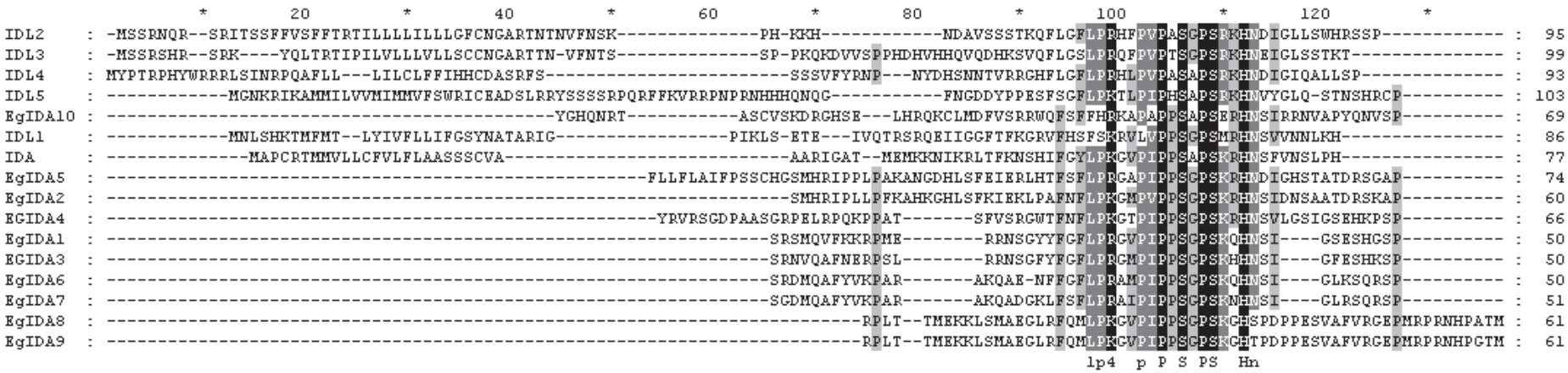

Figure 5. Ten of *IDA* oil palm genes that come in five pairs encoding almost identical preproproteins.

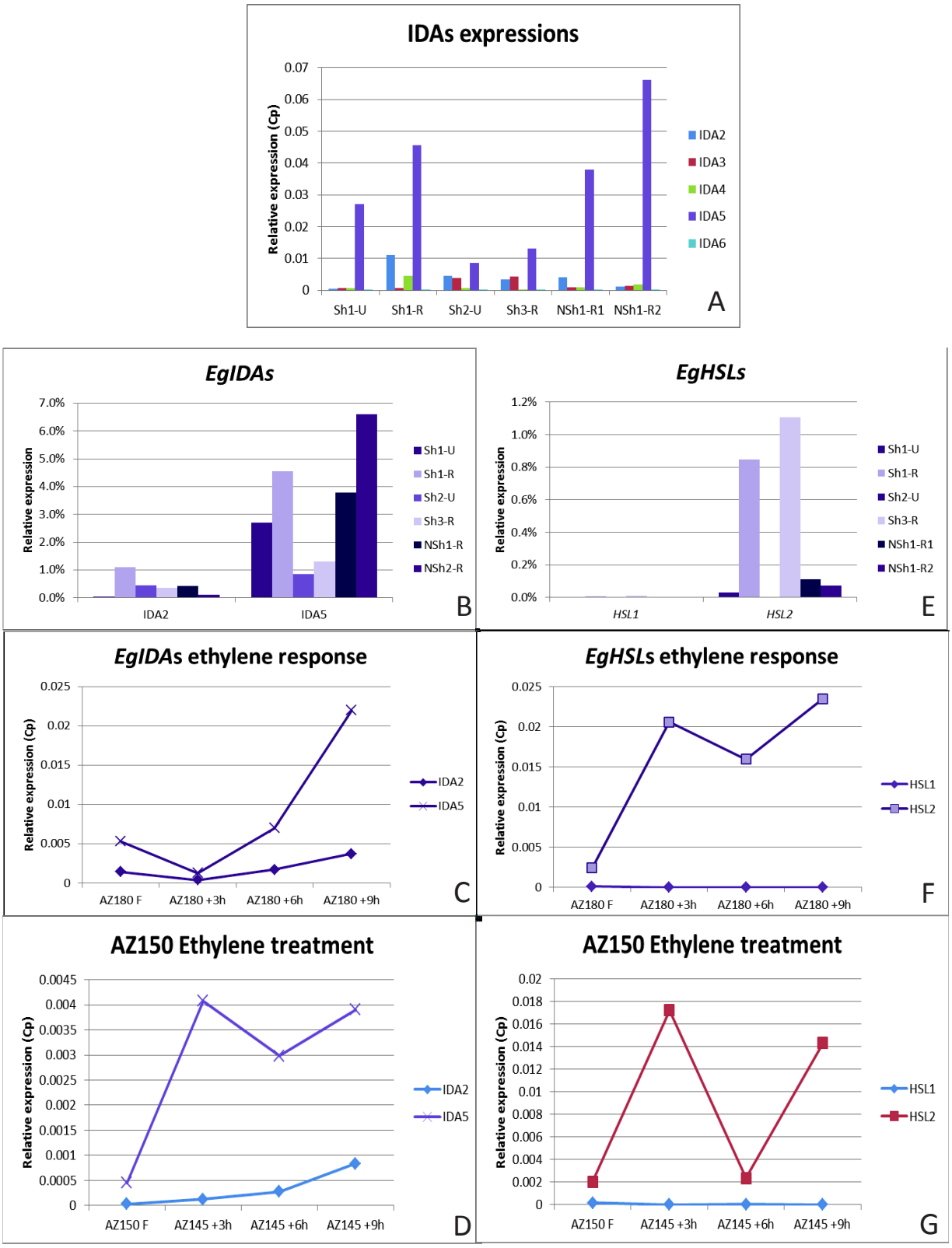

Figure 6. Expression levels of genes encoding IDA ligands and HSL receptors in AZs.
A. Expression levels of additional *EgIDA* genes (*EgIDA2* - *EgIDA6).*
B. qPCR analysis of oil palm *EgIDA2* and *EgIDA5* expression in the AZs of unripe (Sh1-U and Sh2-U) not actively abscising fruit and AZs of ripe (Sh1-R, Sh3-R) actively abscising fruit, as well as AZs from ripe fruit of a non-abscising tree (NSh1-R1, NSh1-R2).

C. qPCR analyses of oil palm *EgIDA2* and *EgIDA5* expression during ethylene-induced abscission in ripe 180 DAP fruits. Samples were taken after 0, 3, 6 and 9 h treatment with ethylene. Similar results were obtained when treating 145 DAP fruits (Figure 6F). In both experiments fruit separated by 9h of ethylene treatment.
D. qPCR analyses of oil palm *EgIDA2* and *EgIDA5* expression during ethylene-induced abscission in ripe 145 DAP fruits. Samples were taken after 0, 3, 6 and 9 h treatment with ethylene.
E. qPCR analysis of oil palm *EgHSL1* and *EgHSL2* expression in AZs from unripe (Sh1-U and Sh2-U) not actively abscising fruit and AZs of ripe (Sh1-R, Sh3-R) actively abscising fruit, as well as AZs from ripe fruit of a non-abscising tree (NSh1-R1, NSh1-R2).
F. qPCR analyses of oil palm *EgHSL* expression during ethylene-induced abscission in ripe 180 DAP fruits. Samples were taken after 0, 3, 6 and 9 h treatment with ethylene. Similar results were obtained when treating 145 DAP fruits (Figure 6C). In both experiments fruit separated by 9h of ethylene treatment.
G. qPCR analyses of oil palm *EgHSL* expression during ethylene-induced abscission in ripe 145 DAP fruits. Samples were taken after 0, 3, 6 and 9 h treatment with ethylene.

IV. Is there an AZ specific cell wall composition?

The specificity of cell separation localized to the AZ layer may also be determined by the composition of the cell walls in the AZ where cell separation occurs. To provide evidence to respond to the question whether the AZ cell walls have a different composition than the adjacent tissues, mesocarp (M), pedicel (P) and AZ samples were sent to the Complex Carbohydrate Research Center in Georgia, USA (http://www.ccrc.uga.edu/) for analyses, which included pectin isolation, initial pectin quantification, glycosyl composition and Uronic acid linkage analysis. From the pectin isolation, the HPLC graphs revealed that the separation of all three samples gives a huge neutral peak and smaller pectin peak (Figure 7). For samples P and AZ, the neutral peak area is about 75% of the total, pectin 25% for both P and Z, while the sample M neutral portion is 95%, with the pectin peak comprising only 5% of the total area of the chromatogram. The M sample had less pectin than the P or AZ.

For the glycosyl composition analysis, the three tissues could be resolved by PCA (Principle Component Analysis) of the neutral and pectin fractions, which suggests each tissue has distinguishable residue compositions (Figure 8A). In particular, the AZ pectin fraction was close to P pectin fractions, which is consistent with the fact that the AZ samples consist of both P and M tissues. PCA of the composition analysis from the fractions reveals that Galacturonic acid (GalA) is associated to the pectin fractions as predicted. In addition, Rhamnose (Rha) residues appear more closely associated to the AZ fraction than the P or M pectin fractions (Figure 8B).

From a PCA of the glycosyl linkage results, three tissues are clearly separated which suggests they have different linkage structures (Figure 9A). Furthermore, t-Araf and 4-GalA appear to be associated with the AZ sample (Figure 9B). Overall, the combined results suggest some compositional characteristics of the AZ are apparent, but these results need to be validated by other approaches or repetitions of the experiment.

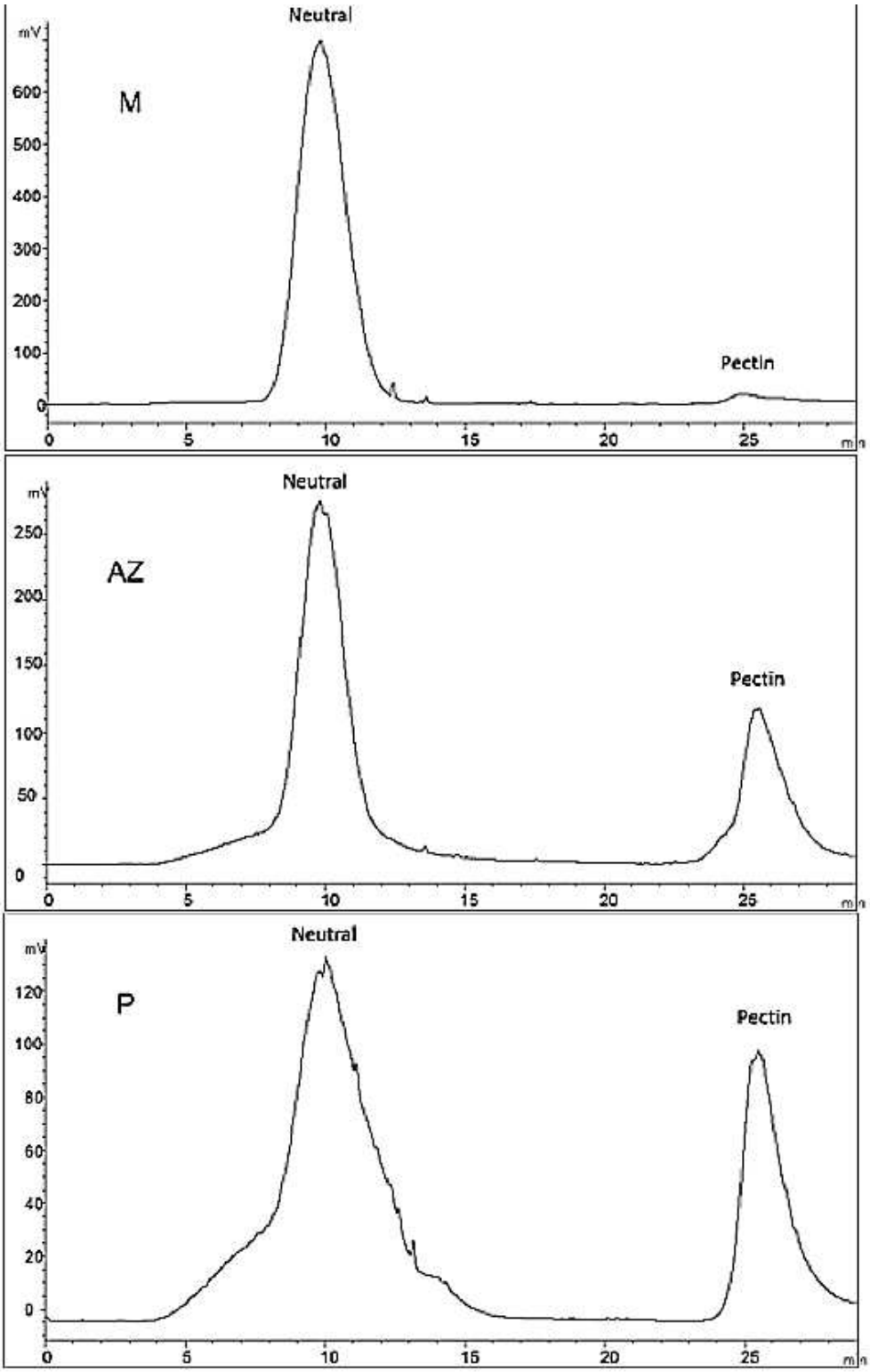

Figure 7. The separation of 3 different tissue M, AZ and P by the HPLC show the separation between Neural and Pectin.

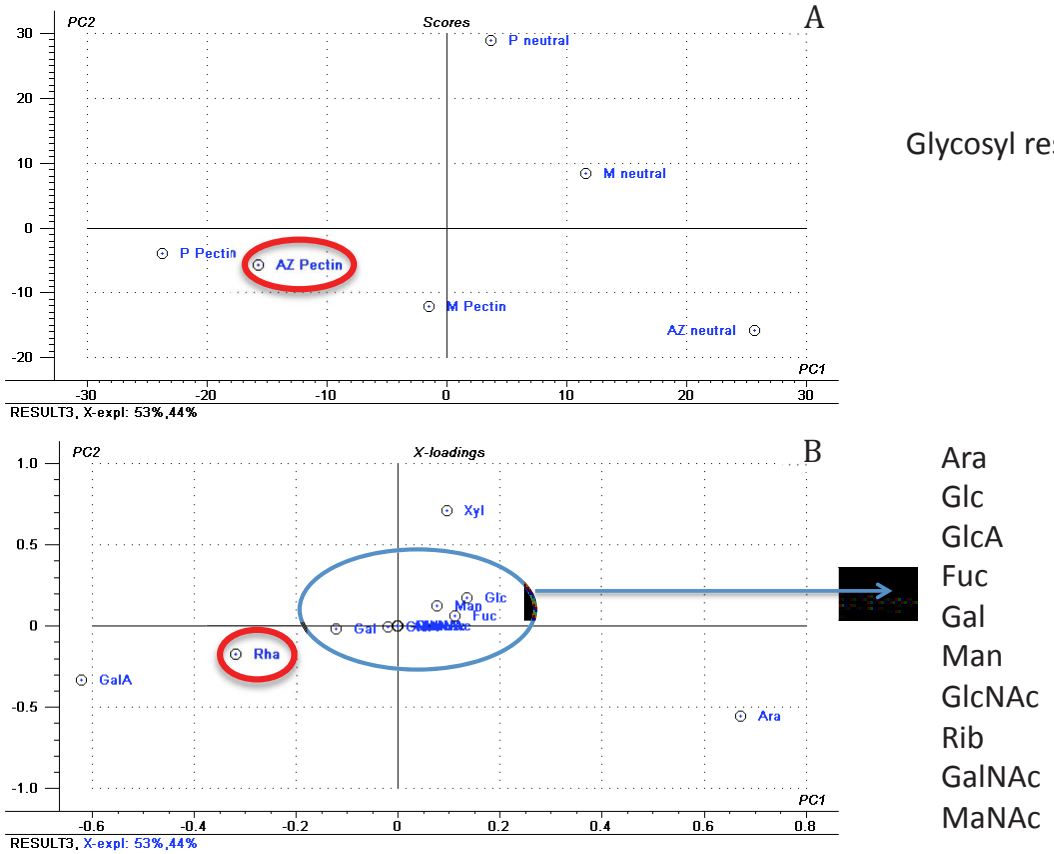

Figure 8. Isolation of pectin and glycosyl composition. A, PCA analysis of pectin and neutral fractions from the mesocarp (M), pedicel (P) and AZ. B, PCA analysis of pectin composition of the samples (M, P, AZ). The glycosyl residues in the central (show on the right hand side) are common to all samples. Ribose (Rib), Arabinose (Ara), Rhamnose (Rha), Fucose (Fuc), Xylose (Xyl), Glucuronic Acid (GlcA), Galacturonic acid (GalA), Mannose (Man), Galactose (Gal), Glucose (Glc), N-Acetyl Galactosamine (GalNAc), N-Acetyl Glucosamine (GlcNAc) and N-Acetyl Mannosamine (ManNAc). Red circle highlights the AZ pectin and the composition closely associated to the AZ.

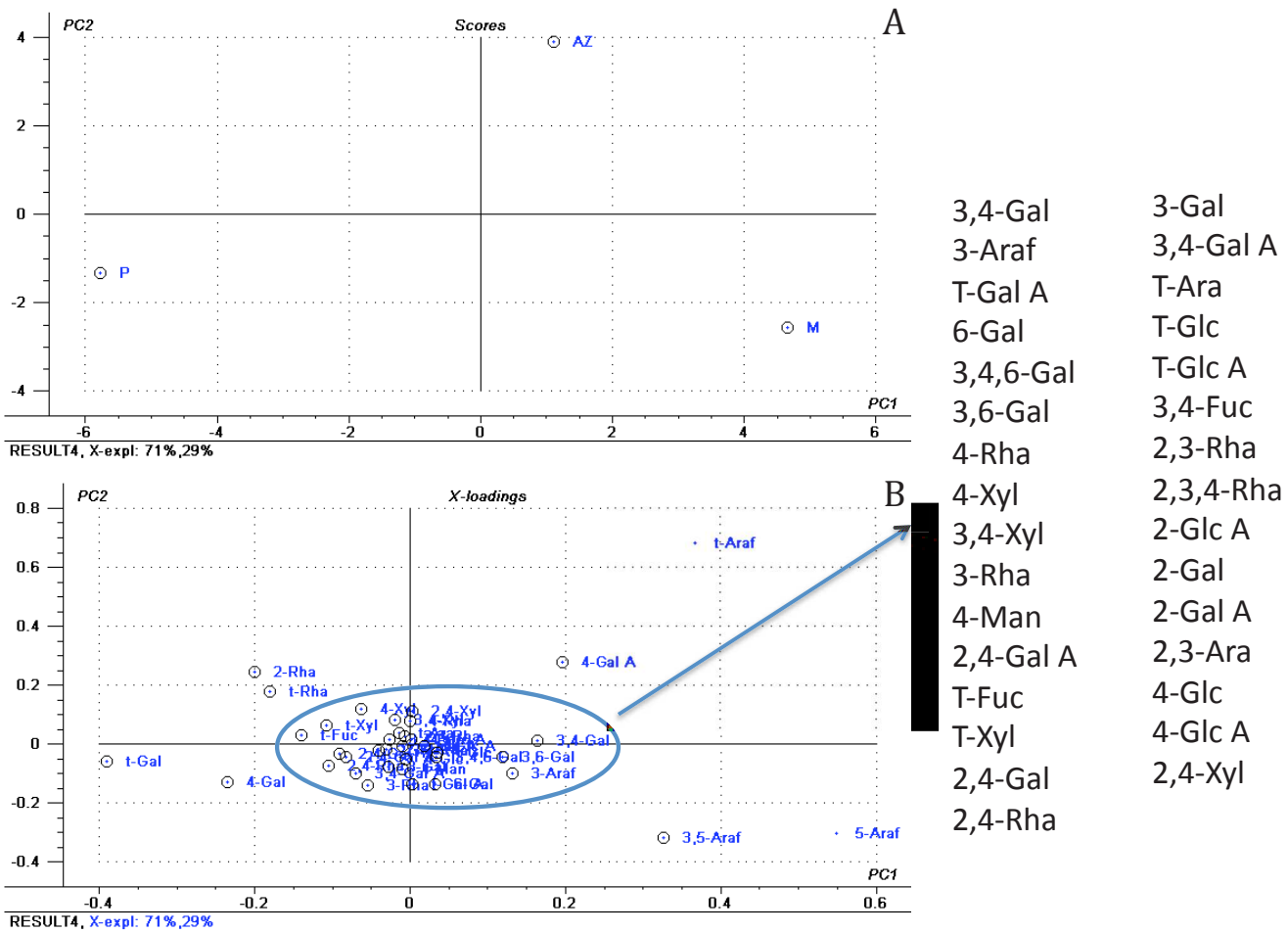

Figure 9. PCA of Uronic acid linkage analysis results. A, PCA resolves linkage results by tissue. B, Details of PCA of uronic acid linkage results. The group in the central show on the right hand side. Terminal, Rhamnopyranosyl residue (t-Rha), Terminal Arabinofuranosyl residue (t-

Araf), Terminal Fucopyranosyl residue (t-Fuc), Terminal Arabinopyranosyl residue (t-Ara), Terminal Xylopyranosyl residue (t-Xyl), 2 linked Rhamnopyranosyl residue (2-Rha), 4 linked Rhamnopyranosyl residue (4-Rha), Terminal Glucopyranosyl residue (t-Glc), Terminal Glucuronic Acid residue (t-Glc A), 3 linked Arabinofuranosyl residue (3-Araf), Terminal Galactopyranosyl residue (t-Gal), Terminal Galacturonic Acid residue (t-Gal A), 4 linked Arabinopyranosyl residue or 5 linked Arabinofuranosyl residue (4-Arap or 5-Araf), 4 linked Xylopyranosyl residue (4-Xyl), 3,4 linked Fucopyranosyl residue (3,4-Fuc), 2,3 linked Rhamnopyranosyl residue (2,3-Rha), 2,4 linked Rhamnopyranosyl residue (2,4-Rha), 2,3,4 linked Rhamnopyranosyl residue (2,3,4-Rha), 2 linked Glucuronic Acid residue (2-Glc A), 3 linked Galactopyranosyl residue (3-Gal), 2 linked, Galactopyranosyl residue (2-Gal), 2 linked Galacturonic Acid residue (2-Gal A), 3,4 linked Arabinopyranosyl residue or 3,5 linked, Arabinofuranosyl residue (3,4-Arap or 3,5-Araf), 4 linked Galacturonic Acid residue (4-Gal A), 2,3 linked Arabinopyranosyl residue (2,3-Ara) 4 linked Glucopyranosyl residue (4-Glc), 4 linked Glucuronic Acid residue (4-Glc A), 2,4 linked Xylopyranosyl residue (2,4-Xyl), 3,4 linked Xylopyranosyl residue (3,4-Xyl), 6 linked Galactopyranosyl residue (6-Gal), 3,4 linked Galactopyranosyl residue (3,4-Gal), 3,4 linked Galacturonic Acid residue (3,4-Gal A), 2,4 linked Galactopyranosyl residue (2,4-Gal), 2,4 linked Galacturonic Acid residue (2,4-Gal A) and 3,6 linked Galactopyranosyl residue (3,6-Gal).

V. Do the different *EgPGs* and other up-regulated candidates have common elements in their promoters?

The up-regulated expression candidates and tissue specific expression observed (Chapter 3) could be due to common promoter elements that coordinate their expression during abscission. To identify common elements in the most robust candidates identified, the upstream sequences for the contigs expressed both in the mesocarp and the AZ including *EgPG4* (CL1Contig10800), *Thioesterase* (CL1Contig1963), and *a/b hydrolase* (CL1Contig9601) and contigs expressed preferentially in the AZ (Chapter 3, Figure 6) including *EgPGAZ1* (CL1Contig6920), *EgPGAZ2* (CLContig9409) and Inositol oxygenase (CL1Contig7452) were isolated. The results reveal that only 2 different Matrix Families can be found, CE3S for the mesocarp contigs and IDDF on the AZ contigs (Table 2).

The CE3 found in the mesocarp and AZ expressed contigs is a response element known to be involved in transcriptional and responses triggered by the phytohormone abscisic acid, and earlier reports with various monocots identified CE3 as a coupling element (CE) associated with ABRE (Gómez-Porras et al., 2007). The CE3 is a binding site related to the ABA Response Element (ABRE) recognized by TRAB1 bZIP transcription factors. ABRE contains an ACGT core, a sequence recognized by plant bZIP proteins (Choi et al., 2000). It has been found that a single copy of ABRE is not sufficient for ABA-mediated induction of transcription, but multiple ABREs or the combination of an ABRE so it is called coupling element (CE) can establish a minimal ABA-responsive complex (ABRC), and thereby confer ABA responsiveness to a minimal promoter (Shen et al., 1996; Choi et al., 2000). In studiy with Arabidopsis and rice found that while ABRE is equally abundant in both species, CE3 is practically absent in Arabidopsis (Gómez-Porras et al., 2007).

For the upstream sequences of AZ specific contigs an IDDF (ID domain factor) binding site was found. The ID domain includes a cluster of three different types of ZINC FINGERs separated from a fourth C2H2 finger by a long spacer. This ID domain protein defines a sub-group of zinc fingers that is highly conserved in higher plants (Colasanti et al., 2006). The core element of the IDDF binding site is TTGT. The upstream regions of these 4 genes contain elements recognized by ID1 transcription factors that have an ID domain as binding domain (Table 2).

Contig (M/AZ)	Annotation	Matrix Family P$CE3S	From	To	(red: ci-value > 60 CAPITALS: core sequence)	Matrix sim.	Transcription Factors	Binding Domain	Description	Associated matrix family
CL1Contig10800	EgPG4	1	425	443	gactgcCGCCtgtcactca	0.792	TRAB1	bZIP	VP1-interacting ABRE-binding bZIP protein	P$ABRE
CL1Contig1963	Thioesterase	1	153	171	caagaaCGCGtgaccttgc	0.880	TRAB1	bZIP	VP1-interacting ABRE-binding bZIP protein	P$ABRE
CL1Contig9601	a-b hydrolase	1	794	812	aactaCGGGtggccttca	0.787	TRAB1	bZIP	VP1-interacting ABRE-binding bZIP protein	P$ABRE

Contig (AZ)	Annotation	Matrix Family P$IDDF	From	To	(red: ci-value > 60 CAPITALS: core sequence)	Matrix sim.	Transcription Factors	Binding Domain	Description	Associated matrix family
CL1Contig6920	EgPGAZ1	3	1520	1532	aggtTTGTcctgg	0.947	ID1	ID domain	ZINC FFINGER PROTEIN ID1	P$IDDF
			1674	1686	cctgTTGTccttc	0.945	ID1	ID domain	ZINC FFINGER PROTEIN ID1	P$IDDF
			1860	1872	agatTTGTcattc	0.934	ID1	ID domain	ZINC FFINGER PROTEIN ID1	P$IDDF
CLContig9409	EgPGAZ2	1	221	233	aggtTTGTcctgg	0.947	ID1	ID domain	ZINC FFINGER PROTEIN ID1	P$IDDF
CL1Contig7452	Inositol oxygenase	1	345	357	ttctTTGTcctca	0.961	ID1	ID domain	ZINC FFINGER PROTEIN ID1	P$IDDF

Table 2. Promoter analysis suggests upstream elements are present that may be involved in the tissue or abscission specific AZ expression of selected candidates. The number in the column "From - To" refers to the position of the conserved area (red).

VI. Future prospects

The application of molecular techniques to study the organ abscission process in model plants has increased our understanding of the biochemical and molecular events leading to separation. It is likely that in the next few years, even more will be discovered, for example, how changing environmental conditions affects the abscission process.

The transcriptome study conducted in the current study lays a foundation for future research and raises many questions. For example, what is the importance of neighboring tissues to the abscission process, and are they an important source of signals to coordinate abscission. In addition, given that the transcriptome data in the current study was performed with a mix of tissues (AZ samples contain portions of mesocarp and pedicel tissues), nothing is known about the specialization of layers within a multilayer AZ found in the oil palm fruit. To test our hypothesis about the expression in neighbor tissues and in layers of the AZ, a laser-microdissected transcriptome study is planned to study individual AZ cell layers and cells of adjacent tissues. The results will address the question whether the middle layers where separation is often observed has a specific mixture of PGs transcripts for separation to take place, as predicted from the current study. This technique will provide the real expression within cells of the AZ and adjacent tissues without interference from tissue mixtures. Validation of the gene candidates found in the current study can be done by qPCR, while very specific cell tissue transcriptome sequencing (NGS) could be used to get a comprehensive understanding of the events in AZ cell layers and cells of neighboring tissues.

The consequence of delayed shedding on fruit oil quality and content has not been fully studied. A combination of information from the oil palm team members who study lipid metabolism in the oil palm would provide information about the oil quality and quantity in the fruit of trees with delayed shedding.

For the genetic approach, projects have been initiated to do the genotypic sequencing to identify the genetic basis of phenotypes with agronomic interest, such as abscission. This approach is simple, quick, extremely specific, highly reproducible, and may reach important regions of the genome that are inaccessible to sequence capture approaches.

To confirm the results obtained from the cell wall analysis, an “Imaging mass spectrometry” could be performed to validate the results. This technique uses an instrument that combines optical microscopy with a mass spectrometer and together allows identification and visualization of the distribution of specific molecules (Hankin et al., 2007; Harada et al., 2009). More recently, the matrix-assisted laser desorption ionization imaging mass spectrometry (MALDI-IMS) is powerful tool for investigating the distribution of molecules within complex tissue samples through the direct

analysis of thin tissue sections (Cornett et al., 2007).

The current and previous thesis (Roongsattham, 2011) show the potential of oil palm fruit AZ for molecular and biochemical studies, and the possibilities to discover many interesting characteristics at the molecular and physiological levels. Indeed, the oil palm fruit could possibly be used as a model to study abscission in monocot fruit bearing trees, including the very large and diverse palm family.

MATERIALS AND METHODS

Plant Materials sampling and preparation

Oil palm *Elaeis guineensis* fruit from Thailand and Ecuador (see chapter 2 and 3).

IDA and their primers

All of the *EgIDA* and *EgHAE*/*HSL2* genes primers were designed for the various Eg*IDA* genes, *EgHSL2* and *EgHSL1* (Table 3). qPCR was performed as previously described (Roongsattham, 2011). All expression was normalized to the *EgEfα1* (accession number: AY550990) expression. No change of *EgEfα1* transcript accumulation was found in the fruit tissues treated or not treated with ethylene. Controls were conducted to validate the absence of DNA in each sample.

Gene	Primer Sequence
EgIDA1_S	AGAGGAGGAATTCGGGCTAC
EgIDA1_AS	ATTTCCGATGGCTTCAGCTC
EgIDA2_S	ACTCCCGGCATTCAACTTC
EgIDA2_AS	TGATGATCGATCGAAAGCTG
EgIDA3_S	GGAGGAATTCGGGCTTCTAC
EgIDA3_AS	AAAGAACCCAACCATGTACATTAAC
EgIDA4_S	AAGAGGCATAACTCGGTGCTC
EgIDA4_AS	GGCAAAAATGATTCAAATAAAGG
EgIDA5_S	GAACGCCTTCACACATTCAG
EgIDA5_AS	TGATCGAAATCCGCATGG
EgIDA6_S	CAAGCGGAGAACTTCTTTGG
EgIDA6_AS	GTGCTGTATAAATTGCCACCTTC
EgIDA7_S	AGCAAGCAGATGGCAAACTC
EgIDA7_AS	ATTTGCTTGCCTCATTCTCG
EgIDA10_S	TATCCCGAAGATGGCAGTTC
EgIDA10_AS	GAAAGAAAAGAAAGCGTTCCAA

Table 3 IDA primer sequences used in the study.

Data mining from transcriptome data

Performed as previously described in Chapter 3 for the transcriptome study. In this chapter tblastx alignments were done with the hormonal related candidates of Arabidopsis (TAIR database) involved in auxin, jasmonic acid and ABA pathways.

Immunohistochemistry sample preparation

Samples for immunohistochemistry were obtained and brought back from Thailand in ethanol 70%, and then all the samples were sectioned by vibratome at 90 and 120 µm longitudinally sectioned. All sections were drenched in PBS 1X and blocking buffer 4% (prepared by 48 ml of 10% blocking buffer plus 78 ml of PBS 1X). Immunohistochemistry was performed with some modifications of the protocol previously described as follows (Roongsattham, 2011). The blocking buffer (BB) Phosphate-buffered saline (PBS) 1:1 was prepared then BB/PBS (500 - 1000µl) solution was added to the glass blocks. Next, add tissue slices on each glass blocks and shake them gently on a shaker for three hours at room temperature (RT). Prepare primary antibody (Table 4) and pipette the previous mixed solution out and add the new mixed solution containing primary antibody (500 – 1000 µl; Table 4) to the glass blocks. Shake them gently on a shaker overnight (18 h) at 4 °C. After that, remove the mixed solution in the glass block, add PBS solution (500 – 1000 µl) shake them gently on a shaker for 15 min, drain out and repeat this step two more times. From this step, do the preparation in a dark room. Prepare secondary antibody (Table 4). Remove the mixed solution in the glass blocks and add the mixed solution with secondary antibody (Alexa Fluor 546, 500-1000 µl at a 1:250 dilution) then cover each glass block and keep in dark and shake them gently on a shaker for 1 h at RT. For the control, no primary antibody was added, while second antibody was added. Add PBS solution (500 – 1000 µl), shake them gently on a shaker for 15 min, drain out and repeat this step for 2 more times. For DAPI, prepare PBS: DAPI at 499:1. Keep the prepared solution in dark and shake them gently on a shaker for 1 h at RT. Add PBS solution (500-1000 µl) shake them gently on a shaker for 15 min, drain out and repeat this step 2 more times. Tissue sections were then put on slides and a few MOWIAL droplets were added and sections were covered with cover slips (No. 0). Then, the solution was allowed to dry for a two weeks at 4 °C in dark. The tissue observations were performed and images captured on a Zeiss LSM 510 Meta Confocal Microscope.

.

Table 4. Antibodies used in the immunocharacterization studies.

1° antibody	1° antibody Dilution	Secondary Antibody (Alexa Fluor® 546)	Epitope	Signal Detected
LM1 (Rat)	1:20	Goat Anti-Rat IgG	Extensin	yes
JIM5 (Rat)	1:20	Goat Anti-Rat IgG	Homogalacturonan with partially methyl-esterified epitopes	yes
LM19 (Rat)	1:20	Goat Anti-Rat IgG	Binds strongly to un-esterified homogalacturonan	yes
LM20 (Rat)	1:20	Goat Anti-Rat IgG	Requires methyl-esters and does not bind to un-esterified homogalacturonan	High signal apparent but need control to confirm
2F4 (Mouse)	1:20	Goat Anti-Mouse IgG	Homogalacturonan specificity to Pectin chain "Egg box"	High signal apparent but need control to confirm
ARF1 (Rabbit)	1:1000	Goat Anti-Rabbit IgG	ARF1, ADP-ribosylation factor 1 (Golgi marker)	yes
LM9 (Rat)	1:20	Goat Anti-Rat IgG	FERULOYLATED-(1-4)- β -D-GALACTAN	Low signal apparent but need control to confirm
LM12 (Rat)	1:20	Goat Anti-Rat IgG	FERULOYLATED POLYMERS	Low signal apparent but need control to confirm

Promoter analysis

The most robust candidates from the transciptome results were selected and their upstream sequences were obtained from the oil palm genome (NCBI). We extracted the area upstream sequence region derived from the blastn alignment to the oil palm genome with the contig sequence. The command line in LINUX was used to extracted sequence upstream in the 5' direction for 3k bases from start codon on open reading frame. With the Genomatix software, first task that we used was MatInspector which is a software tool that utilizes a large library of matrix descriptions for transcription factor binding sites to locate matches in DNA sequences. MatInspector is almost as fast as a search for IUPAC strings but has been shown to produce superior results. It assigns a quality rating to matches and thus allows quality based filtering and selection of matches (Cartharius et al., 2005). The next step was the use of the FrameWorker application which is a complex software tool that allows us to extract a common framework of elements from a set of DNA sequences. These elements are usually transcription factor binding sites since this tool is designed for the comparative analysis of promoter sequences and last application that we used was ModelInspector uses a library of predefined models or models defined with FrameWorker to scan DNA sequences for matches to these models. A model consists of various individual elements (like transcription factor binding sites, repeats and hairpins), their strand orientation, their sequential order, and their distance ranges (Frech et al., 1997). All of the contigs were compared with the controls (selected by the number of contigs from different tissue (AZ30, AZ150 and P150) which is contain no contig in each tissue and time point.

Cell wall pectin analysis: Pectin isolation, glycosyl composition and Uronic acid linkage analysis

Samples that were used for cell wall analysis composed of Me AZ and P. All samples were lyophilized before the analysis and sent to the Complex Carbohydrate Research Center in Georgia, USA (http://www.ccrc.uga.edu/) for analysis. Pectin was isolated from the 3 different tissue samples that were analyzed for glycosyl composition and Uronic acid linkage.

Isolation of pectin fraction

The three samples were initially frozen with liquid nitrogen and ground using a mortar and pestle. The ground samples were then mixed with water and ethanol was added to bring the solution up to 90% alcohol. The solutions were then centrifuged to pellet the insoluble material and the supernatant was discarded. This procedure was repeated twice. The pellet was then dried under

nitrogen and lyophilized. Afterward, the dried samples were then treated with amylases (Sigma) for 48 h at 37 °C to remove starch. The samples were then dialyzed in a 2 kDa Molecular Weight Cut-off (MWCO) membrane against Dionize (DI) water to remove the liberated glucose. After dialysis, the samples were lyophilized.

The dried sample material was then combined with 50 ml of 4M KOH containing 0.1% $NaBH_4$ and stirred for 4 h at 50 °C. The solubilized pectin was then separated from the insoluble material by passing the solution through a glass filter. This procedure was repeated once and the solubilized pectin fractions were combined. The solubilized solutions were then neutralized using acetic acid and dialyzed again. Then 10 mg of each dried sample was dissolved in 100 mM ammonium acetate and run by HPLC using a HiTrap DEAE column. The neutral fraction passed through the column using loading buffer and was collected. The pectic fractions were then eluted from the column by running 1 M ammonium acetate. Each fraction was collected and pooled. The fractions were then lyophilized several times to remove the ammonium acetate. Composition analysis was performed on the six collected fractions.

Glycosyl composition

Glycosyl composition analysis was performed by combined gas chromatography/mass spectrometry (GC/MS) of the per-*O*-trimethylsilyl (TMS) derivatives of the monosaccharide methyl glycosides produced from the sample by acidic methanolysis. The samples amount of 100 and 500 µg were used for the analysis. The samples were placed into test tubes, and 20 µg of inositol was added. Methyl glycosides were then prepared from the dry samples by methanolysis in 1 M HCl in methanol at 80 °C (18 h), followed by re-*N*-acetylation with pyridine and acetic anhydride in methanol (for detection of amino sugars). The samples were then per-*O*-trimethylsilylated by treatment with Tri-Sil (Pierce) at 80°C (0.5 h). These procedures were carried out as previously described in (York et al., 1986; Merkle and Poppe, 1994). GC/MS analysis of the TMS methyl glycosides was performed on an Agilent 7890A GC interfaced to a 5975C MSD, using an Agilent DB-1 fused silica capillary column (30m × 0.25 mm ID).

All of the results were analyzed using the Principle Component Analysis (PCA) which convert a set of observations of possibly correlated variables into a set of values of linearly uncorrelated variables that make the result more easy to interpreted.

Uronic acid linkage

For glycosyl linkage analysis, the samples were permethylated, reduced, repermethylated, depolymerized, reduced, and acetylated; and the resultant partially methylated alditol acetates (PMAAs) analyzed by gas chromatography-mass spectrometry (GC-MS) (York et al., 1986)

Initially, the samples were suspended in 200 µl of dimethyl sulfoxide. The samples were then left to stir for 2 days. The samples were permethylated using potassium dimsyl anion and iodomethane. The permethylated uronic acids were then reduced using lithium borodeuteride. The samples were then permethylated again by the method of (Ciucanu and Kerek, 1984) (treatment with sodium hydroxide and methyl iodide in dry DMSO). This additional permethylation was to insure complete methylation of the polymer. Following sample workup, the permethylated material was hydrolyzed using 2 M trifluoroacetic acid (2 h in sealed tube at 121°C), reduced with $NaBD_4$, and acetylated using acetic anhydride/TFA. The resulting PMAAs were analyzed on an Agilent 7890A GC interfaced to a 5975C MSD (mass selective detector, electron impact ionization mode); separation was performed on a Supelco SP-2380 fused silica capillary column (30m × 0.25 mm ID).

REFERENCES

Choi H-i, Hong J-h, Ha J-o, Kang J-y, Kim SY (2000) ABFs, a family of ABA-responsive element binding factors. Journal of Biological Chemistry **275:** 1723-1730

Ciucanu I, Kerek F (1984) A Simple and Rapid Method for the Permethylation of Carbohydrates. Carbohydrate Research **131:** 209-217

Clausen MH, Ralet MC, Willats WG, McCartney L, Marcus SE, Thibault JF, Knox JP (2004) A monoclonal antibody to feruloylated-(1-->4)-beta-D-galactan. Planta **219:** 1036-1041

Clausen MH, Willats WG, Knox JP (2003) Synthetic methyl hexagalacturonate hapten inhibitors of anti-homogalacturonan monoclonal antibodies LM7, JIM5 and JIM7. Carbohydr Res **338:** 1797-1800

Colasanti J, Tremblay R, Wong AY, Coneva V, Kozaki A, Mable BK (2006) The maize INDETERMINATE1 flowering time regulator defines a highly conserved zinc finger protein family in higher plants. Bmc Genomics **7:** 158

Cornett DS, Reyzer ML, Chaurand P, Caprioli RM (2007) MALDI imaging mass spectrometry: molecular snapshots of biochemical systems. Nature methods **4:** 828-833

Dal Cin V, Barbaro E, Danesin M, Murayama H, Velasco R, Ramina A (2009) Fruitlet abscission: A cDNA-AFLP approach to study genes differentially expressed during shedding of immature fruits reveals the involvement of a putative auxin hydrogen symporter in apple (Malus domestica L. Borkh). Gene **442:** 26-36

Dal Cin V, Danesin M, Boschetti A, Dorigoni A, Ramina A (2005) Ethylene biosynthesis and perception in apple fruitlet abscission (Malus domestica L. Borck). Journal of Experimental Botany **56:** 2995-3005

Dal Cin V, Galla G, Ramina A (2007) MdACO expression during abscission: the use of 33P labeled primers in transcript quantitation. Molecular biotechnology **36:** 9-13

Dal Cin V, Velasco R, Ramina A (2009) Dominance induction of fruitlet shedding in Malus x domestica (L. Borkh): molecular changes associated with polar auxin transport. BMC plant biology **9:** 139

Delker C, Zolman BK, Miersch O, Wasternack C (2007) Jasmonate biosynthesis in Arabidopsis thaliana requires peroxisomal beta-oxidation enzymes--additional proof by properties of pex6 and aim1. Phytochemistry **68:** 1642-1650

Ding X, Cao Y, Huang L, Zhao J, Xu C, Li X, Wang S (2008) Activation of the indole-3-acetic acid-amido synthetase GH3-8 suppresses expansin expression and promotes salicylate- and jasmonate-independent basal immunity in rice. Plant Cell **20:** 228-240

Fan XT, Mattheis JP (1998) Bagging 'Fuji' apples during fruit development affects color development and storage quality. Hortscience **33:** 1235-1238

Gómez-Porras JL, Riaño-Pachón DM, Dreyer I, Mayer JE, Mueller-Roeber B (2007) Genome-wide analysis of ABA-responsive elements ABRE and CE3 reveals divergent patterns in Arabidopsis and rice. BMC genomics **8:** 260.

Hankin JA, Barkley RM, Murphy RC (2007) Sublimation as a method of matrix application for mass spectrometric imaging. Journal of the American Society for Mass Spectrometry **18:** 1646-1652

Harada T, Yuba-Kubo A, Sugiura Y, Zaima N, Hayasaka T, Goto-Inoue N, Wakui M, Suematsu M, Takeshita K, Ogawa K (2009) Visualization of volatile substances in different organelles with an atmospheric-pressure mass microscope. Analytical chemistry **81:** 9153-9157

IM Stø, R Orr, K Fooyontphanich, X Jin, JMB Knutsen, U Fischer, T J Tranbarger, I Nordal and R B Aalen. (2015) The evolutionary conservation of the abscission signaling peptide IDA in Angiosperms: withstanding numerous genome duplications. Frontiers in Plant Science doi: 10.3389/fpls.2015.00931.

Knox JP, Linstead PJ, King J, Cooper C, Roberts K (1990) Pectin esterification is spatially regulated both within cell walls and between developing tissues of root apices. Planta **181:** 512-521

Kondo S, Tomiyama A, Seto H (2000) Changes of endogenous jasmonic acid and methyl jasmonate in apples and sweet cherries during fruit development. Journal of the American Society for Horticultural Science **125:** 282-287

Marais C, Wattelet-Boyer V, Bouyssou G, Hocquellet A, Dupuy J-W, Batailler B, Brocard L, Boutté Y, Maneta-Peyret L, Moreau P (2015) The Qb-SNARE Memb11 interacts specifically with Arf1 in the Golgi apparatus of Arabidopsis thaliana. Journal of experimental botany**:** erv373

Merkle RK, Poppe I (1994) Carbohydrate-Composition Analysis of Glycoconjugates by Gas-Liquid-Chromatography Mass-Spectrometry. Guide to Techniques in Glycobiology **230:** 1-15

Meyer A, Miersch O, Büttner C, Dathe W, Sembdner G (1984) Occurrence of the plant growth regulator jasmonic acid in plants. Journal of Plant Growth Regulation **3:** 1-8

Pedersen HL, Fangel JU, McCleary B, Ruzanski C, Rydahl MG, Ralet M-C, Farkas V, von Schantz L, Marcus SE, Andersen MC (2012) Versatile high resolution oligosaccharide microarrays for plant glycobiology and cell wall research. Journal of Biological Chemistry **287:** 39429-39438

Roongsattham P (2011) Cell separation processes that underlie fruit abscission and shedding in oil palm (Elaeis guineensis Jacq.). UNIVERSITÉ MONTPELLIER 2, Montpellier, France

Roongsattham P, Morcillo F, Fooyontphanich K, Jantasuriyarat C, Tragoonrung S, Amblard P, Collin M, Mouille G, Verdeil J and Tranbarger TJ. (2015) Cellular and cell wall dynamics underlie abscission zone development and function during oil palm fruit abscission. (submitted to Frontiers in Plant Science).

Ruperti B, Bonghi C, Rasori A, Ramina A, Tonutti P (2001) Characterization and expression of two members of the Peach 1−aminocyclopropane−1−carboxylate oxidase gene family. Physiologia Plantarum **111:** 336-344

Saika H, Okamoto M, Miyoshi K, Kushiro T, Shinoda S, Jikumaru Y, Fujimoto M, Arikawa T, Takahashi H, Ando M (2007) Ethylene promotes submergence-induced expression of OsABA8ox1, a gene that encodes ABA 8′-hydroxylase in rice. Plant and Cell Physiology **48:** 287-298

Shen Q, Zhang P, Ho T (1996) Modular nature of abscisic acid (ABA) response complexes: composite promoter units that are necessary and sufficient for ABA induction of gene expression in barley. The Plant Cell **8:** 1107-1119

Steffens B, Sauter M (2014) Role of ethylene and other plant hormones in orchestrating the responses to low oxygen conditions. *In* Low-Oxygen Stress in Plants. Springer, pp 117-132

Vallabhaneni R, Wurtzel ET (2010) From epoxycarotenoids to ABA: the role of ABA 8′-hydroxylases in drought-stressed maize roots. Archives of biochemistry and biophysics **504:** 112-117

Verhertbruggen Y, Marcus SE, Haeger A, Ordaz-Ortiz JJ, Knox JP (2009) An extended set of monoclonal antibodies to pectic homogalacturonan. Carbohydrate Research **344:** 1858-1862

Wang S, Ito T, Uehara M, Naito S, Takano J (2015) UDP-d-galactose synthesis by UDP-glucose 4-epimerase 4 is required for organization of the trans-Golgi network/early endosome in Arabidopsis thaliana root epidermal cells. Journal of plant research**:** 1-11

Willats WG, Limberg G, Buchholt HC, van Alebeek GJ, Benen J, Christensen TM, Visser J, Voragen A, Mikkelsen JD, Knox JP (2000) Analysis of pectic epitopes recognised by hybridoma and phage display monoclonal antibodies using defined oligosaccharides, polysaccharides, and enzymatic degradation. Carbohydr Res **327:** 309-320

York WS, Darvill AG, Mcneil M, Stevenson TT, Albersheim P (1986) Isolation and Characterization of Plant-Cell Walls and Cell-Wall Components. Methods in Enzymology **118:** 3-40

Zhang Y-J, Wang X-J, Wu J-X, Chen S-Y, Chen H, Chai L-J, Yi H-L (2014) Comparative Transcriptome Analyses between a Spontaneous Late-Ripening Sweet Orange Mutant and Its Wild Type Suggest the Functions of ABA, Sucrose and JA during Citrus Fruit Ripening. PloS one **9:** e116056

Résumé

L'abscission des organes chez les végétaux est hautement régulée au cours du développement. Ce processus physiologique qui consiste à diminuer l'adhésion entre deux cellules adjacentes dépend de l'environnement, du stress, de l'attaque de pathogènes ou encore de l'état physiologique de la plante. L'abscission du fruit et de la graine jouent un rôle déterminant dans le cycle de vie de la plante et en particulier, un rôle central dans la dispersion des graines. C'est également un caractère commun de domestication avec des conséquences économiques pour la plus part des espèces cultivées. Le palmier à huile (*Elaeis guineensis*) est largement cultivé dans toutes les zones tropicales et l'huile de palme représente aujourd'hui plus d'un tiers des huiles végétales produites dans le monde. La maturation des fruits au sein des régimes est asynchrone. Ainsi, les fruits les plus murs tombent avant le murissement complet du régime, entrainant une baisse du rendement d'une part et rendant leur collecte manuelle fastidieuse et couteuse d'autre part. Dans ce context, le contrôle ou la réduction de la chute des fruits permettrait une meilleure gestion de la récolte à des couts réduits. Dans le cadre de cette étude, un protocole de phénotypage du processus d'abscission du fruit du palmier à huile a été développé et utilisé pour identifier des génotypes à faible ou retard d'abscision des fruits arrivés à maturité. En parallèle, des analyses comparatives de transcriptomes et de protéomes issus de la zone d'abscission (ZA) du fruit ont été conduites tout au long du processus de séparation cellulaire, déclenché au laboratoire par un traitement à l'éthylène ou bien de manière naturelle au champ. Au total 1957 gènes présentent une expression différentielle significative dans la ZA du fruit au cours du processus d'abscission induit par l'éthylène. Parmi ces gènes, 64 sont spécifiquement (ou majoritairement) exprimés dans la ZA des fruits arrivés à maturité par comparaison avec les tissus où le processus de séparation cellulaire n'est pas observé (pédicelle et mésocarpe des fruits murs ; ZA non fonctionnelle des fruits immatures). Le profil d'expression de ces 64 gènes candidats a été également analysé dans la ZA des fruits mûrs prélevés au champ, afin de conforter leur rôle potentiel au cours de l'abscission déclenchée naturellement. Ainsi, en utilisant les nouvelles technologies de séquençage du transcriptome et du protéome, couplées à une analyse biochimique et cellulaire des modifications de la paroi dans la ZA, ce travail a permis de mettre en évidence la conservation de certains processus moléculaires associés à l'abscission des organes chez les monocotylédones par comparaison avec les espèces modèles dicotylédones, telles que la tomate et Arabidopsis. Par exemple, l'identification de gènes codant des polygalacturonases très proches de celles qui sont impliquées dans l'abscission de la fleur chez Arabidopsis suggère la conservation de leur fonction dans l'hydrolyse de la pectine des cellules des ZA, malgré la divergence phylogénétique entre les espèces. Enfin, ce travail a permis également d'identifier de nouveaux régulateurs associés au processus de séparation cellulaire et fournir une liste de gènes associés à des processus biologiques étroitement liés à la fonction de la ZA chez le fruit du palmier à huile

Summary

Plant organ abscission is a complex developmental process that involves cell separation regulated by the environment, stress, pathogens and the physiological status of the plant. In particular, seed and fruit abscission play a central role in seed dispersion and plant reproductive success, and are common domestication traits with important agronomic consequences for many crop species. Oil palm (*Elaeis guineensis*) is cultivated throughout the tropical regions as one of the most economically important oil crop species in the world. The unsynchronized ripening of the oil palm fruit bunch leads to the abscission of the ripest fruit and consequently high labor cost for harvest and loss of yield. In this context, the control of oil palm ripe fruit abscission is an important agricultural concern for the cultivation of oil palm in a sustainable and cost effective way. In the present study, a protocol to phenotype the oil palm fruit abscission process was developed and used to identify a tree in the field that does not undergo ripe fruit abscission. In parallel, transcriptome and proteome analyses of the oil palm ripe fruit abscission zone (AZ) during abscission induced experimentally by ethylene compared to the AZ undergoing natural abscission in the field was performed. A total of 1,957 candidate genes were identified statistically as differentially expressed in the ripe fruit AZ during ethylene-induced abscission. Furthermore, a total of 64 of these differentially abundant candidates were statistically specific or enriched at least during one time point of the ethylene induced abscission, compared to their profiles in the AZ of immature fruit and the pedicel of ripe fruit, where cell separation is not observed. The profiles of these gene candidates were examined in the ripe fruit AZ undergoing natural abscission in the field to validate their potential role during abscission. Finally, the profiles of selected candidate genes were then examined in the AZ of the tree observed not to undergo fruit abscission in the field. The combined approaches provide evidence of wide scale conservation of the molecular components involved in organ abscission of this monocot compared with the model dicot plants tomato and Arabidopsis. For example, the identification of polygalacturonases very similar to those that function during Arabidopsis floral organ abscission suggests a conservation of the components for pectin disassembly despite the phylogenetic distance between these species. In addition, the data from the global analysis and complementary molecular, cellular and biochemical approaches suggest novel components and provide a robust list of genes and processes important for AZ function during ripe fruit abscission of this important monocot crop species